UNIVERSITAT DE BARCELONA

Role of Fsp27 in lipid homeostasis during nutrient deprivation

Alexandra Carrilho do Rosario

UNIVERSITAT DE BARCELONA

Programa de Doctorat en Biomedicina

Facultat de Farmàcia i Ciències de l'Alimentació

Departament de Nutrició, Ciències de l'Alimentació i Gastronomia

Role of Fsp27 in lipid homeostasis during nutrient deprivation

Memòria presentada per Alexandra Carrilho do Rosário per optar al títol de doctor per la Universitat de Barcelona

Dr. Pedro Marrero	Dra. Joana Relat	Alexandra Carrilho do Rosário
El Director	La Directora	La doctoranda

Aquesta tesi ha estat realitzada gràcies a la concessió d'una beca del
programa "Ajuts per a Personal Investigador predoctoral en Formació "(APIF-UB) de la
Universitat de Barcelona

Agradecimientos

Una tesis es mucho más que un trabajo. Es un aprendizaje, un viaje y muchas veces un test a nuestros propios limites.

Puedo decir que en los últimos 4 años he aprendido mucho, he evolucionado, tanto personal como profesionalmente, muchas veces he puesto en duda mis decisiones y he hecho amigos que se han transformado en familia. Todo esto no sería posible sin el apoyo, de una manera o de otra, de muchas personas.

En primer lugar, quiero agradecer a mis "jefes", Pedro y Diego. Gracias por haberme recibido en vuestro laboratorio en 2011, por haber hecho que fuera posible volver a Barcelona para hacer el doctorado y por todo lo que me habéis enseñado en los últimos años.

Agradezco también a mi nueva "jefa". Gracias Joana, por todo lo que me has enseñado, por la paciencia para explicar las cosas una y otra vez y por las palabras de ánimo.

A las chicas del ST lab, Mariona, Elena y en especial Ana Lu, gracias por haberme acogido de brazos abiertos en el lab, y por hacerme ver que trabajar en un laboratorio no tiene que ser aburrido.

Agradeço também à minha colega de curso, de casa e de muitas experiências (e festas) Joana Gonçalves. Tudo o que já vivemos supera as palavras e sei que sabes bem a importância que tiveste no meu percurso. Obrigada pelo apoio, pelas conversas diárias, pelos artigos e dicas que me envias sempre que preciso.

Gracias Albert, por tu paciencia infinita, por siempre estar dispuesto a explicar las cosas una y otra vez y por no enfadarte con las infinitas preguntas que te hacía a diario. Puedo decir que todo lo que he aprendido en el laboratorio durante el doctorado lo he aprendido contigo.

Gracias Maite, Vivi y Úrsula, por acogerme tan bien y con tan buena disposición en el nuevo laboratorio. Gracias por ayudarme cuando hacía falta.

No puedo dejar de agradecer también a todas las personas del departamento que de una manera o de otra, sea dejándome una hora en la real time o dejándome un bote de reactivo, me han ayudado.

Y como no podía ser de otra manera, un agradecimiento muy especial a mi pequeña "familia" del departamento, Maria José, Maria Alexandra y Carlos. Gracias, por todos los momentos que hemos pasado juntos. Gracias por todos los buenos momentos, por todas las fiestas, por la compañía, por los findes pasados en el laboratorio. Desde esa primera cerveza hace 4 años muchas cosas han cambiado. Me siento afortunada de teneros en mi vida.

Aos tugas que me fizeram sentir em casa quando cheguei, obrigada. Obrigada Ângelo, foram muitas festas, idas ao cinema, infinitos jantares, dias de Praia (etc etc) que fizeram com que estar longe de casa não custasse tanto.

Obrigada Pai e Mãe, por acreditarem em mim mais do que eu própria acredito.
Obrigada por fazerem possível que os meus sonhos se tornassem realidade.
Obrigada Margarida e João, sem o vosso apoio (e visitas) nao seria a mesma coisa.
Vocês são o meu porto seguro.
Aos meus avós, à Rita e ao Tiaguinho, agradeço o apoio nas fases complicadas da minha vida, que fez com que fosse possível chegar aqui.

A mis nuevos nuevos compis de Roche, Anna y Marc, gracias por no dejar que me vuelva loca estos últimos meses.

Obrigada a todos os meus amiguinhos de Portugal, em Portugal e espalhados pelo mundo, que mesmo longe sei que estão a torcer por mim.

A mi pequeño Zakk, un agradecimiento especial, que aunque no pueda hablar, me transmite su apoyo y alegría sin querer nada a cambio.

Por último el agradecimiento más importante. Gracias David, por haberme esperado, por aguantar mi mal humor, por entender lo que estoy pasando y por apoyarme, siempre. Has sido el mejor descubrimiento de mi investigación y sé que todo este camino ha merecido la pena si lo terminamos juntos. *T'estimo.*

INDEX

INDEX

INDEX

PRESENTATION AND OBJECTIVES

PRESENTATION AND OBJECTIVES

The main goal of this project is to study new mechanisms by which FSP27 regulates cell physiology and to define its putative role on PPAR signaling during fasting.

FSP27 is a lipid-droplet associated protein expressed in liver and white and brown adipose tissues, which promotes intracellular lipid accumulation and prevents lipolysis (Puri 2013).

There are two different isoforms of FSP27 that encode for two different proteins, the FSP27α that is mainly expressed in white adipose tissue and FSP27β, the unique form expressed in liver and also expressed in brown adipose tissue. The alternative β isoform contains 10 additional amino acids at the N terminus of the original FSP27α (Xu et al. 2015).

The expression of *Fsp27*β is induced by the cyclic-AMP-responsive element-binding protein H (CREBH), a transcription factor that regulates lipid and glucose metabolism (Xu et al. 2015). Previous work developed in our lab identified *Fsp27* as a key gene up regulated in the liver on the early response to fasting. *Fsp27* is induced in an early fasting (6-15h), but not during longer periods of starvation, suggesting that Fsp27 is specifically responsive to the signals of an early response to fasting. (Vilà-Brau et al. 2013)

It is known that the *"new fat",* fat that comes from diet or from *de novo* synthesis via fatty acid synthase (FASN) is capable of activating PPARα, but the *"old fat",* the fat stored in the adipocytes, cannot. This leads to an important paradox, since PPARα target genes are expressed in fasting situations, but PPARα itself should not be active (Chakravarthy et al. 2005). The activation of PPARα target genes is impaired when the FASN is not active or absent (in a knockout mice), and that led to the discovery of 1-palmitoyl-2-oleoyl-sn-glycerol-3-phosphocholine (16:0/18:1 PC) as a ligand for PPARα (Chakravarthy et al. 2010). Another phosphocholine species, the 18:0/18:1 PC, was described as being a serum lipid regulated by diurnal hepatic PPARα activity (Liu et al. 2013).

All together uncovers a link between *Fsp27* expression pattern and its role in the unilocular lipid droplet formation, and the availability of PPARα ligands coming from the new fat, in fasting and feeding situations. In this context the hypothesis of this Thesis is that the activity of FSP27 could promote the intrahepatic accumulation of newly synthesized phospholipids during the early fasting state, which would then be released into circulation, thus regulating the availability of endogenous ligands of PPARα.

The work developed in this Thesis was divided into three different chapters, the regulation of *Fsp27* during the fasting adaptation, the transcriptional regulation of *Fsp27* in liver and finally the role of FSP27 as a lipid-droplet protein in PPARα signaling, with the purpose to understand the following objectives:

1) To describe the expression pattern of FSP27 during fasting adaptation in different tissues and different fasting times.
2) To define the transcriptional mechanisms responsible for hepatic expression of FSP27 during fasting specially the ones that cause the fall of Fsp27β expression during late fasting.
3) To identify the role of Fsp27β in PPARα signaling by studying its ability to control the store/release of specific endogenous ligands of PPARa from lipid droplets.

INTRODUCTION

1. Liver Fatty Acid Metabolism

Deregulation of lipid metabolism lies at the base of the most common medical disorders in western populations, such as cardiovascular disease, obesity, diabetes, and fatty liver conditions. However, a gap of knowledge still exists in both the basic science and the clinical fields regarding the impact of altered lipid storage on human disease.

The liver can both oxidize and synthetize fatty acids. In humans the overall rate of fatty acid synthesis from other molecules (glucose in particular) is usually small in comparison with dietary fatty acid intake, nonetheless this pathway has a special significance in coordinating glucose and fat metabolism, and in generating the ligands for the appropriated PPARa activation, as discussed below.

1.1Fatty acid oxidation in liver during adaptation to fasting

The hepatic fatty acid oxidation (FAO) plays a central role in the adaptive response to fasting. The plasma hormone profile in this situation, low insulin and high glucagon, induces the release of large amounts of fatty acids from the adipose tissue to be used by peripheral tissues and spare glucose consumption. Therefore, the liver of a starved animal actively oxidizes fatty acid, which provides the energy necessary to sustain gluconeogenesis. It also supplies the acetyl-CoA needed for active ketone body synthesis, which replaces glucose as the energy substrate for the brain and other tissues (McGarry and Foster 1995).

Two enzymes determine the metabolic fate of fatty acids in the liver of starved animals: carnitine palmitoyltransferase-1 (CPT1) A and hydroxymethylglutaryl CoA

synthase 2 (HMGCS2). *Cpt1A* encodes a malonyl-CoA-sensitive protein that regulates mitochondrial long chain fatty acid oxidation (McGarry and Foster 1995), whereas *Hmgcs2* encodes a mitochondrial protein that controls the 3-hydroxy-3-methylglutaryl-CoA (HMG-CoA) cycle, by which acetoacetate, b-hydroxybutyrate, and NAD^+ are generated (Hegardt 1995). The expression of both genes is regulated by peroxisome proliferator-activated receptor α (PPARα) (Napal, Marrero, and Haro 2005; Ortiz et al. 1999; Rodríguez et al. 1994; Hsu et al. 2001), a fatty acid-activated nuclear receptor that regulates metabolic changes in the liver associated with starvation (see below). Consistently, during starvation, PPARα null mice show severe hypoglycemia and hypoketonemia (Kersten et al. 1999). The hypoglycemia is due to a reduced capacity for hepatic gluconeogenesis secondary to a 70% lower rate of fatty acid oxidation. The liver *Hmgcs2* expression during fasting is relevant to produce ketone bodies that will avoid glucose utilization, but also to maintain an active FAO (Figure I1). Thus, knocking down *Hmgcs2* expression impairs fatty acid oxidation (Vilà-Brau et al. 2011a).

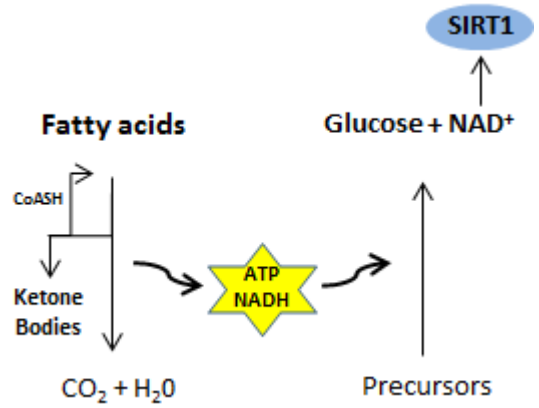

Figure I1. Role of liver FAO in generating the energy and reduction power needed to produce glucose during fasting. Energy is obtained from FAO to perform gluconeogenesis from precursors (lactate, glycerol or alanine). Complete oxidation of FA is compromised by the gluconeogenic use of oxaloacetate. Ketone body production allows the incomplete b-oxidation and liberates the Ac-CoA molecule needed for fatty acid activation. Gluconeogenesis produces NAD^+, an essential, and consumed, substrate for Sirt1 activity. Adapted from Foster and McGarry (McGarry and Foster 1995) and Vilá Brau *et al.*(Vilà-Brau et al. 2011a; Vilà-Brau et al. 2013).

In addition to this network of genes regulated by PPARα activation, another enzyme may contribute to the metabolic adaptation to fasting: SirT1 (sirtuin 1). This NAD^+-dependent protein deacetylase is a general regulator of energy homeostasis in response to nutrient availability (Nemoto, Fergusson, and Finkel 2004). Thus, the

adaptation program to fasting in liver can be divide into two temporally distinct phases: the onset of fasting (<12–18 h) and sustained fasting (>12–18 h) that are distinguishable by the NAD^+ mediated SirT1 activation (Dominy et al. 2010). The activation of SIRT1 results in the deacetylation of transcription factors and co-activators providing a mechanism to further amplify gluconeogenic gene expression in response to prolonged fasting (Altarejos and Montminy 2011).

1.2Hepatic SIRT1 activity in long Fasting and its target genes

At the onset of fasting, circulating levels of glucose fall, there is an increase the levels of glucagon and a decrease in insulin. In the first phase of fasting (<12h-18h) gluconeogenesis is upregulated in liver. The transcription of gluconeogenic enzymes is initiated by activation of cAMP response element binding protein (CREB) and its coactivator CRTC2. However, in longer periods of fasting (>12-18h) CRTC2 protein degradation is signaled by SIRT1 deacetylation (Lay et al. 2010). Therefore, the maintenance of the gluconeogenic response in prolonged fasting will be mediated by PGC1-α and its related transcription factors (Figure I2). An increase in PGC1α levels facilitates increased hepatic glucose output by promoting the expression of gluconeogenic genes such as *Pepck* and *G6Pase*(Dominy et al. 2010).

In addition to co-activators, SIRT1 mediated deacetylation can modulate the activity of several transcription factor. Thus, SIRT1 may support residual expression of the gluconeogenic program during late fasting by deacetylation and enhancing the activity of the forkhead activator FOXO1 (Y. Liu et al. 2009). Importantly, activation of PGC1α and FOXO1 also stimulate fatty acid oxidation (Napal, Marrero, and Haro 2005) and ketogenesis(Nadal, Marrero, and Haro 2002), when insulin is absent, respectively.

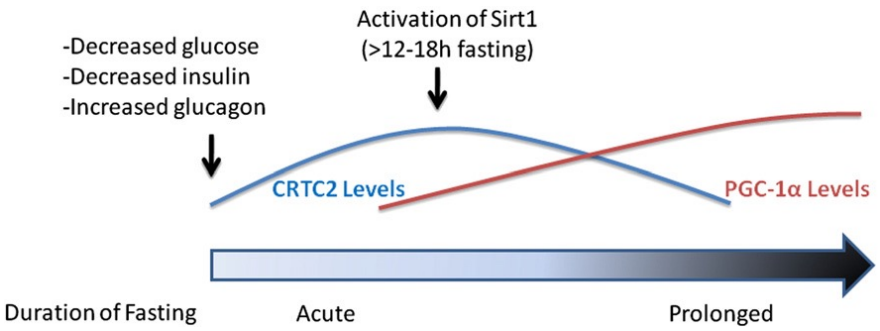

Figure I2. A proposed theory for the temporal regulation of two major transcriptional coactivators involved in hepatic gluconeogenesis during fasting. CRTC2 deacetylation facilitates ubiquitination and degradation. PGC1a deacetylation increases protein stability. Deacetylation of FOXO1 and CREBH stimulates and reduces, respectively their transcriptional activity.

1.3Role of CREBH acetylation during fasting adaptation

CREBH (CREBH: cyclic-AMP-responsive element binding protein H) is an Endoplasmic Reticulum transcription factor, which possesses similarity to SREBP as regards its localization and the activation process of its cleavage system. CREBH is involved in the regulation of several metabolic pathways, such as lipogenesis, FA and cholesterol metabolism and lipolysis, under metabolic stress conditions in order to maintain lipid homeostasis (C. Zhang et al. 2012).

During fasting CREBH expression is induced by the glucocorticoid receptor (GR)/PGC-1α complex, and the HNF4α/PGC1α complex (M. W. Lee et al. 2010). The mature form of CREBH up-regulates gluconeogenic genes such *Pepck* and *G6Pase* (M. W. Lee et al. 2010) in the livers of mice in fasted state via directly binding to CRE (cAMP responsive element). CREBH also stimulates FAO and ketogenesis in the liver of fasted animals throughout an indirect mechanism that involves FGF21, a unique member of the FGF family with hormone-like actions(Kharitonenkov, A. Shiyanova et al. 2005). CREBH directly binds to the proximal region of the *Fgf21* promoter and upregulates its expression (H. Kim et al. 2014). FGF21 is a key mediator of starvation that activates

lipolysis in white adipose tissue (WAT) and increases fatty acid oxidation and ketogenesis in the liver (Kharitonenkov, A. Shiyanova et al. 2005).

Fgf21 is also a bona fide PPARα target gene (Badman et al. 2007; Inagaki et al. 2007), although the presence of CREBH is needed for the PPARa-mediated Fgf21 induction during fasting (Danno et al. 2010). In addition, CREBH is acetylated in the liver upon fasting in a time-dependent manner and this acetylation is crucial to maintain the hepatic lipid homeostasis in a fasting state (Hyunbae Kim et al. 2015a). Therefore, a cooperative model (Figure I3) between CREBH and PPARα has been proposed to explain upregulation of *Fgf21* expression by both CREBH and PPARα (Danno et al. 2010; Hyunbae Kim et al. 2015a). In this model, upon states of fasting, cleavage of the CREBH protein occurs (see below). The cleaved activated form of CREBH will be released and moved to the nucleus, where the histone acetyltransferase PCAF mediates the acetylation of CREBH at K294. At the same time, SIRT1 modulates the acetylation phenomenon through its deacetylation activity (Figure I3). Globally, this acetylation process is essential for the interaction between CREBH and PPARa, and therefore for the activation of its target genes in fasting (Hyunbae Kim et al. 2015a).

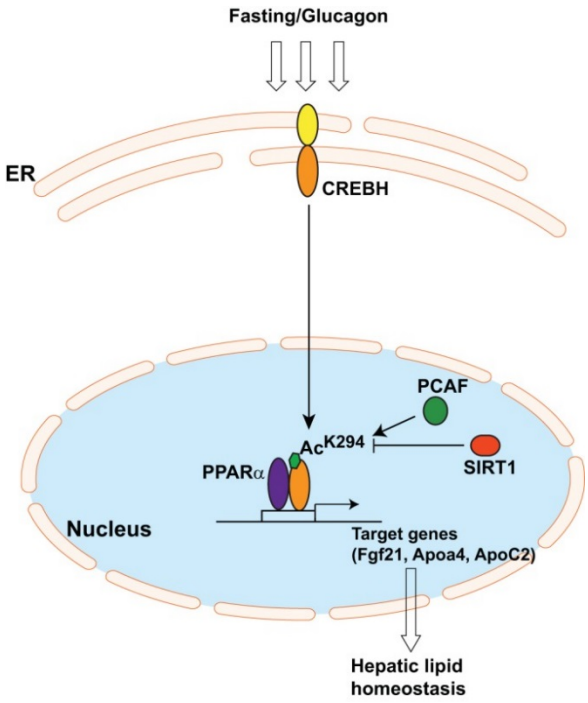

Figure I3. Model for the regulation of CREBH activity by acetylation in fasted states. Cooperative action of PPARa and nuclear form of CREBH on genes like *Fgf21*. CREBH is stimulated by PCAF-dependent acetylation (Kim *et al.* 2015).

NEFAs arriving from WAT are involved in the CREBH nuclear protein accumulation under fasting by promoting CREBH cleavage. Hence, in the fasted state, the expression of CREBH mRNA and nuclear protein are both suppressed by refeeding in the wild-type mice, but not in the ob/ob mice (Danno et al. 2010). Interestingly, animals in which WAT lipolysis has been ablated (CGI-58-ATko), and there is not a FA supply upon fasting, shown a marked defect in liver PPARa-signaling and nuclear CREBH translocation (Jaeger et al. 2015). Therefore, CREBH cleavage in the ER could be relevant to signaling the presence of this old fat (see below) in liver throughout PPARα-mediated FGF21 activation (Figure I4)

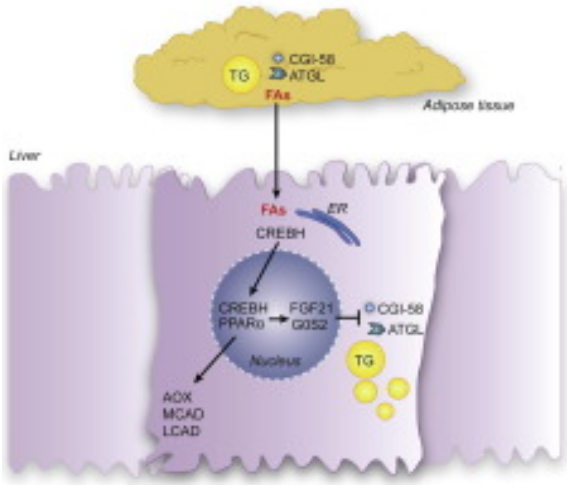

Figure I4. Proposed moldel for FA stimulation of CREBH translocation to nucleus. CGI-58, Comparative gene identification-58 (ATGL co-activactor); G0S2, G0/G1 Switch Gene 2 (ATGL inhibitor); ATGL, Adipose triglyceride lipase; AOX; Acyl-CoA oxidase; MCAD, Medium-chain acyl-CoA dehidrogenase; LCAD, Long-chain acyl-CoA deshidrogenase; ER, endoplasmic reticulum. AOX, MCAD, and LCAD are PPARa target genes. From Jaeger *et al.* 2015.

2. Peroxisome Proliferator Activated Receptors (PPARs) as Regulators of Fat Metabolism

The PPARs belong to the ligand-activated nuclear receptor family and the steroid receptor superfamily. The nuclear receptors (NR) are a family of transcription factors that can exert their effects as monomers, homodimers or heterodimers by binding to

specific sequences of DNA called Nuclear Receptors Responsive Elements (NRRE) with a repetitive consensus hexamer (AGGTCA) that is recognized by the DNA binding domain (DBD) of the NR. All of the NRs share a common structure, a NH2 terminal region (A/B), a conserved DBD (region C) that includes two ZN fingers, a linker region (D) responsible for nuclear localization, and finally a well conserved carboxy-terminal ligand-binding domain, the LBD, or region E. Some of the NR may possess an extra F domain, with unknown functions so far, a highly variable carboxy-terminal tail (Feige et al., n.d.; Sever and Glass 2013).

PPARs regulate the expression of genes involved in a variety of processes, concerning the metabolic homeostasis by controlling the metabolism of glucose and lipids, (Monsalve et al. 2013). For the PPAR-mediated transcriptional activation of its target genes it is necessary the heterodimerization of a PPAR with RXR, and the binding of the heterodimer to a PPRE sequence, producing a change in chromatin structure indicated by ligand activation of the complex and histone H1 release. The binding of the ligand triggers a conformational change that will generate new specific contacts with coactivators (Desvergne, Michalik, and Wahli 2006). Like PPARs are controlling lipid homeostasis (lipid synthesis and oxidation) and are activated by lipids (or a closely related derivate) that are acting as ligands (see below), necessarily the mechanism of activation by lipids may be far baroque than the description presented here.

2.1PPAR isotypes and metabolic integration

Despite their different tissue distribution, this subfamily of nuclear receptors function in an integrated network to regulate metabolism (Evans 2004). The PPARs function as lipid sensors, in a way that can be activated by both dietary fatty acids and their derivatives in the body and consequently redirect metabolism.

The alpha isoform of the PPARs (PPARα) has a crucial role in FAO and therefore is found mainly in highly oxidative tissues, its mRNA is expressed in liver, and at a lesser extent in heart, kidneys, skeletal muscle and BAT. PPARa is shown to have a crucial role in the adaptive response to fasting by regulating genes involved in FAO (Napal, Marrero, and Haro 2005; Rodríguez et al. 1994), therefore having consequent indirect effects on other metabolic pathways and energy homeostasis(Kersten et al. 1999; Desvergne, Michalik, and Wahli 2006; Evans 2004).

PPARψ is highly enriched in both BAT and WAT. It is induced during adipocyte differentiation and it is thought to be an important regulator of fat cells(Lazar 2002; Tsai, Y.S., and Maeda 2005). This member of the PPARs is a master effector of adipogenesis in a transcriptional cascade involving C/EBP (Z. Wu et al. 1999) and has an important role in the regulation of glucose and lipid metabolism. It also participates in the regulation of cardiovascular disease, inflammation, organ development and tumor formation (J. H. Kim, Song, and Park 2015). According to its functions, PPARψ-adipose KO mice are protected from HFD-induced obesity and insulin resistance(Jones et al. 2005) and in humans, a dominant negative mutation in a single allele of PPARG (encoding for PPARψ) leads to insulin resistance and lipodystrophy phenotype. Finally, this transcription factor is of great clinical importance, since it is the molecular target for the thiazolidinedione (TZD). TZDs are a class of antidiabetic agents, which improve peripheral insulin sensitivity and assist in glycemic control in type 2 diabetic patients (Lehmann et al. 1995).

The third member of this family, PPARδ, has been the more elusive one. It expression is quite ubiquitous and originally its functions were center on fatty acid catabolism and energy homeostasis (Evans 2004). It is considered an important metabolic regulator in different tissues, such as adipose tissue, skeletal muscle and heart (Barish, Narkar, and Evans 2006).

The transcriptional activation of PPARδ enhances fatty acid catabolism and energy uncoupling, decreasing TG stores, improving endurance performance and enhancing

cardiac contractility. Its receptor activation decreases macrophage inflammatory responses and modulates lipoprotein metabolism to lower TG and on the other hand, to raise HDL cholesterol. In liver, the activation of this transcription factor ameliorates glucose homeostasis, by repressing hepatic glucose output (Barish, Narkar, and Evans 2006).

In muscle it is attributed a fundamental role in the regulation of mitochondrial fatty acid oxidation. Thus, overexpression of PPARδ in muscle increases the oxidative capacity in a very marked way. In fact, mice that express large amounts of PPARd in muscle (marathon mice) can run for hours without stopping (Y. X. Wang et al. 2004)(Y. X. Wang et al. 2004).

However, in liver, PPARδ plays a lipogenic role as indicated by overexpression (adenovirus) experiments(S. Liu et al. 2011) or knockout animal models(Barish, Narkar, and Evans 2006). Recently, it has been shown that PPARδ controls diurnal expression of lipogenic genes in the dark/feeding cycle (S. Liu et al. 2013). Surprising, liver-specific PPARδ activation increases, whereas hepatocyte PPARδ deletion reduces, muscle fatty acid uptake(S. Liu et al. 2013) (see below).

2.2New Fat are the PPARα endogenous ligands

As mentioned, PPARα-null mice develop a phenotype characterized by hypoglycemia, hyperlipidemia, hypoketonemia, and fatty liver due to its inability to meet the energy demands in a fasting state (Kersten et al. 1999). The FASKOL mice lack the capacity of synthetizing fatty acid from carbohydrate, by the deletion of fatty acid synthase (FASN). This animal when either fed with a fat free diet or exposed to prolonged fasting showed the same hypoglycemic phenotype than PPARα-null mice, with decreased expression of PPARα target genes. FASKOL mice also developed a cholesterol phenotype, not dependent on diet. Both the hypoglycemia/steatohepatitis

and the cholesterol phenotypes were reversed by administration of a PPARα agonist such as WY14643 (Chakravarthy et al. 2005). Since the *"new fat"* is the fat that comes from diet or from *de novo* synthesis via FASN, this experiment led to the concept that only *"new fat"* is capable of activating PPARa and promoting gluconeogenesis and FAO. By contrast, the *"old fat",* the fat mobilized from peripheral fat stores and transported to the liver where it accumulates, fails to activate PPARα (see Figure I5).

Later, by immunoprecipitation of PPARα, an endogenous ligand with nanomolar affinity was described for PPARa activation: that the 1-palmitoyl-2-oleoyl-sn-glycerol-3-phosphocholine (16:0/18:1 PC) (Chakravarthy et al. 2010).

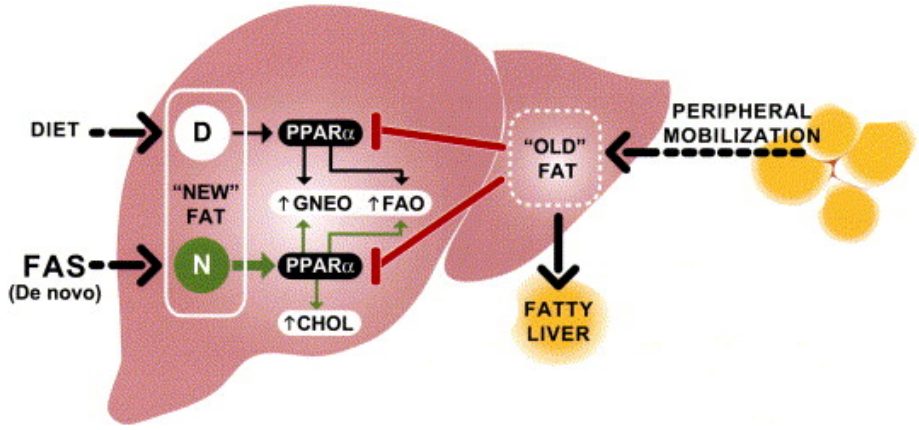

Figure I5. "Proposed model for differential effects of hepatic lipid. Fat absorbed from the diet or synthesized de novo via FAS in the liver constitutes "new" fat, capable of activating PPARα to ensure normal glucose and lipid homeostasis. Fat derived from peripheral mobilization of adipose stores constitutes a different hepatic compartment ("old" fat) that does not appear to activate PPARα as effectively as new fat, leading to fatty liver. In contrast to de novo synthesized fat, dietary fat is inadequate for the maintenance of cholesterol homeostasis, suggesting different PPARα pools" (Chakravarthy et al. 2005).

Hence, PPARα is activated by specific fatty-acid pools synthesized by hepatic FASN or derived from diet, but not from peripheral FA and this leads to an important paradox, since PPARα target genes are expressed in fasting situations, when PPARα itself should not be active (see Discussion Section).

2.3PPARδ can generate the PPARa endogenous ligands

PPARδ overexpression (adenoviral-mediated PPARδ) up-regulates glucose utilization and *de novo* lipogenesis pathways (S. Liu et al. 2011). Liver-specific PPARδ activation increases, whereas hepatocyte-PPARδ deletion reduces, muscle fatty acid uptake (S. Liu et al. 2013). Therefore, apparently a PPARd dependent signal couples liver lipid metabolism to muscle FAO (S. Liu et al. 2013).

Profiling of lipid metabolites of samples from wild type and LPPARDKO mice revealed that the main differences in serum occurred during the dark cycle, when PPARδ controlled lipogenesis is active. Nonetheless, daytime feeding led to serious differences in serum lipidomes of the two genotypes, showing that LPARDKO mice were unable to adjust their lipogenic gene expression program.

Acetyl-CoA carboxylase (*Acc1*), rate-limiting enzyme in *de novo* lipogenesis, is induced by PPARd overexpression (adPPARδ). While transitory *Acc1* knockdown (LACC1KD) mice shows: i) reduced hepatic TAG, ii) increased serum TAG, and iii) decrease FFA uptake in isolated soleus muscle. Muscle FA uptake decreased in LACC1KD mice in the dark/feeding cycle, when the lipogenic program is active and additionally there was a slower clearance of circulating [3H] oleic acid. Thus, *de novo* lipogenesis is linked to muscle FA use(S. Liu et al. 2013).

Unbiased metabolite profiling identifies 1-stearoyl-2-oleoyl-sn-glycero-3-phosphocholine (PC 18:1/18:0) as a serum lipid regulated by diurnal hepatic PPARδ activity. PC (18:0/18:1) reduces postprandial lipid levels and increases fatty acid use through muscle PPARα. Put together, this links the hepatic PPARδ-controlled lipogenic program to serum lipid concentrations and muscle fat use.

PPARδ expression peaks at night, parallel to the mRNA levels of the molecular clock Bmal1 in the liver. Therefore, it is feasible that hepatic PPARδ alter the expression of muscle genes and FA use through PC (18:0/18:1), indicating that a hepatic PPARδ-PC (18:0/18:1)-muscle PPARα signaling cascade coordinates fat synthesis and use. That PPARα ligands are products of the de novo synthesis of FA illustrates a link between

hepatic lipogenesis and peripheral FAO. This link can explain how tissues like muscle oxidize fatty acids, depending on circadian hepatic synthesis, at specific times coinciding to the animal activity.

3. Fat-Specific protein FSP27/CIDEC

The production of endogenous ligand of PPARa requires an esterification and re-hydrolysis cycle (Ong et al. 2011), suggesting that lipid droplet (LD) formation during the fed-to-fasting transition could be necessary for PPARSYMBOL
activation. In vivo attenuation of liver ketogenesis (siRNA) downregulate FAO and *Fgf21* expression (Vilà-Brau et al. 2011a). In this model, mRNA analysis indicates that *Fsp27* is one of the genes induced by liver knock down of *Hmgcs2* (Vilà-Brau et al. 2013). *Fsp27* (CIDEC in humans) is a lipid droplet (LD) formation protein and call our attention since was induce during starvation in liver(Vilà-Brau et al. 2013).

The CIDE family of proteins comprises three distinct isotypes; CIDEA, CIDEB and CIDEC (FSP27 in mice) that were first identified by their sequence homology with the N terminal domain of the DNA fragmentation factor (DFF) and described as apoptosis activators. When transfected in adherent cells, they induce morphological changes, nuclear condensation and fragmentation, key characteristics of apoptosis (Inohara et al. 1998). The CIDE proteins are essentially lipid droplet-associated proteins and important regulators of lipid storage and formation of lipid droplets in adipocytes and hepatocytes but their roles seem to be more complex and intricate in the regulation of lipid metabolism and be crucially involved in metabolic disorders, such as obesity, diabetes mellitus, liver steatosis and cardiovascular diseases (Gong, Sun, and Li 2009). The proteins isotypes are expressed differently throughout the tissues. CIDEB is expressed mainly in liver, and in smaller amounts in kidney, small intestine and colon

(C. Wu et al. 2008). By contrast, CIDEA and CIDEC are mainly expressed in the adipose tissue, regulating the formation of lipid droplets in white and brown adipocytes (C. Wu et al. 2008). Additionally, CIDEA is expressed in the mammary glands of lactating or pregnant mice, possibly acting as a transcription coactivator with C/EBP to control the expression of several downstream targets (W. Wang et al. 2012). Finally, CIDEC (Fsp27) was also found to be expressed in the steatotic and fasted liver(Vilà-Brau et al. 2013; Matsusue et al. 2008).

3.1Fat-specific protein 27/CIDEC isoforms and tissue-specific distribution

Fat-specific protein 27 (*Fsp27*) was originally identified from mouse adipocyte TA cell lines as a mature adipocyte-specific gene (Danesch, Hoeck, and Ringold 1992). It is an important regulator of metabolic homeostasis and it is involved in the regulation of FAO (Matsusue et al. 2008). Nowadays there are two isoforms of FSP27 described: alpha and beta. FSP27α (CIDEC1 in humans) is mainly expressed in WAT, while FSP27β (CIDEC2) is expressed in steatotic and fasted livers but it also is the predominant isoform in brown adipose tissue (BAT). Concretely, *Fsp27*β is highly expressed in the livers of *ob/ob* and fasted mice while in WAT the predominant isoform is *Fsp27*α*,* both in wild-type and *ob/ob* mice (Xu et al. 2015). Despite the specific tissue distribution between isoforms, a deficiency in these proteins leads to the same lean phenotype; resistance to HFD induced obesity, improved insulin sensitivity and an increased whole body metabolic rate (L. Z. Wu et al. 2014; Zhou et al. 2003).

The presence of two isoforms was described through the characterization of CREBH knockout mice in which *Fsp27* expression fails (J. H. Lee et al. 2011), contrary to other CIDE family of lipid droplet proteins such as CIDEB, or Plin1, which expression remains unaltered(Xu et al. 2015).

In the case of *Fsp27*, although its mRNA was induced by CREBH there was no activation of a luciferase reporter containing an *Fsp27* promoter fragment extending from -994bp to +23bp from the transcription start site. 5' RACE experiments, using a complementary primer located in exon 3, yielded two different PCR products from the liver (Figure I6). This data led to the identification of an alternative promoter between exon 1 and exon 2, which would drive the transcription of an alternative *Fsp27* mRNA (*Fsp27β*). The PCR amplification generated a single product in mRNA from WAT (the α isoform). In WAT transcription started in exon 1a, although the transcription-starting site was 4 bps downstream of the previously determined start site. In liver, the expressed mRNA starts in an alternative exon 1b (Xu et al. 2015).

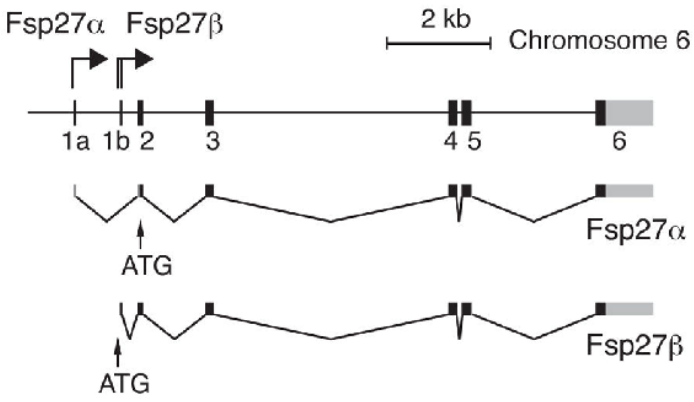

Figure I6. Identification and characterization of alternative promoters for Fsp27 transcription. Schematic representation of the mouse Fsp27 gene. Boxes denote exons. Dark and shaded boxes represent protein-coding and untranslated regions, respectively. Arrows indicate transcription start sites (Xu et al. 2015).

Both isoforms share the same open reading frame. However, FSP27β is predicted to contain 10 additional amino acids at the N-terminus, which allows for a better stability (Xu et al. 2015) and gives different characteristic as a lipid droplet formation protein (see below). The characterization of the two transcriptions start site can explain how liver *Fsp27* (*Fsp27β)* could be pharmacologically induced by PPARα ligands in liver (Langhi and Baldán 2014), despite its induction is not affected in starved PPARα KO mice (Langhi and Baldán 2014), since we know that CREBH is induce by PPARα activation (Danno et al. 2010).

In summary *Fsp27α* promoter is regulated by C/EBP(Danesch, Hoeck, and Ringold 1992), CREB (Vilà-Brau et al. 2013) and PPARγ (Matsusue et al. 2008) in WAT; while *Fsp27β* is mainly regulated by CREBH in liver (Xu et al. 2015).

Most of the data regarding *Fsp27* expression was obtained before knowing the existence of both isoforms. However, the strong tissue specific expression of both isoform: *Fsp27β* in liver, BAT and intestine, and *Fsp27β* in WAT makes possible to assume old data in the new context, and this assumption has been corroborated in this Thesis. The knowledge about the isoform existence was later used to design a strategy to obtain *Fsp27* tissue specific knock-out (see discussion).

3.2FSP27α and β function

LDs are dynamic organelles, constantly forming, growing or shrinking. They are mostly formed in the endoplasmic reticulum (ER), where enzymes catalyzing neutral lipid synthesis (*e.g.,* acyl-CoA cholesterol acyltransferases (ACATs) for sterol esters and acyl CoA: diacylglycerol acyltransferases (DGATs) for TGs) predominantly reside (Natalie Krahmer, Farese, and Walther 2013). In fatty acid excess conditions, LDs rapidly increase their volumes, as seen for example in cell culture or murine small intestine. During LD growth, the synthesis of neutral lipids and phospholipids is coordinated: as LD volume increases, surfaces expand, and phospholipids are needed to shield the neutral lipid core, reduce surface tension, and prevent LD collapse (N. Krahmer et al. 2011). Thus, changes in LD phospholipid composition are important in determining their morphology and may play a role in diseases with altered lipid storage.

Originally, FSP27 was thought to be uniquely involved in the formation of unilocular lipid droplets in WAT during adipogenesis, as its expression was highly increased during this process (Puri et al. 2007; Nishino et al. 2008). Both alpha and beta isoforms of FSP27 are localized around the LDs, and therefore were thought to promote the

formation of large LDs, and suppress lipolysis. However, they differ in the first 10 amino acids residues and shown tissue-specific distribution; therefore, it was expect that they might vary in their specific functions.

The LD size is variable and their growth is thought to occur by two different mechanisms: the first one is the growth of LD itself (as mentioned before), the second one is by fusion of the already existence LDs. In this context, full length FSP27 seems not to be necessary for the formation of large LDs (Tamori et al. 2016), since LD expansion depends on the carboxy-terminal domain of FSP27 (amino acids 131-239). However, the amino-terminal domain of FSP27 are relevant for the size of the formed lipid droplet (Nishimoto et al. 2017).

As shown in Figure I7, FSP27 isoform expression can regulate lipid droplet size. That is an important issue since it can determine the fate of the accumulated fatty acids. In WAT, FSP27α expression will promote big unilocular lipid droplets that are ideal for efficient lipid storage because lipolysis, from the LD surface, is restricted due to the minimum LD surface area. In BAT, FSP27β expression will promote small multilocular LD formation, that is ideal for efficient intracellular lipolysis from the LD surface and the subsequent facilitation of FFA transport to mitochondria that are adjacent to LDs for β-oxidation in BAT(Nishimoto et al. 2017; Nishimoto and Tamori 2017).

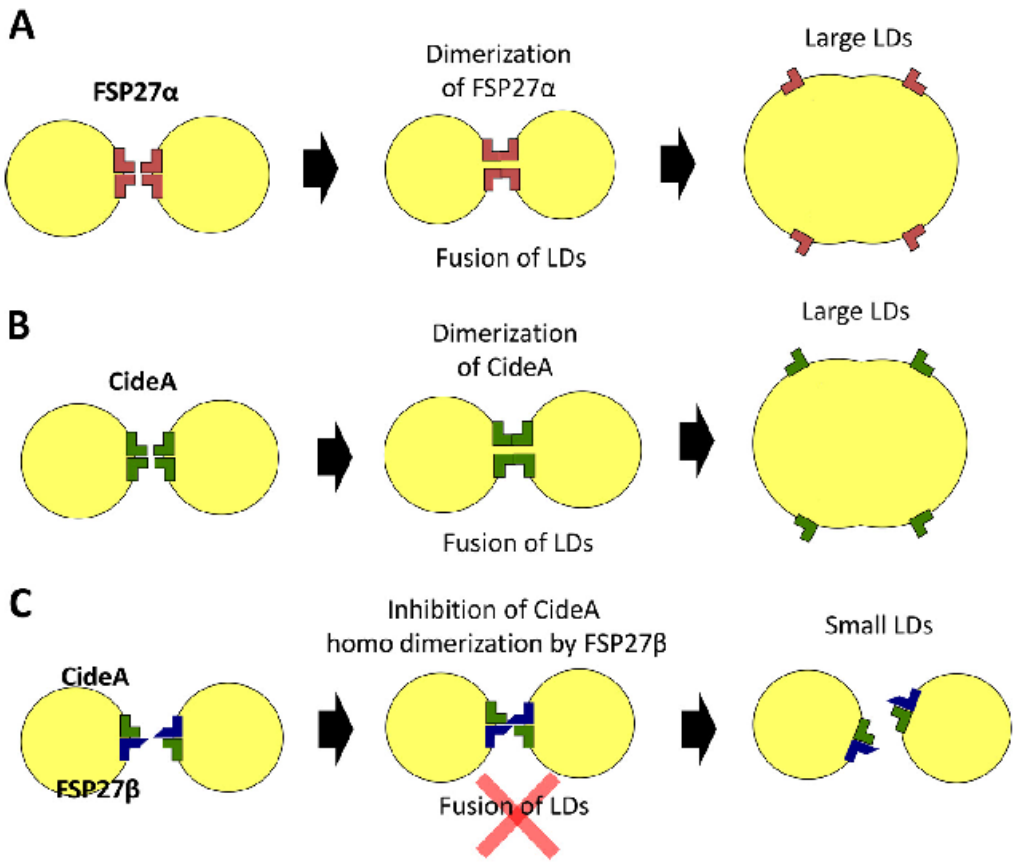

Figure I7. Proposed mechanisms by which the Cide protein family regulates LD sizes in WAT and BAT. In WAT, FSP27a on neighboring LD induces homo dimerization, resulting in the fusion of LD, subsequent lipid exchange, and formation of larger LD (A). CideA also mediates the formation of large LD in the same manner (B). In BAT, FSP27b inhibits the homo dimerization of CideA and suppresses the formation of large LD (C).

In concordance with this working model, FSP27β is the isoform expressed in liver, were FAO has to occur to push gluconeogenic process. However, the role of FSP27β could be more sophisticated, since *Fsp27β* expression is first up regulated in early fasting, and then down regulated during late fasting. Since CREBH, until now, is the only factor known to regulate *Fsp27β* expression, and CREBH is induce in both early and late fasting (see results), the mechanism controlling *Fsp27β* expression during fasting still elusive at this moment.

4. REV-ERBα and HNF6 in lipid metabolism

Rev-Erbα is a nuclear receptor that participates in the clock circuitry and regulates lipid metabolism, adipogenesis and vascular inflammation (Duez and Staels 2008). It was considered an "orphan receptor" due to its lack of known ligands, until the porphyrin heme was demonstrated to function as a ligand for both **REV-ERBα** and **REV-ERBβ** (Duez and Staels 2008; Burris 2008).

REV-ERBα and REV-ERBβ lack the activation function-2 region, associated with the ability of nuclear hormone receptors to recruit co-activators and are considered as constitutive repressors of transcription.

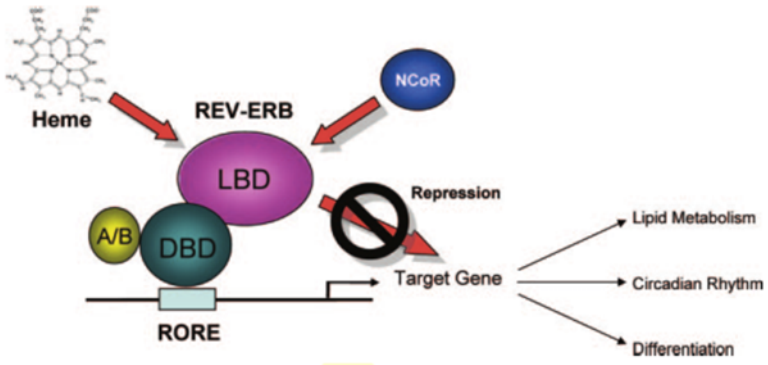

Figure I8. Proposed model for REV-ERB as a repressor of transcription.(Burris 2008)

The ligand heme modulates the activity of REV-ERB nuclear receptors, by binding directly to the ligand binding domain (LBD) of REV-ERB and increasing its affinity for the corepressor NCoR (Figure I8). This complex will lead to gene repression due to histone deacetylase activity from the nuclear receptor co-repressor (NCoR)/histone deacetylase complex (Burris 2008).

Modulation of clock and metabolism by Rev-Erbα is accomplished through different pathways. To regulate clock control genes, it binds directly to the genome at its cognate sites competing with activating ROR transcription factors; on the other hand, to regulate metabolic genes it works by recruiting the histone deacetylase 3 (HDAC3) through NCoR so its transcriptional repression effects are mediated through its interactions with DNA-bound factors (Y. Zhang et al. 2015) Deletion of HDAC3 or REV-ERBa in mouse liver causes hepatic steatosis (Burstein et al. 2013).

More recently, it was described that REV-ERB⟨ works cooperatively with the transcription factor HNF6 to regulate hepatic lipid metabolism. The mechanisms of action involve the HNF6 tethering of REV-ERBa to repress lipid metabolic genes, such as *Lp1*, *Scd1*, *Acacb*, *Cd36* and *Fasn*, that are up-regulated in the HNF6 knockout and the direct activation of other hepatic genes by HNF6 (Y. Zhang et al. 2016b).

Thus, HNF6 regulates hepatic lipid metabolism in adult livers through a mechanism that involves the HNF6-dependent tethering of REV-ERBα. Together they repress a variety of lipid metabolic genes that were shown to be up-regulated in the HNF6 knockout. HNF6 can also activate directly another set of hepatic genes.

As for REV-ERBα, besides working cooperatively with HNF6, it has independent effects on hepatic lipid metabolism through tethering factors and on the regulation of the liver circadian clock, as seen in figure I 6 (Y. Zhang et al. 2016b).

Materials and Methods

1. Cell Culture

The **AML12** (*alpha mouse liver 12*) cell line was established from hepatocytes from a mouse (CD1 strain, line MT42) transgenic for human TGF alpha and it exhibits typical hepatocyte features such as peroxisomes and bile canicular like structure.
These cells were a kind gift from Dra. M. Martinez Chantar.
The cells were cultured in a 1:1 mixture of Dulbecco's Modified Eagle Medium and Ham's F12 medium(DMEM:F12, supplemented with 0,005 mg/ml insulin, 0,005 mg/ml transferrin, 5 ng/ml selenium, 40 ng/ml dexamethasone, 4 mM glutamine, 100 units/ml penicillin G, 100ug/ml streptomycin, and heat-inactivated 10% (v/v) Fetal Bovine Serum (FBS).

The **HepG2 (***human liver carcinoma*) cell line was derived from the liver tissue of a fifteen years old male with differentiated hepatocellular carcinoma. These cells are adherent, epithelial-like, growing as monolayers and in small aggregates.
The cells were cultured in Eagle's Minimum Essential Medium (MEM) supplemented with 4 mM glutamine, 100 units/ml penicillin G, 100ug/ml streptomycin, and 10% (v/v) Fetal Bovine Serum (FBS).

The **HEK-293A** cell line is a subclone of the **HEK-293** *(human embryonic kidney)* cell line. Its relatively flat morphology facilitates the initial production, amplification and tittering of replication- incompetent adenovirus. This cell line contains a stably integrated copy of E1 gene that supplies the E1a and E1b proteins that are necessary to generate adenoviruses.
The cells were cultured in Dulbecco's Modified Eagle Medium (DMEM), supplemented with 4 mM glutamine, 100 units/ml penicillin G, 100ug/ml streptomycin, and 10% (v/v) Fetal Bovine Serum (FBS).

The cells were incubated at 37^{o}C in a humidified atmosphere containing 5% CO2. Culture medium was discarded and changed each 2 to 3 days. To pass the cells, the plates were rinsed twice with 1x PBS and a 0,05% Trypsin-EDTA solution was added. Once the cell layer was dispersed (from 2 to 5 minutes at 37oC depending on the cell line), the trypsin solution was deactivated by adding complete growth medium.
The cells were either split in a 1:3 dilution every 3 days or counted and plated for the experiments.

1.1Reagents used in Cell Culture

1.1.1 Cell culture maintenance

Dulbecco's Modified Eagle Medium and Ham's F12 Medium (DMEM:F12) – GIBCO 11320074

Minimum Essential Medium (MEM) – GIBCO 61100-087

Dulbecco's Modified Eagle Medium (DMEM)– GIBCO 12100-061

Fetal Bovine Serum (FBS) – GIBCO 10270-106

Penicillin Streptomycin (Pen Strep) – GIBCO 15140-122

Sodium Bicarbonate solution 7,5% - Sigma Aldrich S8761

L-Glutamine 200 mM – GIBCO 25030-024

Insulin-Trasnferrin-Sodium Selenite Supplement- GIBCO 11074547001

Dexamethasone – Sigma-Aldrich D2915

Tripsin-EDTA 10X – GIBCO 15400-054

1.1.2 Cell Culture Transfection

OPTI-MEM® I Reduced serum media – GIBCO 31985-047

Lipofectamine LTX Reagent – Invitrogen 15338-100

PLUS Reagent– Invitrogen 11514015

1.1.3 Cell Culture Treatments

WY14643 *(Sigma, C7081)* – Selective PPARα agonist, dissolved in DMSO to 10 mM.

Hemin*(Sigma- Aldrich, H9039)***–** Natural ligand of Reverbα. Small molecule present either free or bound to hemoglobin in the bloodstream of mammals. Dissolved in 1.4M NaOH to 30 mM.

2. DNA oligonucleotides

All of the DNA oligonucleotides mentioned in this chapter were synthesized by *Sigma-Aldrich*, with technology ultra-high base coupling efficiency, combined with optimized cartridge purification and 100% quality control by mass spectrometry.

3. Vectors

3.1Cloning vectors

The ampicillin resistant **pGEM®-T** vector (Promega A36000) is linearized by digestion with the restriction enzyme *EcoRV*, and has additional 3' terminal thymidine at both ends. These 3'-T overhangs facilitate the insertion of the PCR products with A overhangs synthesized by the *Taq* polymerase.
The vector contains the Sp6 and T7 RNA promoters, that flank the multiple cloning site with several restriction sites.

The insertion of the PCR products within the polylinker disrupts the codifying region of the *lacZ* gene and the β-galactosidade activity. In a medium supplemented with ampicillin (100mg/L), IPTG (8 mg/L) and X-Gal (40 mg/L), the recombinant colonies

will be white, due to the impossibility to hydrolyse the X-gal substrate, while the colonies that incorporated the empty vector will be blue, due to the presence of the products of the X-gal hydrolysis.

3.2Eukaryotic Expression Vectors

The **pcDNA3** vector is a mammalian expression vector with the CMV promoter and a neomycin resistance marker.

3.3Reporter vectors

The reporter vectors are used in the transitory transfection of eukaryotic cells. After transfection, the enzymatic activity can be measured by chemiluminescence.

The **pGL3Basic** (Promega E1751) is ampicillin resistant and has a multiple cloning site upstream of the LUC gene. It does not have a eukaryotic promoter, or *enhancer* sequences; therefore the activity of the luciferase enzyme in the transfected cells is dependent on the activity of the inserted promoter, object of study.

The **pRL-CMV** (Promega E2261) vector is a wild-type Renilla luciferase (Rluc) control reporter vector.
It is used as a control of the efficiency of mammal cells transfection.

4. Plasmid Constructs

All of the constructs were generated by PCR from mouse genomic DNA from C57BL/6, using Taq Polymerase (Biotools) and sequence specific primers (table 1) introducing restriction sites.

The correspondent PCR products were cloned in the pGEM-T vector (Promega) and sequenced.

The plasmids were digested with the corresponding restriction enzymes and subcloned into pGL3b vector (Promega) or pCDNA3 vector.

The sequences and orientations of the constructions were verified by sequencing (Macrogen sequencing service).

The Fsp27β promoter (*-900, +76, relative to +1*β) was amplified by PCR from mouse genomic DNA using sequence specific oligonucleotides (table 1) and cloned into the pGL3-basic vector (*Promega*), using the restriction sites *Xho* and *MluI*.

The Fsp27 promoter including both α and β isoforms (Fsp27αβ- pGl3b) *(-2024 to +1013, relative to +1*α*),* was amplified by PCR from mouse genomic DNA using sequence specific nulceotides (table 1) and cloned into the pGL3-basic vector (Promega) using the restriction sites *XhoI* and *MluI*.

The Fsp27β promoter was also cloned including different deletions, amplified by PCR from mouse genomic DNA using sequence specific nucleotides for each deletion (table 1) and cloned into the pGL3basic vector using the restriction sites *XhoI* and *MluI* :

The first deletion of the Fp27β promoter (Fsp27β1-pGL3b) comprised 660 nucleotides *(-548,+76, relative to +1*β);

The second deletion of the Fp27β promoter (Fsp27β2-pGL3b) comprised 376 nucleotides *(-300,+76, relative to +1*β);

The third deletion of the Fp27β promoter (Fsp27β3-pGL3b) comprised 166 nucleotides *(-90,+76, relative to +1*β).

Fsp27α cDNA was amplified by PCR from mouse cDNA using sequence specific oligonucleotides (Table 1) and cloned from the translation initiation site ATG to the stop codon TGA into pcDNA3 expression vector, using the restriction sites *HindIII* and *EcorI.*

Crebh-nuclear cDNA was amplified by PCR from human cDNA using sequence specific oligonucleotides (Table 1) and cloned from the translation site ATG to the stop codon TGA into pcDNA3 expression vector, using the restriction sites *XbaI* and *EcorI*.

Table 1. Primers for PCR amplification.

	Primers Forward (5'-3')	**Primers Reverse**
Fsp27b-pGL3b	*TTAACGCGTAGGAGCTGGGGTATATGGCT*	*TTACTCGAGTGTTTCTCCGACCCAAGCTG*
Fsp27ab-pGL3b	*TTAACGCGTCTGCAACTCATTCTGTAGCCC*	*TTACTCGAGTGTTTCTCCGACCCAAGCTG*
Fsp27a- pcDNA3	*AAGCTTTGACAAGGATGGACTACGCC*	*GAATTCACTCGGGTCTTCATTGCAGC*
Crebh-N-pcDNA3	*TTGAATTCCATCTGCAGACAGAACTGGATGG AC*	*AATCTAGATCATGTCTGGGCTGACTTGCTGGTGGAC*
Fsp27b1-pGL3b	*TTAACGCGTGTCCTTCTGCCAGTTATTGG*	*TTACTCGAGTGTTTCTCCGACCCAAGCTG*
Fsp27b2-pGL3b	*TTAACGCGTTAGAAGTGCAGAGTCAGCTC*	*TTACTCGAGTGTTTCTCCGACCCAAGCTG*
Fsp27b3-pGL3b	*TTAACGCGTTGACTTTCAGGTCCCTCACA*	*TTACTCGAGTGTTTCTCCGACCCAAGCTG*

Mouse PPARα expression vector (PPARα-pSG5) was a gift from Dr. S. Green, Maclesfield.

The thymidine kinase promoter under the control of three PPRE elements ((PPRE)3-Tkluc) was a gift from Dr. F.Villaroya.

Human RevErbα expression vector (pSG5-hRevErba) and human RORa1 expression vector (pSG5-RORa1) and was a gift from Dr. J.C. Rodríguez.

The putative acetylation site of human CREBH, Lys294, was target of site-directed mutations. Two different mutations were introduced, the K294R mutation, where AAG changed to AGG, or K294Q, where AAG changed to CAG. The site directed mutagenesis was achieved by using as template human CREBH expression plasmid and the primers described in table 2, using the Q5 Site-directed Mutagenesis kit *(BioLabs)* following the manufacturer's instructions.

Mutants	Forward Primers (5'-3')	Reverse Primers(5'-3')
K294Q	GCATCTCGAGcagCAAAACCTGTC	AAGACTTTCCTCTGTAACTCC
K294R	GCATCTCGAGaggCAAAACCTGT	AAGACTTTCCTCTGTAACTCC

Table 2. Primers used for the site-directed mutagenesis of human CREBH

5. Transient transfection and Luciferase assay

Aml12 cells were seeded at a density of $4x10^4$ cells/well and HepG2 cells were seeded at a density of $6x10^4$ cells/well, in 24-well plates and transfected using Lipofectamine LTX and Plus reagent (*Invitrogen*), following the manufacturer's instructions. The cells were co-transfected with 400 ng of the reporter gene construct (Fsp27β-pGl3b or (PPRE)3-TK-Luc) and between 150 to 200 ng of the eukaryotic expression vector (pcDNA3, CREBH-N, K294Q, K294R, Fsp27α, PPARα, RevErbα, Sirt1,FoxA2, FoxO3a). 10 ng of the plasmid pRL-CMV were used as an internal transfection control.

The total amount of transfected DNA was kept constant amongst experimental groups by addition of empty pcDNA3 plasmid.

48h following transfection, cellular extracts were prepared for analysis of luciferase activity, by washing the cells with cold PBS and harvesting them in 100 ul of 1x Passive lysis buffer (*Promega*). A 10 ul aliquot of the the lysates were collected and used for Firefly luciferase assays, using the dual luciferase reporter assay system (*Promega*).

Relative luciferase activity was given as the ration of relative luciferase unit/relative Renilla unit.

6. Recombinant adenovirus generation

The adenovirus encoding a shRNA against Fsp27 was generated and kindly supplied by Dr. Ángel Baldán.

The adenovirus enconding a ShRNA control was purchased from Vector Biolabs (#1122), and contains a scramble RNA sequence under the control of the U6 promoter with the GFP co-expression under CMV promoter.

6.1Reagents and solutions for adenovirus generation

DMEM 10% FBS

Phosphate buffer solution

CsCl solution (filter sterilized/ - 10mM TrisHCl pH8 ; 0,51g CsCl/mL

Adenovirus storage buffer 2x (filter sterilized) – 10mM Tris pH8; 10 mM NaCl; 0,1% BSA;50% glycerol

Dialysis solution pH8– TBS/ 30% glycerol (filter sterilized)

137 mM NaCl; 20 mM Tris Base;30% glycerol (v/v)

6.2Adenovirus amplification

For the adenoviruses amplification, HEK-293A cells were plated at $10x10^6$ cells/flask ($75cm^2$) with a final volume of 15 mL of DMEM 10% FBS.

The plated cells were infected from 6 to 15 hours with a viral dosis of 10 *pfu* (plaque forming unit) per cell ($10x10^7$) per flask.

After the first 24 hours, the cells start to show morphological changes, starting to round up and detach. The cells are recovered between 24 and 48 hours after infection.

The recovered cells are centrifuged for 10 minutes, at 4^{o}C and 1500 rpm, and the pellet is ressuspended in a final volume of 8 mL of PBS.

To cells were then lysed through 4 cycles of freezing, with a mix of dry ice and ethanol, and defrosting, in a 37oC bath.

After the lysis, the cells are centrifuged for 15 minutes, at 4^{o}C and 5000 rpm, and the resulting supernatant is recovered to a 15mL corning and stored at -80^{o}C.

6.3Adenovirus purification

For *in vivo* use, the amplified adenoviruses must be purified.

CsCl was added to the amplified adenoviruses to a final density of 1,34g/mL and the mix was transfered to quickseal polyallomer tubes *(Beckman 342413)* with the aid of a syringe. The tubes were filled to the top with an already prepared and sterilized solution with the corrected density of 1,34g/ml.

Both tubes were carefully sealed and centrifuged overnight at a temperature of 22^{o}C, with a Beckam NVT 65 rotor, at 6300 rpm. The centrifuge was set with no brakes.

After centrifugation, the tube containing the adenovirus was carefully punctured and the opaque viral band was recovered with a 3 mL syringe set with an 18 gauge needle, and transferred to new quickseal polyallomer tubes, filled with the CsCl solution and centrifuged at a temperature of 22oC for 5 hours, at 6300 rpm. The centrifuge was set with no brakes.

After centrifugation the adenoviral band was recovered from each tube with a 1 mL syringe set with a 21 gauge needle and transferred into a Slide-A-lyzer dialysis cassette (*Pierce #66370*), adding an equivalent volume of adenovirus storage buffer 2x.

The solution was dialyzed overnight in TBS 30% glycerol, agitating and at 4oC.

Recover the next day and store at -80oC.

6.4Adenovirus tittering

To quantify the viral stock, HEK-293A cells were plated with a density of $1x10^5$ cells/ well in a 12 multi-well.

The cells were infected with a series of dilutions of the adenovirus (from 10^{-3} to 10-8).

48h after the infection the cells were observed in a fluorescence microscope (the adenovirus expressed the green fluorescence protein) and the green cells were counted.

The calculation of the viral stock was obtained counting the cells (x20 lens) in 3 different fields. The following equation was used to obtain pfu/mL:

Pfu/ml=((infected cells/field)x594)/ (0,1x dilution factor)

7. Animal Experiments

For the i*n vivo* experiments, mice were used. The mice were housed in cages on a 12h light: 12h dark cycle at controlled temperature (25±1).

All experiment protocols with mice were performed with the approval of the animal ethics committee of the Universitat de Barcelona, Barcelona, Spain.

7.1Fasting Kinetics Experiment

10 week-old C57BL/6J male mice (supplied by Charles River) were used. Mice were divided in two groups, one fed Ad Libitum (ZT12) with a standard chow diet or fasted for 6h (ZT18), 15h (ZT13) or 24h (ZT12) and euthanized at the indicated Zeitgeber time (ZT).

7.2High Fat Diet experiment

For the comparison of Fsp27β expression between the fed and fasted state, with a control and high fat diet in mice liver, 12 week-old male mice with mix background c57bl6/sv129, where used. The mice were either fed Ad Libitum or fasted for 24 h.
These mice were a kind gift from Toni Vidal-Puig lab from the University of Cambridge.

For the comparison of Fsp27α and Fsp27β expression throughout different tissues 10 week-old C57BL/6J male mice were used. Mice were divided in two groups, one fed a standard chow (CHO 62%; Prot 17%; Fat 17%) and the other fed a High-Fat diet (CHO 25%; Prot 15%;Fat 60%) for 21 weeks. Both diets contained the same proportion of micronutrients to avoid effects that did not derived from the difference in fat.
The mice were fasted for 8 hours before being euthanized.

7.3FSP27 knockdown Experiments

Adenoviruses encoding shRNA control or a shRNA against *Fsp27* (kindly supplied by Dr. Ángel Baldán, SLU) were administered to 8 week old C57Bl/6J male mice by tail-vein injection ($5x10^9$ pfu/animal).

Nine days after injection, mice were either fed ad libitum with a standard chow diet (7 animals per group, both control and shFsp27) or fasted for 17h (6 animals per group, both control and shFsp27) and euthanized at ZT5 (i.e. 5h after the onset of the 12h light span) and sacrificed at the indicated Zeitgebertime (ZT).

7.3.1 Tissues Harvesting

Mice were fully anesthetized using isoflurane inhalation (4% for induction and 2% for maintenance), the thoracic cavity was opened and blood was collected by intracardiac

puncture. After sacrificing the animals, tissues were isolated and immediately snap frozen in liquid nitrogen. Tissues were stored at -80oC for future analysis.

7.3.2 Serum extraction

Mice serum was obtained by clotting whole blood (30 minutes, RT) following a centrifugation (1500G, 15 min, 4oC). Serums were stored at -80oC for posterior analysis.

7.3.3 Phospholipids measurements

7.3.3.1 Solid Phase Extraction Method

Serum samples were diluted with PBS followed by a liquid/liquid extraction with methanol and a solution of the internal standard (16:0D31-18:1 PC) in chloroform (final concentrations of PBS: MeOH: CHCl3 were 1:1:2). The mixture was thoroughly vortexed and then centrifuged at 10,000 rpm to provide two liquid phases (one aqueous layer on the top and an organic layer at the bottom) separated by a disk of white solid material. An aliquot of the lipid-containing layer (organic phase) was evaporated to dryness using a constant stream of nitrogen and re-dissolved in hexane/methyl-tert-butyl-ether (MTBE)/acetic acid (100:3:0.3) followed by fractionation using a column purification method, as described (24). Briefly, Bond Elut SS-NH2 cartridges (3 ml, 500 mg, 47-60 mm, Varian) were equilibrated 3 times with acetone/water (7:1) and washed with two 1 ml portions of hexane. Lipids were loaded onto the column and were eluted sequentially with hexane, hexane/CHCl3/AcOEt (100:5:5), CHCl3/iPrOH (2:1), CHCl3/MeOH/AcOH (100:2:2) and finally the phospholipid fraction was eluted with CHCl3/MeOH/H2O (5:10:4), evaporated to dryness under a stream of nitrogen and reconstituted with CHCl3 prior to LC-MS analysis.

7.3.3.2 LC–ESI–MS/MS procedure

The HPLC system consisted of an Agilent 1290 Infinity (*Waldbronn, Germany*) binary pump equipped with a thermostated (10 °C) autosampler. For the analysis of the extracts, a Mediterranea Sea C18 column (100 × 2.1 mm, 2.2 µm) (*Teknokroma*) was used, mantained at 50 °C. Mobile phase A consisted of 95:5 water:methanol and mobile phase B was composed of 60:35:5 isopropanol:methanol:water. Both A and B were supplemented with 0.1% formic acid and 5 mM ammonium formate. The flow rate was 0.5 ml min-1 and the injection volume 2 µl. A linear gradient profile with the following proportions of solvent B was applied (t, %B): (0, 20), (5, 20), (20, 100), (25, 100), (26, 20), (35, 20). MS/MS experiments were performed on an QTRAP 6500 mass spectrometer (*AB SCIEX, Concord, Ontario, Canada*). All the analyses were performed using the *IonDrive™* source in positive ion mode with the following settings: capillary voltage 5500 V, temperature 500 ºC, curtain gas (N2) 25 (arbitrary units), GS1 (N2) 50 (arbitrary units), GS2 (N2) 30 (arbitrary units), collision gas Medium (arbitrary units), declustering potential (DP, Table 3), entrance potential 10 V, collision energy (CE, Table 3), collision cell exit potential (CXP, Table 3). All the MS/MS parameters were optimized in infusion experiments: individual standard solutions of 18:0-18:1 PC, 16:0-18:1 PC and 16:0D31-18:1 PC (100 ng µl−1) were infused at a constant flow rate of 5 µl min−1 into the mass spectrometer. Relative quantification of phosphocoline species was done using stable isotope dilution mass spectrometry with the spectrometer operated in MRM (multiple reaction monitoring method). Transitions were used to identify and quantify the analyses (Table 3).

Table 3. Transitions used to identify and quantify the analyses of mass spectrometry.

Compound	Transitions	DP	CE	CXP
18:0-18:1 PC	788.5/184.0	196	39	18
	788.5/85.9	196	101	10
16:0-18:1 PC	760.6/184.1	171	39	16

	760.6/86.1	171	101	10
16:0D31-18:1 PC	791.6/184.1	136	41	10
	791.6/86.0	136	103	10

The integrated peak area for each species was normalized to the peak area of the internal standard.

7.3.4 Triglyceride measurements

Lipids from the livers of mice were extracted with 5% NP40/ddH2O and TG levels in livers and serums were analyzed with a TG measurement kit (*LabAssay Triglyceride Wako*).

7.3.5 RNA analysis

7.3.5.1 RNA extraction

Frozen tissues were chopped in liquid nitrogen and crushed in TRI Reagent solution with the help of a politron and the RNA was isolated following the manufacturer's instructions.

The RNA was pre treated with DNAse I (*Ambion*) to eliminate genomic DNA contamination and

dissolved in DEPC-water (*Sigma-Aldrich*) and the concentration and purity of each sample was obtained from A260/A280 and A260/A230 measurements in a micro volume spectrophotometer *Nanodrop-1000* (Nanodrop Technologies, Inc. Thermo Scientific).

7.3.5.2 Analysis of mRNA expression

The cDNAs were prepared from total RNA of tissues and were subjected to quantitative real time polymerase chain reaction (qPCR) to measure the mRNA levels of the genes of interest, using SYBR Green or Taqman reagents.

One microgram of total RNA was used to synthesize the cDNA by M-MLV reverse transcriptase (Invitrogen) with random hexamers (Roche Diagnostics) and dNTPs (Attend Bio) according to manufacturer's instructions.

The SYBR Green PCR Master Mix and Taqman Gene Expression Master Mix, was supplied by Applied Biosystems (ThermoFisher Scientific) and used for the PCR step.

Amplification and detection were performed using the Step-One Plus Real-Time PCR System (Applied Biosystems, ThermoFIsher Scientific).

The PCR assays were carried out in 96-well plates and each mRNA single sample was measured in duplicate using 18S, beta-actin and b2m as housekeeping genes.

The results were obtained by the Relative Standard Curve Method and expressed as the Ct method and expressed as fold increase versus the experimental control.

The probes (table 6) and primers (table 7) used are shown below:

Table 4. qPCR probes for Taqman assays

Name	*Probes*
mCpt2	Mm00487202_m1
mFgf21	Mm00840165_g1
mFsp27	Mm00617672_m1
mHMGCS2	Mm00550050_m1
18S	X03205.1

Table 5. qPCR primer pairs for Sybr green assays.

Name	*Forward Primers (5'-3')*	*Reverse primers (5'-3')*
B2M	ACTGATACATACGCCTGCAGAGTT	TCACATGTCTCGATCCCAGTAGA
Cpt1b	GCGTGCCAGCCACAATTC	TCCATGCGGTAATATGCTT
Fsp27α	GCCACGCGGTATTGCCAGGA	TCCATGCGGTAATATGCTT
Fsp27β	TGACCACAGCTTGGGTCGGA	TCCATGCGGTAATATGCTT
Ucp1	CCCGCTGGACACTGCC	ACCTAATGGTACTGGAAGCCTGG

18S	CGGCTACCACATCCAAGGAA	GCTGGAATTACCGCGGCT

8. Statistical analysis

All results are expressed as mean ± SEM. Significant differences were assessed using the two-tailed Student's t-test. P <0,05 was considered statistically significant.

9. Additional Information

Any missing information regarding the experimental procedures means that the procedure was performed according to the detailed information given by "Molecular Cloning, a Laboratory Manual" (Sambrook, Frisch and Maniatis) and "Current Protocols in Molecular Biology" (Ausubel, Bent, Kingston, Moore, Seidman, Smith and Struhl) or fol

RESULTS

1. Regulation of FSP27 during the fasting adaptation

Fsp27 is a response gene in the fasted liver, it has a particular expression pattern, showing changes in liver during the fasting period by increasing at the beginning (6-15h) and lowing in the long fasting (24h) *(Vilà-Brau et al. 2013).* For this reason, it was important to study the mechanisms underlying this regulation, as explained in more detail below.

1.1 Expression pattern of Fsp27α and Fsp27β in different tissues

Two different isoforms (FSP27α and FSP27β), differing in the first 10 amino acids and driven by different promoters are expressed from the same gene (Xu et al. 2015). In order to compare the mRNA expression of both isoforms in different tissues under fasting conditions we perform a gene expression analysis through a qPCR approach. C57BL6/KJ mice were fed with a control diet (CD) or a HFD for 21 weeks and the mRNA levels were evaluated in various tissues after 12h fasting. Figure R1 shows that FSP27β is the isoform mainly expressed in BAT, small intestine and liver in animals fed either with a control diet (CTL) or with a HFD.

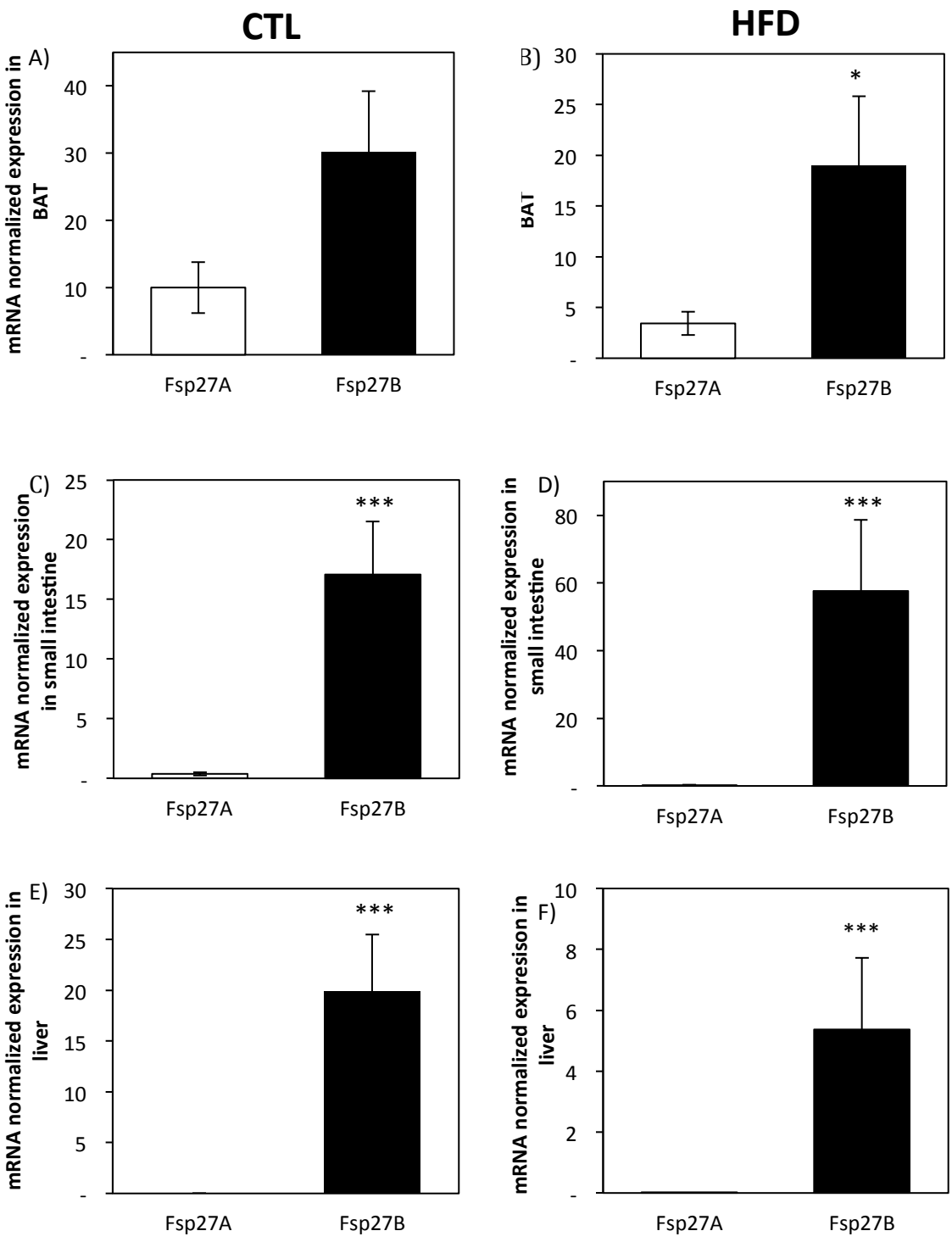

Figure R 1. Expression levels of *Fsp27α* (white bars) and *Fsp27β* (black bars) in different tissues. - RT-PCR analysis of Fsp27a and Fsp27b C57BL/6J mice fed with a control diet (CTL) or HFD for 21 weeks and starved for 12 hours before sacrifice (n=8) in A,B) BAT, C,D) small intestine and E,F) liver. As the comparison were performed in the same tissue the values represented are absolute quantifications rather than relative levels. Error bars represent the mean ±standard error of the mean (SEM) * p <0,05 and *** p < 0,001relative to the expression of *Fsp27α*.

1.2 Expression pattern of Fsp27β in the adaptation to fasting

In 2013, our group described the hepatic expression pattern of *Fsp27* during fasting adaptation (Vilà-Brau et al. 2013). These results were published before the two different isoforms were described. As FSP27β is the main isoform expressed in liver we analyzed the expression pattern of the beta isoform of the *Fsp27* gene during a fasting time-course experiment. This way, the specific expression and the regulation of *Fsp27β* in the adaptation to fasting could be evaluated, as it was done before with total Fsp27. *Fsp27β* and *Fsp27α* mRNA levels were measured in livers of fasted mice at different time points (0, 6, 15 and 24 hours). As figure R 2 shows, *Fsp27β* has the same expression pattern as total *Fsp27* (Vilà-Brau et al. 2013). As the mRNA of alpha isoform was not detected in liver (*data shown*) this experiment confirmed that FSP27β is the main/unique isoform expressed in fasted in liver and also the responsible of the *Fsp27* role in the fasting adaptation of the liver metabolism.

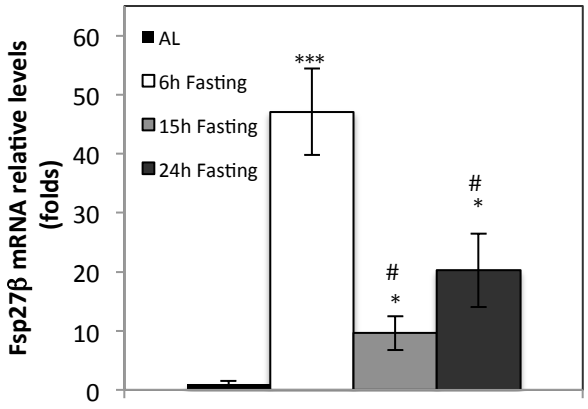

Figure R 2. *Fsp27β* is a responsive gene in the fasted liver. mRNA levels of ***Fsp27β*** **in the livers of fasted mice (n=5 per group), at different time periods (black bars: Ad Libitum, white bars: 6 hours fasting, light grey bars: 15 hours fasting, dark grey bars: 24 hours fasting). Error bars represent the mean ±standard error of the mean (SEM) . * p< 0,05 and *** p<0,001 relative to *Fsp27β* expression Ad Libitum; # p<0,05 relative to *Fsp27β* expression at 6 hours fasting.**

1.3 Impact of a High-Fat diet on the expression of Fsp27β

Fsp27β expression is induced under different nutritional inputs, HFD, MD, but also by fasting. To explore how *Fsp27β* is regulated by both HFD and fasting, an *in vivo* experiment using C57Bl6/J mice was designed. Animals were divided into four different groups. In two of the groups the mice were fed *Ad Libitum* either CD or a HFD; in the remaining two groups, the mice were also fed a CD or a HFD, but were fasted 12h before being sacrificed.

This experiment combines the adaptation to fasting and a HFD (Figure R3) to a better understanding of *Fsp27* regulation, as it is not only a possible regulator in the adaption to fasting but it is also expressed in the steatotic liver, under the regulation of PPARγ. (Matsusue et al. 2008)

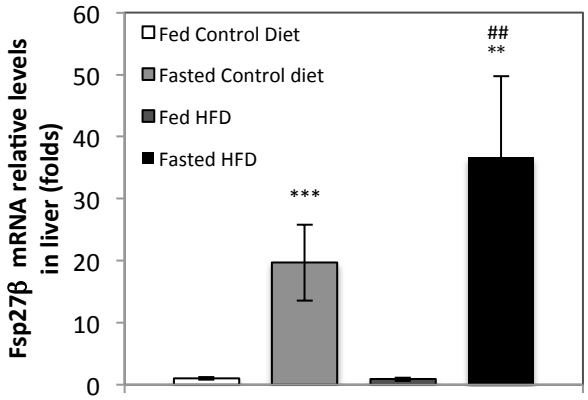

Figure R 3. Fsp27β is fasting dependent and up regulated by a HFD. Gene expression (mRNA levels) in the livers of fed and fasted mice, previously fed a control or HFD (white bars: Fed, control diet; light grey bars: Fasted, control diet; dark grey bars: Fed,HFD black bars: Fasted, HFD. Error bars represent the mean ±standard error of the mean (SEM) . ** p< 0,01 and *** p<0,001 relative to Fsp27b expression Fed, control diet; ## p<0,01 relative to *Fsp27β* expression fasted, control diet.

Interestingly, and although *Fsp27β* is already significantly up regulated in fasting when the mice were previously fed with a CD, its expression is much higher in a fasting condition, when fed previously with a HFD.

Nonetheless, no significant changes are seen between the mice fed a CD and HFD, meaning that possibly the pattern of expression of *Fsp27* is always fasting dependent (Figure R3).

2. Transcriptional regulation of Fsp27 in liver

To study its importance in the adaptation to fasting and thus have a better understanding of FSP27 expression pattern, its transcriptional regulation was studied. Globally the experimental approach used to solve this part of the work was based on transient transfection assays. A hepatic cell line model (AML12) was used to co-transfect luciferase reporter constructs that include different regions of the Fsp27 promoters with various combinations of plasmids that codify for the transcription factors we were interested on.

2.1 CREBH and Rev-Erba as possible Fsp27 regulators in fasting

The focus of this part of the study was to understand by which mechanisms Fsp27β is up regulated in an early fasting and down regulated in a late fasting. As for the first part of the question, the proposed responsible for the up-regulation of *Fsp27β* is the transcription factor Cyclic-AMP-responsive-element-binding-protein H (CREBH). For the second part, lower induction in late fasting, we proposed either the acetylation levels of *CREBH* or *Rev-Erbα* expression.

In figure R 4, the mRNA expression pattern of *CREBH* (Figure R 4A) and *REV-ERBα* (Figure R 4B) were analyzed, at the same fasting times as *Fsp27β (*Figure R 3), to check if these two factors are implied in the mRNA changes of *Fsp27β*.

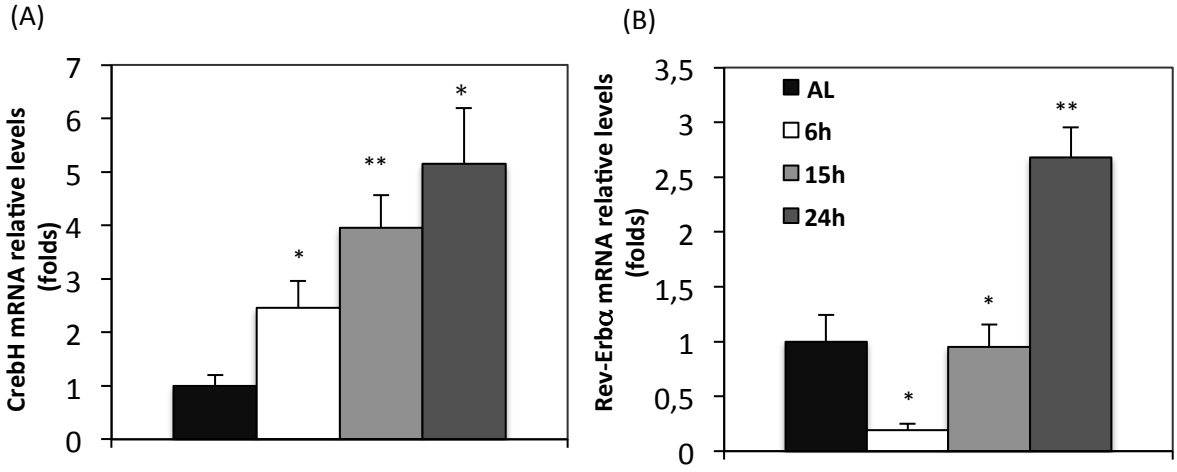

Figure R 4. CREBH and Rev-Erbα are possible *Fsp27β* regulators (A) *CREBH* and (B) *Rev-Erbα* gene expression in the livers of fasted mice, at different time periods (black bars: Ad Libitum, white bars: 6 hours fasting, light grey bars: 15 hours fasting, dark grey bars: 24 hours fasting). Error bars represent the mean ±standard error of the mean (SEM) * p< 0,05 and **p< 0,01 relative to expression Ad Libitum.

In figure R 4A, the *CREBH* mRNA expression is induced constantly during the course of the fasting period, therefore showing an up-regulation in fasting state. As for *Rev-Erbα,* its expression pattern shown in figure R 4 B illustrates that its mRNA levels are opposite to the *Fsp27β* levels. *Rev-Erbα,* is down-regulated in an early fasting (6 hours), being this tendency reversed in a late fasting, once the levels rise at 15 hours of fasting, and keep rising. This profile would be compatible with the possible role of REV-ERBα as a FSP27β repressor. Consequently, arises the hypothesis that FSP27 regulation could be due to the PGC1α-Rev-Erbα axis. In addition, It is also reported that Rev-Erbα negatively affects Fgf21 expression by a mechanism that involves the expression of ALAS-1, the rate limiting enzyme in heme biosynthesis (Estall et al. 2009).

2.1 Fsp27 promoter

The two isoforms of FSP27 have different tissue expression patterns and their mRNA levels are regulated by different signals and transcription factors. Looking for the response elements that were responsible to the transcriptional regulation of FSP27 expression and moreover this differential expression pattern, the promoter of FSP27 and the differential regulatory elements between both isoforms were analyzed.

As it is shown in figure R 5, the *Fsp27* promoter contains different response elements, marked in figure R 5, along with the *Fsp27*α transcription starting site (+1α) and *Fsp27*β transcription starting site (+1β).

Concretely, it contains two different putative CREB response elements, *CRE (-1792, -1787* relative to +1α and *-375,-366* relative to +1α), a PPAR response element, *PPRE* (-116, -1150 relative to +1b) and a CREBH response element, *CHRE* (-35,-24 relative to +1b). Additionally, in figure R 5 it is also marked a predicted site for REV-ERBα, outside the range of the constructs assayed.

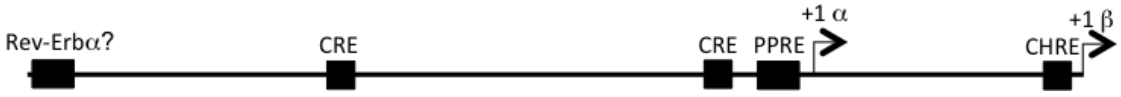

Figure R 5. Map of total *Fsp27*β promoter (-2024, +1013 relative to +1b) , with the Fsp27 α transcription starting site (+1a) and *Fsp27*β transcription starting site (+1b), the two putative CREB response elements CRE2 (-1792,-1787 relative to +1a) and CRE1 (-375, -366 relative to +1a),PPAR response element PPRE (-1163,-1150 relative to +1b) and CREBH response element (-35,-24relative to +1b) and a predicted Rev-Erba putative binding site .

In the course of this study, different constructs of the promoter driving the luciferase gene expression were used (Figure R6). The *Fsp27*$\alpha\beta$ construct (-2024 to +1013 relative to +1α) includes both transcription starting sites (+1α and +1β) and the elements of response for CREB (CRE), PPAR (PPRE) and CREBH (CHRE). The *Fsp27*α construct (-2024, +13 relative to +1α) encodes for the alpha isoform, and contains the response elements for CRE and PPRE. Finally, to study more specifically the regulatory

elements that control *Fsp27β* expression various constructs with different deletions encoding for the β isoform and containing the CHRE response element were generated: The *Fsp27β(-900)* (-900 to +76 relative to +1β), *Fsp27β(-584)* (-584 to +76, relative to +1β), *Fsp27β(+300)* (-300 to +76 relative to +1β), *Fsp27β(-90)* (-90 to + 76 relative to +1β).

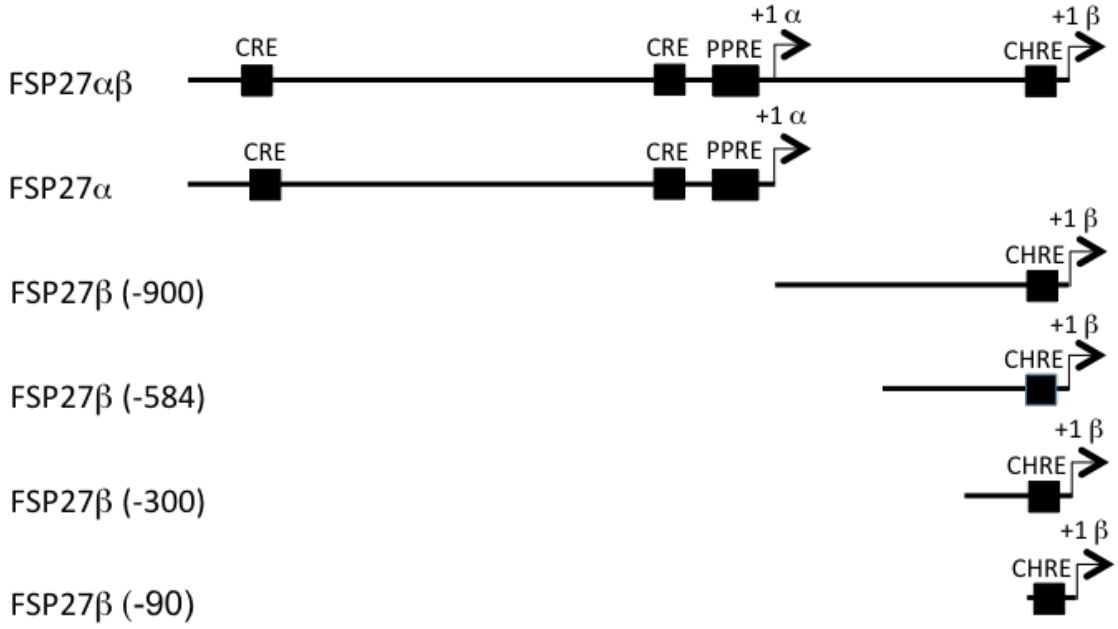

Figure R 6. Map of the different Fsp27 promoter constructs. (A) *Fsp27 α β* (-2024 +1013 relative to +1 β) containing the CREB responsive elements CRE (-1792,-1787 relative to +1a and -375, -366 relative to +1 α), PPAR response element PPRE (-1163,-1150 relative to +1 β) and CREBH response element (-35,-24 relative to +1 β) ; (B) *Fsp27 α* (2024, +18 relative to +1α)containing the CREB responsive elements CRE (-1792,-1787 relative to +1 α and -375, -366 relative to +1 α), PPAR response element PPRE (-1163,-1150 relative to +1 β) and (C) Fsp27 β (-900,+76 relative to +1 β), (D) *Fsp27 β* (-584,+76 relative to +1 β), (E) Fsp27(-300, +76 relative to +1 β) and (F) Fsp27 β (-90, +76 relative to +1 β) , CREBH response element (-35,- 24 relative to +1 β).

2.2 Fsp27β is a CREBH but not a PPARα target gene

As stated above, there is a CHRE site, a CREBH response element in the *Fsp27β* promoter, and consequently CREBH is an activator of the alternative β isoform. The promoter sequence described for *Fsp27α* contains a PPRE element, that is not present in the specific promoter sequence for the β isoform. In order to study the effects of both CREBH and PPARα in the regulation of *Fsp27*, the *Fsp27β* promoter was co-transfected in AML12 cells with CREBH and PPARα (Figure R 7A). Although the

promoter is activated by CREBH, there is no effect of PPARα, neither on the promoter's basal activity, nor in the CREBH activated promoter.

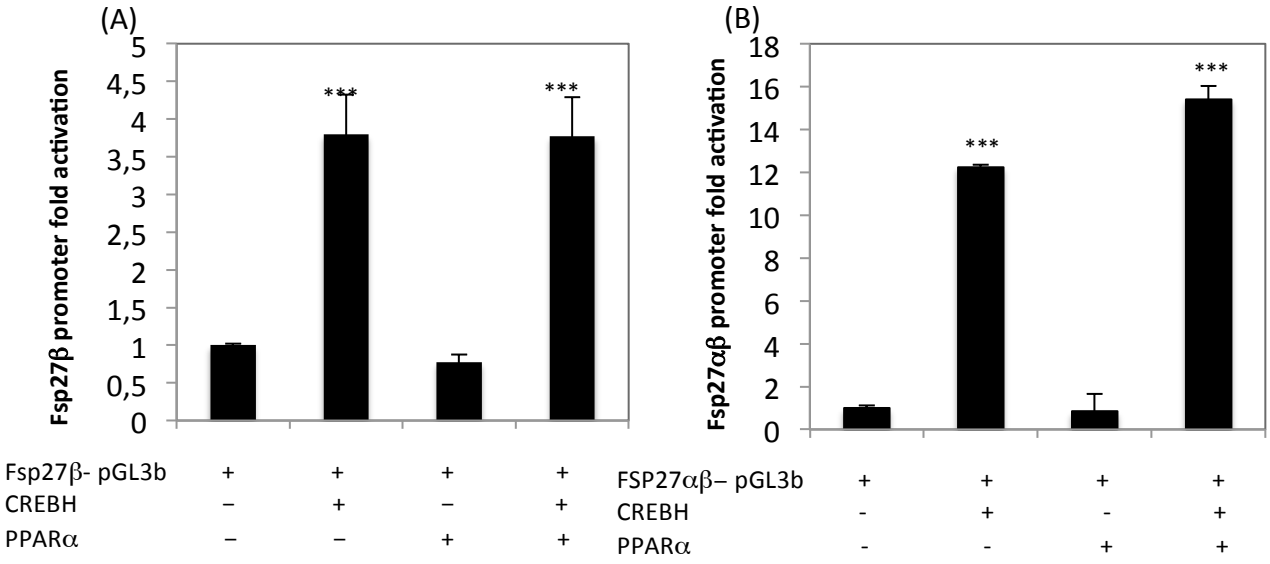

Figure R 7. *Fsp27* promoter is activated by CREBH but not by PPARα. (A) *Fsp27β* and (B) *Fsp27αβ* promoter activation in AML12 cells co-transfected with the transcription factors CREBH and PPARa. Values are given as ± s.d. ***p<0,001 relative to *Fsp27* promoter's basal activity.

The same assay was performed using the *Fsp27αβ* promoter (Figure R 7B), that contains the PPRE response element, and the same results were observed.

Therefore, this data indicates that *Fsp27* is a CREBH but not a PPARα target gene.

2.3Fsp27β activation is dependent on CREBH acetylation

The fasting dependent CREBH acetylation is crucial for its transcriptional activity. The acetylation and deacetylation of CREBH are catalysed by the lysine acetyl transferase PCAF and the deacetylase SIRT1, respectively (Hyunbae Kim et al. 2015b). This information led to the hypothesis that *Fsp27* down-regulation in late fasting could be due to deacetylation of CREBH, making the modulation of *Fsp27* activity dependent of the lysine acetylation of CREBH.

To pursue this hypothesis two different mutants were generated, the mutant K294Q, mimicking the acetylated state of CREBH, and the deficient acetylation mutant K294R. These mutants were transfected in AML12 cells with the *Fsp27β* reporter plasmid (Figure R 8).

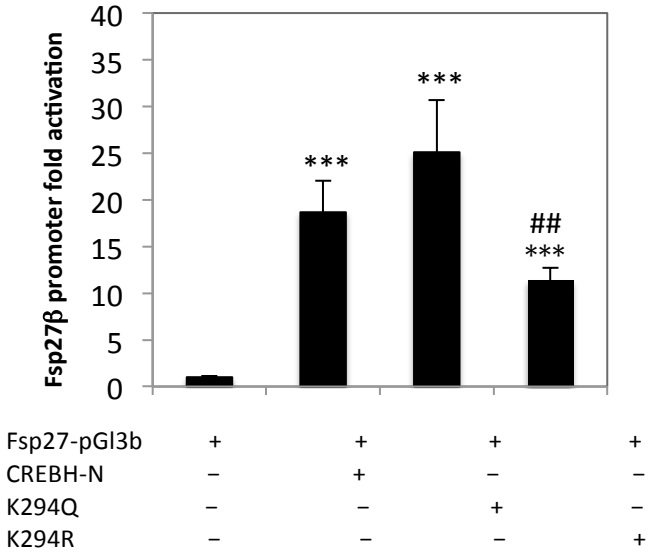

Figure R 8. Regulation of *Fsp27β* is dependent on the acetylation state of CREBH. *Fsp27β* promoter activity in AML12 cells co-transfected with wild type CREBH and the mutants K294Q and K294R. Error bars represent the mean ±standard error of the mean. *** p<0,001 relative to the promoter's basal activity and ## p<0,01 relative to the promoter activation by CREBH.

The mutant K294Q showed similar effects as the wild-type CREBH Nuclear, and the K294R acetylation deficient mutant K294R failed to induce *Fsp27β i*n the same extent.

These results point out that Fsp27β activation by CREBH is dependent on its acetylation state.

2.4 The role of REV-ERBα and HNF6 in Fsp27 repression

As shown before, REV-ERBα is a possible candidate for the repression of FSP27, due to its pattern of expression in fasting (Figure R 4B). To evaluate this hypothesis AML12

cells were co-transfected with the *Fsp27β* promoter, CREBH and REV-ERBα. In this context, REV-ERBα was not able to repress the promoter activation produced by CREBH (Figure R 9).

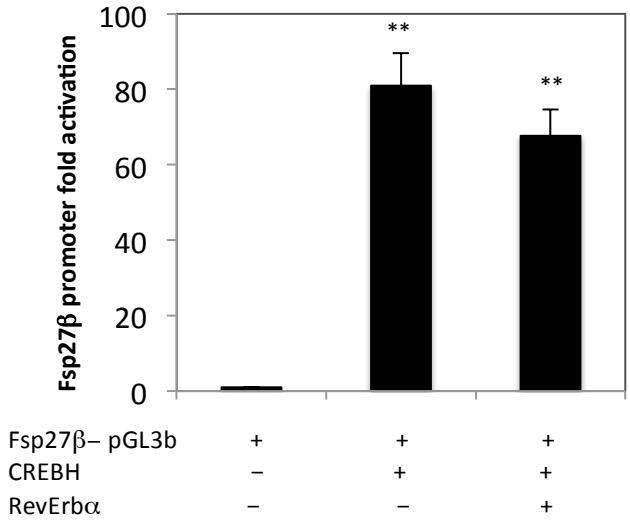

Figure R 9. *Fsp27 α β* regulation through CREBH and REV-ERBa. *Fsp27 β* promoter (-900 to +76, relative to +1B) activity in AML12 cells co-transfected with the transcription factors CREBH and REV-ERBa. Values are given as mean ± s.d ** p< 0,01 relative to Fsp27 β promoter' s basal activity.

Moreover, both the *Fsp27αβ* and the *Fsp27β* promoter were co-transfected with RORα, a transcription factor that competes for the same binding sites as REV-ERBα, but no effect was shown (Figure R 10). This data indicates that REV-ERBα may not be a direct repressor for FSP27.

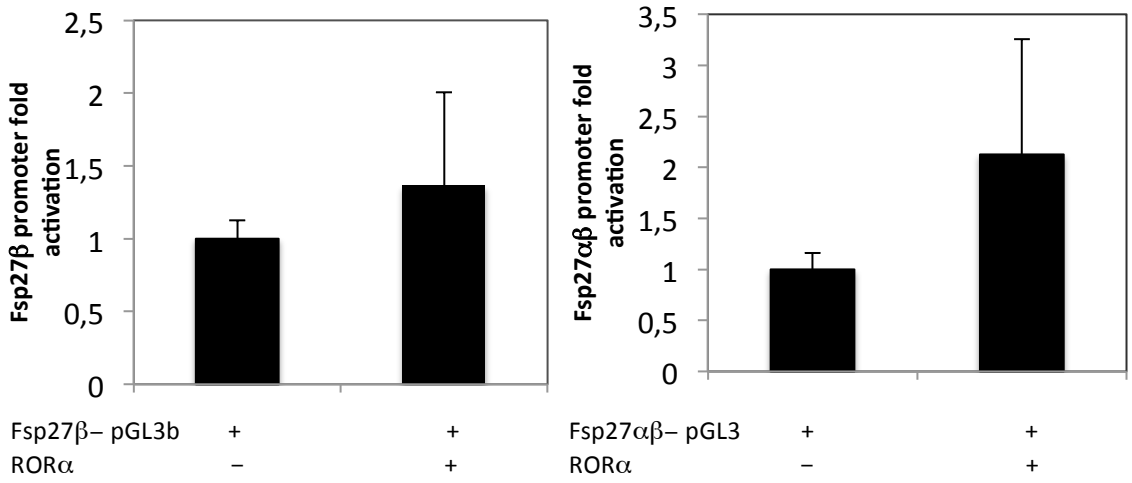

Figure R 10. *Fsp27* promoter activation does not depend on ROR. (A) *Fsp27 β* promoter (-900 to +76, relative to +1B) and (B) *Fsp27a β* (-2024 +1013 relative to +1 *β*) activity in AML12 cells co-transfected with the transcription factor ROR.

Based on the results that indicate that REV-ERBα is not a direct repressor of the *Fsp27β* promoter and knowing that REV-ERBα works cooperatively with the transcription factor HNF6 to regulate the hepatic lipid metabolism (Y. Zhang et al. 2016a) AML12 cells were co-transfected with the *Fsp27β* promoter and the HNF6 transcription factor, CREBH and REV-ERBα. Although REV-ERBα itself cannot repress the activation shown by CREBH, HNF6 repressed the promoter activity (Figure R 12).

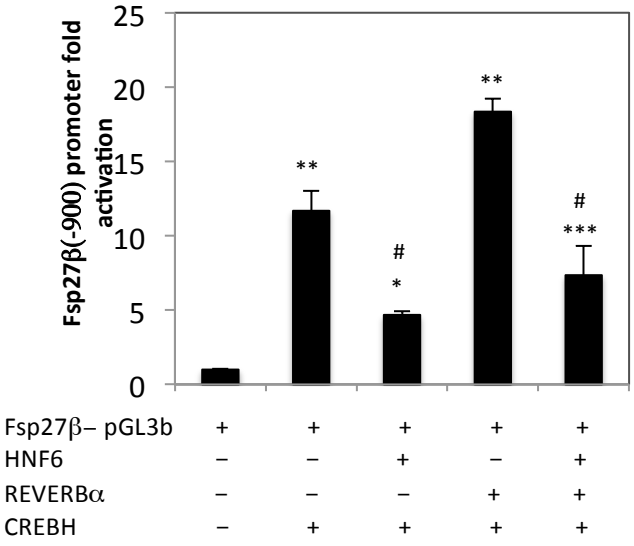

Figure R 11. HNF6 as a possible *Fsp27β* repressor. Fsp27β promoter (-900 to +76, relative to +1B) activity in AML12 cells co-transfected with the transcription factors HNF6, REV-ERBα and CREBH. Error bars represent the mean ±standard error of the mean * p<0,05; ** p<0,01 and *** p<0,001 relative to the promoter's basal activity and # p<0,05 relative to the promoter's activation by CREBH.

With this result, the next step was to map the HNF6 putative binding site, that is predicted to be at -155 to -141 relative to +1β, performing deletions of the promoter as detailed previously (Figure R 6). The different constructs (Fsp27β*(-584),* Fsp27β*(-300)* and Fsp27β*(-90))* were transfected in AML12 cells with or without HNF6, as seen in figure R 13 A,B and C, respectively. In figure R 13C, the shorter promoter construct, *Fsp27β (-90)* does not loss its activation by CREBH completely, but it is significantly reduced. Since the construct *Fsp27β (-90)* should exclude the HNF6 putative binding site, this result raises the question of whether HNF6 is acting directly on the promoter or is involved in an indirect response. In figure R 13D, an experiment was performed to test the effect of HNF6, by co- transfecting different amounts of CREBH and a fixed concentration of HNF6. The result shows that the effect of HNF6 depends on the CREBH concentration, meaning that it is probably a squelching phenomenon between CREBH and HNF6.

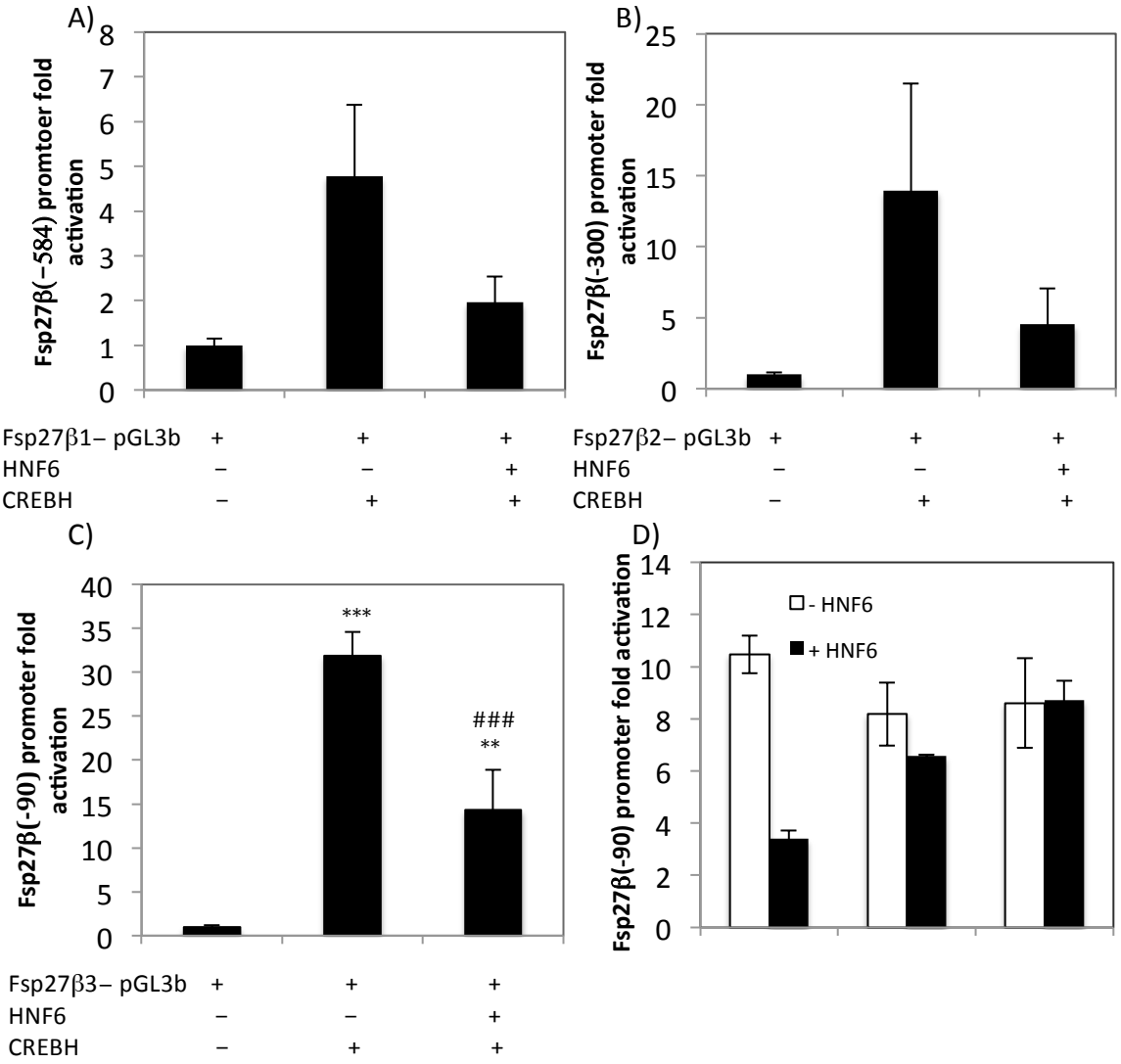

Figure R 12. HNF6 affects *FSP27β* regulation, through CREBH. (A) *Fsp27 β* (-584) (-584 to +76, relative to +1 β), (B) Fsp27 β (-300) (-300 to +76, relative to +1 β), (C) Fsp27 β (-90) (-90to +76, relative to +1 β) activity in AML12 cells co-transfected with the transcription factors HNF6 and CREBH co-transfected with the same amount of each transcription factor and (D) Fsp27 β (-90) (-90to +76, relative to +1 β) activity in a dependent dosis of CREBH. Values are given as ± s.d. p<0,01 and *** p<0,001 relative to the promoter's basal activity and ### p<0,005 relative to the promoter's activation by CREBH.**

Finally and looking for the role of REV-ERBα we analyzed the results of a ChIPseq experiment published by Mitchell Lazar's group (GSM1659686). They used livers from 129S1/SvlmJ mice to extract protein and performing the chromatin immunoprecipitation with a REV-ERBα antibody. After After the immunoprecipitation through the DNA sequencing it is possible to check the enriched-regions and to

identify where REV-ERBα binds. The result of this analysis indicates that Reverbα has indeed some putative binding sites on the *Fsp27* promoter (Figure R 11), although these sites (approximate coordinates -3070 to -133 relative to +1β) are outside of the range of the *Fsp27* promoter constructs used in this thesis.

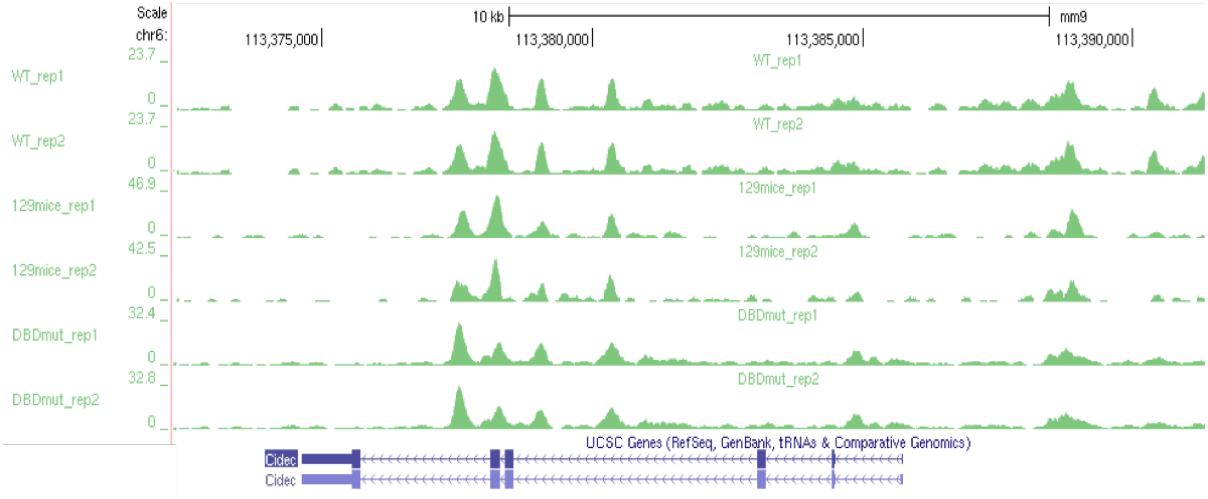

Figure R 13. Analysis of ChIP-seq results from Mitchell's Lazar group (GSM1659686); showing sequences enrichment after immunoprecipitation of Rev-ERBα is shown in green. WT: liver of C57BL/6J mouse. 129 mice:liver of 129S1/SvlmJ. DBDmut: liver of C57BL/6J RevErba DNA binding domain(DBD) mutant mouse. FSP27/CIDEC representation is shown in blue.

3. The role of FSP27 as a lipid-droplet protein in PPARα signaling

PPARα is an important regulator of the FAO, although its regulation mechanism is not clearly understood. While PPARα is activated in feeding periods, and not by adipose stores (Chakravarthy et al. 2005), its target genes are expressed in fasting but its expression is impaired when FASN is absent (FASKOL). Nowadays two phosphocholines (16:0/18:1 and 18:0/18:1) has been described as PPARα ligands *(Chakravarthy et al. 2010)*(S. Liu et al. 2013). Therefore, this may uncover a link between Fsp27, with its

particular expression pattern *(Vilà-Brau et al. 2013)* and with its role in the unilocular lipid droplet formation and the availability of PPARα ligands.

To determine the role that FSP27 plays in PPAR signaling, two different approaches were used, *in vitro* and *in vivo*.

3.1Interference of PPARα signaling by Fsp27β *in vitro*

For the first approach, a hepatic cell line model (*HepG2*) was used to transfect the TK (thymidine-kinase) luciferase reporter construct under the control of three *PPRE* (peroxisome proliferator responsive element). The cells were co-transfected with the expression vector for PPARα, FSP27α, and both of the constructs simultaneously.

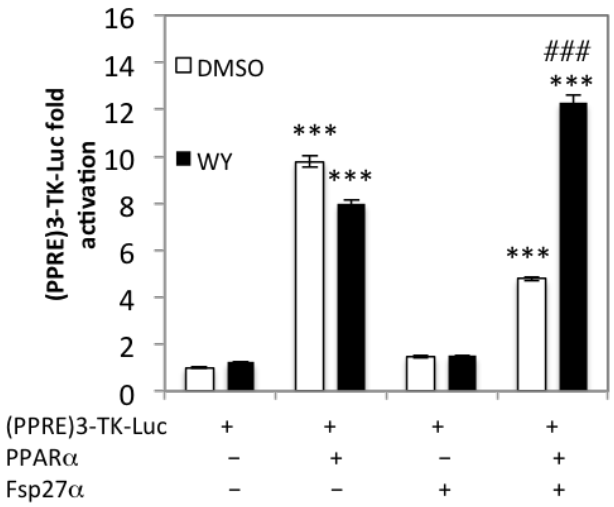

Figure R 14. FSP27 interferes with PPAR signaling. TK luciferase reporter activity in HepG2 cells co-transfected with PPARα and FSP7α. Error bars represent the mean ±standard error of the mean . *< 0,001 relative to the promoter's basal activity and ### < 0,005 relative to the promoter co-transfected with PPARα and FSP27α, with DMSO.**

Figure R 14 corroborates that FSP27 is somehow involved in the regulation of PPARα, by disturbing PPARα activation of the TK promoter. This disturbance is reversed in the presence of a synthetic agonist of PPARα (*Wy14643*), revealing that in these conditions

PPARα activation may be mediated by endogenous ligands. This result evidences that although *Fsp27* is not a direct PPARα target gene, it may interfere indirectly in its signaling.

3.2 Effects of hepatic FSP27β absence in PPAR signaling *in vivo*

To evaluate the role of FSP27β expression in PPAR signaling *in vivo*, its hepatic expression was knocked-down in fed and starved animals, by using an adenovirus-mediated shRNA. The mice were divided in two different groups, the control group, with a shRNA control adenovirus and the shFSP27 group, with a shRNA silencing FSP27.

The experiment was conducted in two different conditions, Ad Libitum, and at 17 hours fasting. This time frame was chosen by combining the *Fsp27* expression pattern *(Vilà-Brau et al. 2013)* and the variation of the phospholipids in serum, described as PPARα endogenous ligands. (S. Liu et al. 2013)

3.2.1 Fsp27β hepatic knockdown

The success of the experimental design was confirmed by analysis of the mRNA expression of *Fsp27β* in the livers of mice.

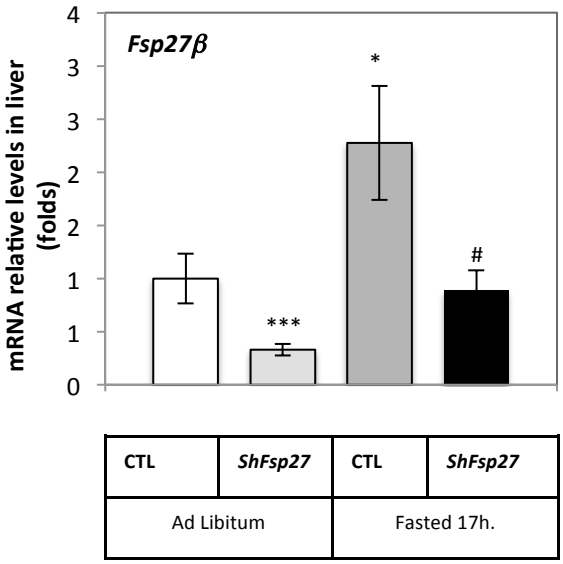

Figure R 15. Successful *Fsp27β* hepatic knockdown. *Fsp27β* gene expression in the livers of mice fed Ad Libitum or fasted for 17 hours treated with shRNA control adenovirus (CTL: white or dark grey bars, respectively) or sh*Fsp27* specific adenovirus (shFSP27: light dark or dark respectively). Error bars represent the mean ±standard error of the mean (SEM) *<0,05 and *< 0,001 relative to Ad Libitum control; # < 0,05 relative to fasting control.**

As expected, there is an increase in the expression of the hepatic *Fsp27β* in fasting, concomitant with *Fsp27* pattern of expression in this condition *(Vilà-Brau et al. 2013)*, relative to the control ad libitum mice. In both conditions, there is a significant down-regulation of the gene expression both Ad Libitum and in the 17 hours fasting, meaning that the knockdown was successful (Figure R 15).

3.2.2 Hepatic Fsp27β expression is essential for liver long-term expression of PPARα target genes

After analysis of PPARα target genes mRNA expression, it is confirmed that silencing of FSP27 affects the expression of genes like *Fgf21* and *Hmgcs2* (Figure R 17A and B, repectively) , showing that their induction in fasting is dependent on *Fsp27* expression.

Unexpectedly, the expression of *Cpt2*, an early-fasting responsive gene, is not altered (Figure R 16C). Therefore, it seems that FSP27 only affects the expression of late fasting responsive PPARα target genes.

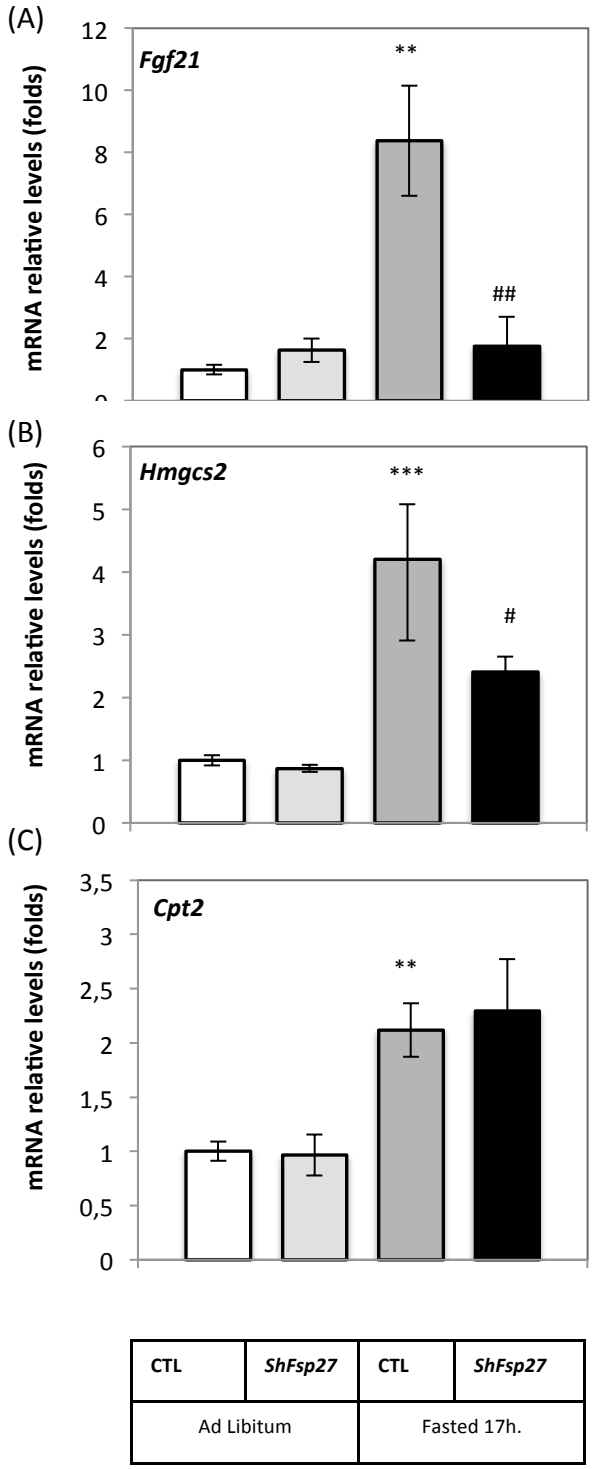

Figure R 16. Effects of hepatic *Fsp27β* knockdown in liver. Gene expression in the livers of mice. (A) *Fgf21*, (B) *Hmgcs2*, (C) *Cpt2*. Mice were fed Ad Libitum or fasted for 17 hours treated with shRNA control adenovirus (CTL: white or dark grey bars, respectively) or sh*Fsp27* specific adenovirus (shFSP27: light dark or dark respectively). Error bars represent the mean ±standard error of the mean (SEM) **<0,01 and *< 0,001 relative to Ad Libitum control; # < 0,05 and ## < 0,01 relative to fasting control.**

3.2.3 Hepatic FSP27β expression affects serum phospholipids levels

In 17 hours fasting, the TAG levels in serum rise in wild type animals, although this does not occur in the mice lacking hepatic fsp27β (figure R 17A). In liver, there is also a rise in the TAG levels in fasting, and it can be concluded that FSP27β is essential for the accumulation of TAG, both in the fed and the fasted state (Figure R 17b).

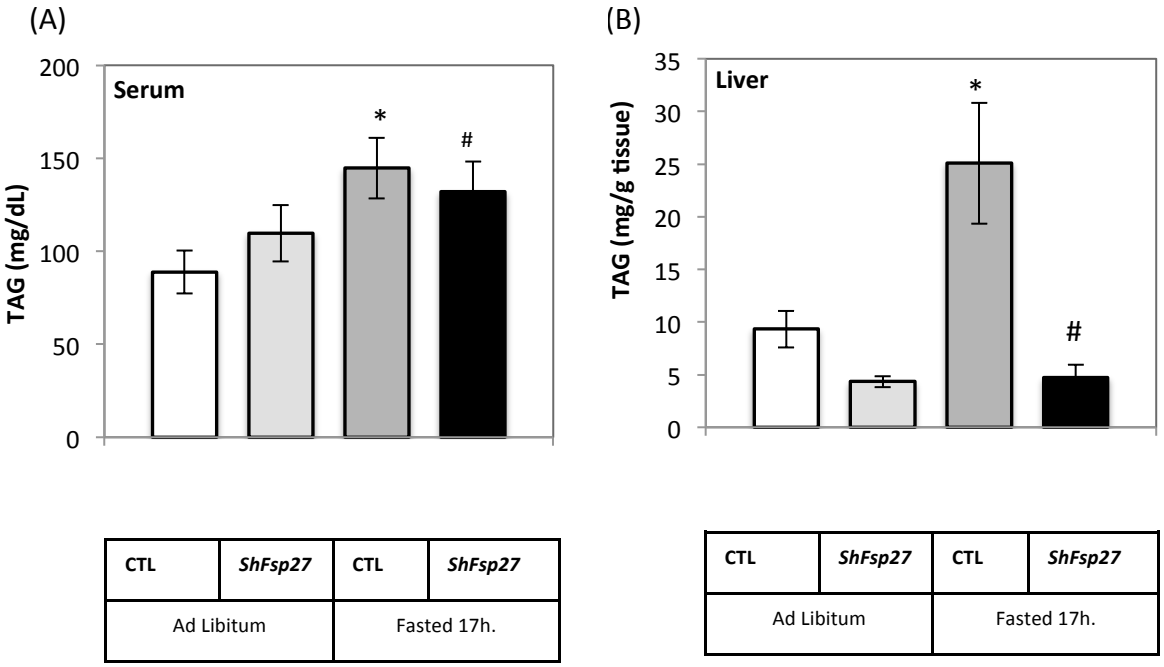

Figure R 17. *Fsp27* hepatic knockdown alters TAG levels. (A) Serum levels (mg/dL) and (B) liver levels (mg/g tissue) of TAG. Mice were fed Ad Libitum or fasted for 17 hours treated with shRNA control adenovirus (CTL: white or dark grey bars, respectively) or sh*Fsp27* specific adenovirus (shFSP27: light dark or dark respectively). Values are given as mean ± SEM *<0,05 relative to Ad Libitum control; # < 0,05 relative to fasting control.

When analyzing the serums of the animals, it was discovered that the concentration of phospholipids was lower in fasted animals in comparison with the fed animals. Nonetheless, in the animals lacking hepatic *Fsp27β*, the levels of phospholipids in serum are higher, in both conditions (Figure R 18). These two results put together suggest that *Fsp27β* expression is essential to accommodate TAG in liver and to preserve the phospholipids needed for the formation of the lipid droplets.

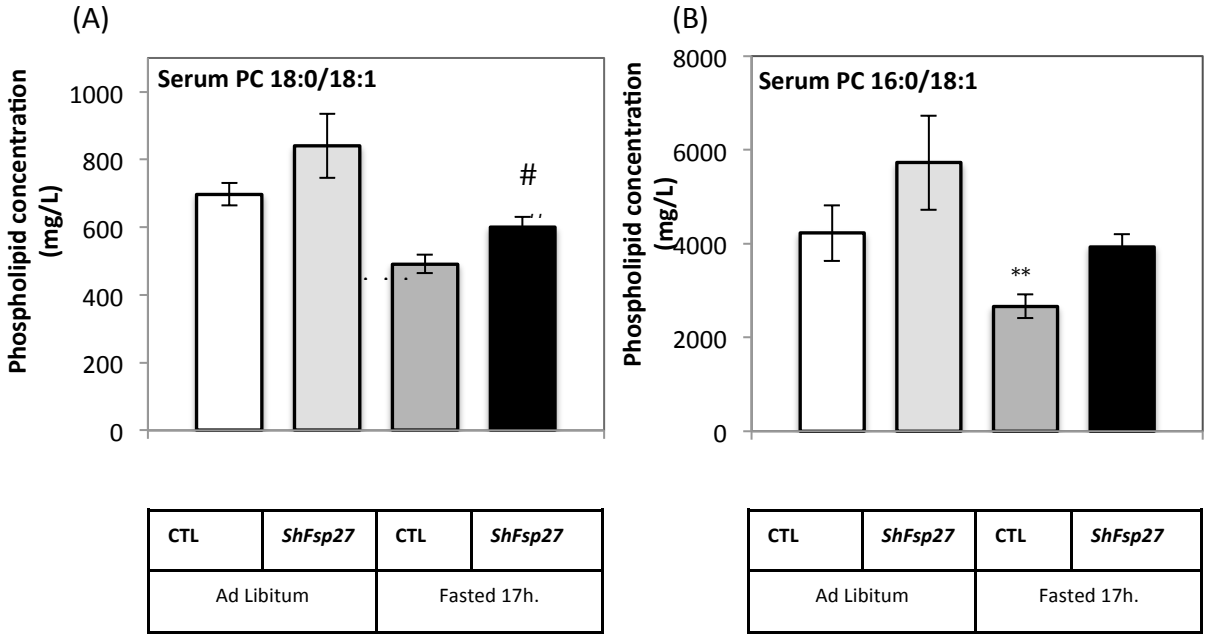

Figure R 18. *Fsp27* hepatic knockdown alters phospholipids (PC) levels. (A) Serum levels (ug/L) of 1- palmitoyl-2-oleoyl-sn-glycerol-3-phosphocholine (PC 18:0/18:1) ; (D) Serum levels (ug/L) of 1-stearoyl-2-oleoyl-sn-glycerol-3-phosphocholine (PC 16:0/18:1). Mice were fed Ad Libitum or fasted for 17 hours treated with shRNA control adenovirus (CTL: white or dark grey bars, respectively) or sh*Fsp27* specific adenovirus (shFSP27: light dark or dark respectively). Error bars represent the mean ±standard error of the mean (SEM) *<0,05 relative to Ad Libitum control; # < 0,05 relative to fasting control.

3.2.4 Hepatic Fsp27β expression affects the expression of PPARα target genes in Brown Adipose Tissue

The increase in the levels of phospholipids in serum of *Fsp27β* knockdown animals (Figure R 18) correlates with a decrease in PPARα late fasting responsive genes, such as *Fgf21* and *Hmgcs2* (Fig 16). Therefore, it is possible that endogenous PPARα ligands are being secreted from the liver, losing lipid droplet formation capacity. To further study the implications of the absence of *Fsp27β* in liver, the expression pattern of PPARα target genes were also studied in BAT and muscle (Figure R 19).

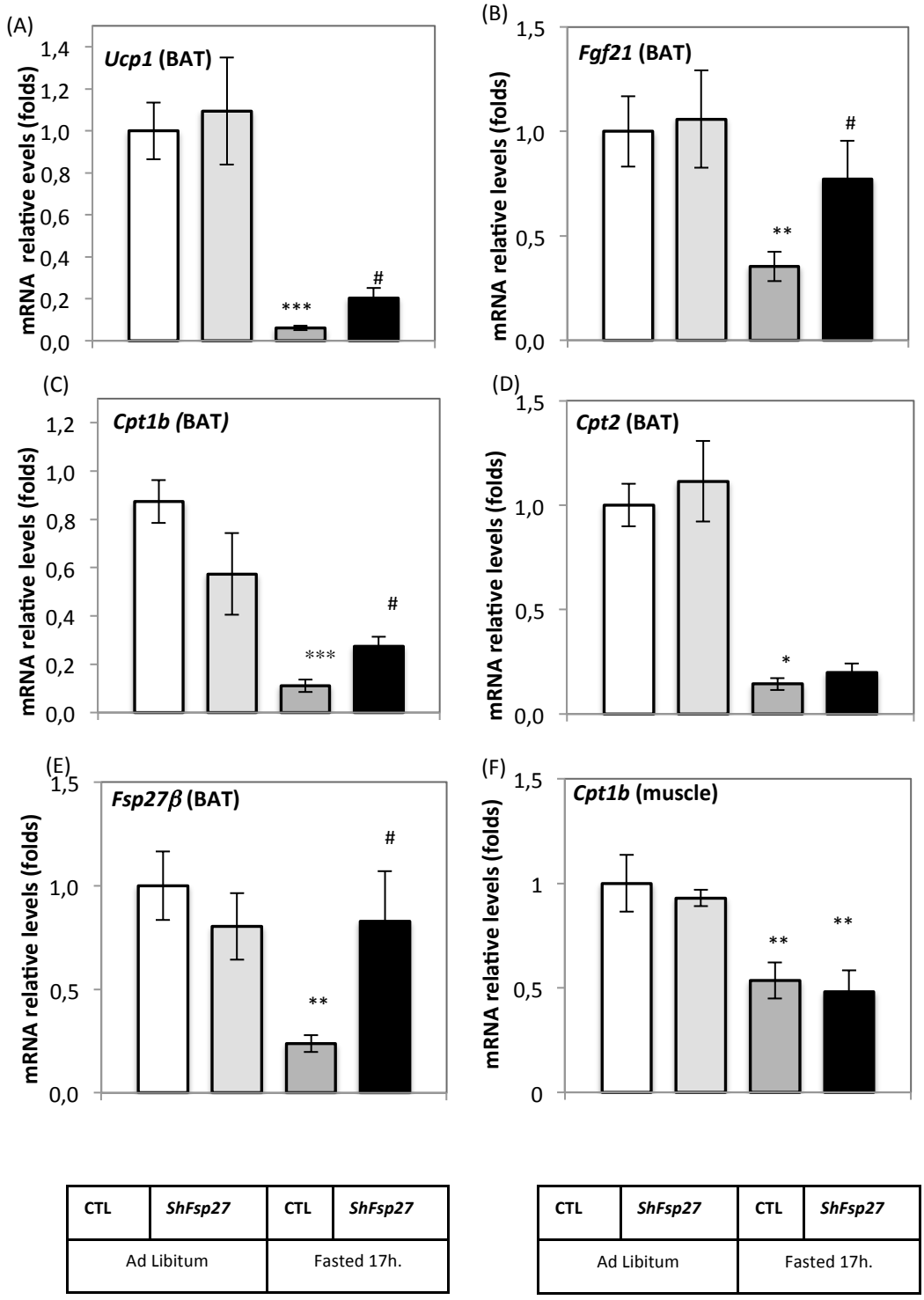

Figure R 19. Effects of liver knockdown in extra-hepatic tissues. Gene expression in BAT and muscle soleus of mice fed Ad Libitum or fasted for 17 hours treated with shRNA control adenovirus (CTL: white or dark grey bars, respectively) or sh*Fsp27* specific adenovirus (shFSP27: light dark or dark respectively). (A-E) BAT *Ucp1*, *Fgf21*, *Cpt1b*, *Cpt2*, *Fsp27b*, respectively. (F) Muscle *Cpt1b*. Error bars represent the mean ±standard error of the mean (SEM) *<0,05, **< 0,01 and *< 0,001 relative to Ad Libitum control; # < 0,05 relative to fasting control.**

Fasting down regulates *UcpI* (Figure R 19A), *Fgf21* (Figure R 19B), *Cpt1b* (Figure R 19C) and *Cpt2* (Fig 19D) in BAT, and this down regulation is partially restored in the BAT of the shFsp27β animals were the phospholipids levels in serum are increased, except for *Cpt2*. In Figure R 19 *Fsp27β* is down regulated by fasting and up regulated by liver knockdown. In muscle, fasting down regulates *Cpt1b*, but this effect is independent of the expression of *Fsp27β* in liver or phospholipids in serum.

Globally, these results suggest that during fasting, PPARα ligands are accumulated in the steatotic liver, preventing an excessive PPARα activity in BAT.

DISCUSSION

At the beginning of the 1960s, a diverse group of pesticides (clofibrate) was recognized as capable of causing the proliferation of peroxisomes in rat liver. Subsequently, it was identified that these compounds bound to a nuclear receptor that was known as peroxisome proliferator activated receptor (PPAR).

We now know that the endogenous ligands of PPAR are the fatty acids, or products derived from them like certain prostaglandins. PPARs are the way to regulate gene expression according to the availability of fatty acids.

The three PPARs, PPARα, PPARβ/δ and PPARγ, show distinct tissue distributions and regulate various aspects of lipid metabolism. The best-described functions for these receptors include the adipogenic and insulin-sensitizing effects of PPARγ and regulation of fatty acid catabolism/mitochondrial oxidative metabolism by PPARα and PPARδ in liver and muscle, respectively. In the liver, PPARα and PPARδ exhibit opposing activities in the control of diurnal lipid metabolism**.** PPARα is up-regulated in the fasted state to regulate fat catabolism (Kersten et al. 1999). By contrast, PPARδ is more active in the fed state and controls the transcription of lipogenic genes (Sanderson et al. 2010; S. Liu et al. 2011; S. Liu et al. 2013).

The most important contribution to identify the endogenous ligands of PPARα was made in the FASKOL animal model (Chakravarthy et al. 2005). This animal is unable to synthesize fats, and when fed with a zero fat diet and subjected to fasting, is hypoglycemic. In fact, this model shows a phenotype similar to a fasted PPARα knockout animal. By pharmacologically activating PPARα in the FASKOL mice, these effects were reversed. Thus, it can be said that metabolic abnormalities in FASKOL mice are driven by the failure to activate PPARα (Chakravarthy et al. 2005).

Therefore, in the absence of dietary fat, FAs synthesized *de novo* through FAS (fatty acid synthase) are able to act as PPARα ligands (Chakravarthy et al. 2005). Later on, the phospholipid 1-palmitoyl-2-oleoyl-sn-glycerol-3-phosphocholine (16:0/18:1 GPC) has been identified as an endogenous ligand with nanomolar affinity for

PPARα (Chakravarthy et al. 2010). This observation supports the model that only *"new fat",* either from the diet or from FAS-dependent synthesis, and not the *"old fat"* recruited from peripheral stores, produces PPARα ligands. Down regulation (siRNA) of CEPT1 (Kennedy pathway) decreased the expression of PPARα-dependent genes, that were rescued by exogenous 16:0/18:1-GPC. This line of evidence indicates that when 16:0/18:1-GPC binds to PPARα in the nucleus it activates the transcription machinery, inducing the expression of PPARα-dependent genes and affecting lipid metabolism(Chakravarthy et al. 2010).

However, this model generates a new paradox in the PPAR field. The expression of PPARα is circadian (Lemberger, Desvergne, and Wahli 1996), with a decrease of this receptor protein in the fed state and an increase during fasting, coinciding with the need for FA oxidation to maintain the energy balance. Since the 16:0/18:1 GPC production and peak of PPARα activity are anti-phasic, it could be postulated that if FAS is essential for producing the PPARα ligand, then additional regulation is required to present the ligand to PPARα when needed. In this Thesis, we are proposing that this additional mechanism could be related with lipid droplet formation during the early fasting period (see below).

The physiological role of PPARδ has been more elusive, although today we know that expression of PPARδ in liver is a key element in the production of lipids necessary for the activation of PPARα in liver and muscle.

PPARδ shows an ubiquitous pattern of expression. In muscle it is attributed a fundamental role in the regulation of mitochondrial fatty acid oxidation. Thus, overexpression of PPARδ in muscle increases the oxidative capacity in a very marked way. In fact, mice that express large amounts of PPARδ in muscle (marathon mice) can run for hours without stopping (Y. X. Wang et al. 2004).

However, in liver, PPARδ plays a lipogenic role as indicated by overexpression (adenovirus) experiments (S. Liu et al. 2011) or knockout animal models(C.-H. Lee et al. 2006). Recently, it has been shown that PPARδ controls diurnal expression of lipogenic genes in the dark/feeding cycle (S. Liu et al. 2013). Liver-specific PPARδ activation increases, whereas hepatocyte PPARδ deletion reduces, muscle fatty acid uptake. An unbiased metabolite profiling identified the phospholipid 1-oleico-2-oleoyl-sn-glycerol-3-phosphocholine (18:0/18:1 GPC) as a serum lipid regulated by diurnal hepatic PPARδ activity. Interestingly, 18:0/18:1-GPC reduces postprandial lipid levels and increases fatty acid use through muscle PPARα (S. Liu et al. 2013).

PPARδ expression peaks at night parallel to the mRNA levels of the molecular clock *Bmal1* in the liver. Therefore, it is feasible that hepatic PPARδ alters the expression of muscle genes and FA use through PC (18:0/18:1), indicating that an hepatic PPARδ-PC(18:0/18:1)-muscle PPARα signalling cascade coordinates fat synthesis and use.

That PPARα ligands are products of the *de novo* synthesis of FA illustrates a link between hepatic lipogenesis and peripheral FAO. This link can explain how tissues like muscle oxidize fatty acids, depending on circadian hepatic synthesis, at specific times coinciding to the animal activity. However, as mentioned before, the requirement of de novo synthesis to activate FAO presents a significant problem during the fasting state, where PPAR in liver becomes active to promote FAO and ketogenesis, but there is not any endogenous ligand supply available by diet or de novo synthesis.

During periods of fasting, the liver needs to adapt its metabolism to maintain the production of glucose and keep a state of normoglycemia. Gluconeogenesis takes action when the reducing power (NADH) is made available through the mitochondrial oxidation of FAs mobilized from WAT during fasting (McGarry and Foster 1995). The liver synthesizes ketone bodies, which are soluble products of incomplete oxidation of FAs that, in addition to replace glucose as an energy source, increases the FAO rate (Vilà-Brau et al. 2011b). As proposed by Denis McGarry in 1980 (McGarry and Foster 1995) a powerful oxidation of fatty acids is needed to maintain normoglycemia (Vilà-

Brau et al. 2013). More relevant, ketogenesis is needed to maintain the β-oxidation flux of fatty acids, probably because releases free CoA from the acyl-CoA allowing the activation of new acyl molecules. In agreement, *Hmgcs2*, the gene that controls ketogenesis (Ayté et al. 1990), is involved in the induction of fatty acid oxidation mediated by PPARα in HepG2 cell line(Vilà-Brau et al. 2011b). Thus, the expression of a specific shRNA in liver of fasted animals, that reduced hepatic *Hmgcs2* activity by 50%, correlated with a 20% decrease in liver FAO(Vilà-Brau et al. 2013).

Seeking for new mechanisms involved in liver gene expression during starvation, a microarray was performed to compare the expression pattern of wild type with HMGCS2 knockdown animals. One of the genes that was up regulated when ketogenesis, and therefore FAO, was blocked was *Fsp27β/CIDEC*. Similar result was obtained when a pharmacological inhibition of CPT1A was used to blunt FAO in liver(Vilà-Brau et al. 2013).

Fsp27β (formerly referred as *Fsp27*) shows a peculiar pattern of expression during liver adaptation to fasting (Figure R1). Thus, is highly expressed in the early period (6 h) of fasting but over longer periods of fasting (15-24 h), the expression of *Fsp27β* decreases. FSP27 is as a lipid-droplet formation protein, and its induction during fasting was unexpected. Nonetheless, in humans more than 60% of the FAs that reach the liver during fasting are re-esterified (Kalhan et al. 2001) and a futile cycle of TG/FA has been proposed in fasting (Hanson and Reshef 2003). Interestingly, FSP27β was shown to be a direct mediator of PPARγ-dependent hepatic steatosis(Yu et al. 2003), and that forced expression of recombinant tagged-FSP27α in hepatocytes significantly decreases mitochondrial β-oxidation (Matsusue et al. 2008). This observation suggests that expression of FSP27β may promote LD formation in hepatocytes. The LDs created will transitorily accommodate, not only the flood of fatty acids coming from WAT, but also the endogenous phospholipids needed for the LDs generation. In concordance, *Fsp27β* expression drops when PPARα target genes are robustly expressed (> 15 h of fasting) and FAO is rate is maxim (Puri et al. 2007). Hence, we hypothesize that

FSP27β, in addition to participate in the accumulation/export of the newly synthesized TGs may also be involved in PPARα signaling in the steps of adaptation to fasting.

From this point, two main objectives were set to understand:

1) If the peculiar pattern of Fsp27β expression in liver plays a role in PPARα signaling by accumulating/liberating specific endogenous ligands.
2) The transcriptional mechanisms responsible for the drop of Fsp27β expression during late fasting.

The discovery of two forms of FSP27 (α and β) (Xu et al. 2015) did not change our first objective since FSP27β is the main form expressed in liver (Figure 1 and (Xu et al. 2015)). However, it affects our strategy of studying the role of FSP27β in liver. A floxed mouse line was generated in which the first loxP site was introduced in the first intron of the *Fsp27* gene (Tanaka et al. 2015), before discovering that *Fsp27* gene has an alternative promoter that drives the expression of β isoform (Xu et al. 2015). Sequence of the floxed allele (A. Baldan, personal communication) shows that the loxP sequence disturbed the CREBH element, present upstream of exon 1B, that is essential for it expression (Figures 6-8 and (Xu et al. 2015)), therefore this animal has down regulated the CREBH-dependent Fsp27β expression in all tissues and was discarded for this study.

Therefore, we decided to use adenovirus-mediated interference, to acute down regulate Fsp27β expression in liver of fasted animals, and study the effect of iRNA in TAG and GPC (18:0/18:1, and 16:0/18:1) levels in liver and serum. In addition, we studied in this experimental model, the expression pattern of bona fide PPARα target genes in liver, WAT, BAT and muscle.

Our data indicates that while *Fsp27β* does not appear to have an impact in total TAG in the serum of starved animals (Figure R 17A), however, it appears critical for the liver

steatosis induced by fasting (Figure R 17B). Importantly, liver *Fsp27β* expression appears also important for TAG accumulation in liver under feeding conditions (Figure R 17B). Fasting reduces the analyzed GPC in serum, but in the animals lacking hepatic Fsp27β, the phospholipids in serum are higher (Figure R 18). Therefore, despite the role of *Fsp27β* in liver lipid droplet formation, this result encouraged the analysis of PPARα-target gene expression in liver and extrahepatic tissues, since it appears that PPARα ligands are overflowing in a liver that lacks *Fsp27β* expression. It is important to note that in untreated animals, fasting induces serum TAG (Figure R 17A) but reduced serum phospholipids (Figure R 17B), that is probable related with the precedence of TAG (WAT) and phospholipids (liver).

Overflow of PPARα ligands from liver correlates with lower expression of PPARα-target genes (Figure R 16). However, not all transcripts characterized as PPARα target respond in the liver to *Fsp27β* knock down. In fact, the loss of *Fsp27β* induction during fasting (Figure R 15) appears to affect mostly genes that show a late induction during fasting, like *Fgf21* (Figure R 16A)(Estall et al. 2009) or *Hmgcs2* (Figure R 16B) (Vilà-Brau et al. 2013), rather than early responsive genes like *Cpt2* (Figure R 16 C)(Vilà-Brau et al. 2013). This observation reinforces our proposed model for PPARα signaling during fasting. In addition, no effect was observed in a muscle PPARα target gene (Figure R 19F), suggesting that further signals are necessary for the expression of those genes, which are not present during nutrient sparseness.

The role of PPARα signaling in BAT is quite intriguing since down-regulation of Fsp27β in liver avoids the hepatic steatosis (Figure R 17B) without any stimulation of liver FAO (Figure R 16 and (Langhi and Baldán 2014)) nor serum TAG (Figure R 17A and (Langhi and Baldán 2014)). The induction of *Fsp27β* in BAT (Figure R 17E) indicates that our adenovirus specifically targets the liver of treated animals and hits inside the open debate about if *Fsp27* is a PPARα target gene. Others (Matsusue et al. 2008) and we (Vilà-Brau et al. 2013) have indicated that liver expression of *Fsp27β* is not dependent of PPARα signaling. However, Baldan group had shown that Fsp27β expression is stimulated by pharmacological activation of PPARα (Langhi and Baldán 2014), despite

no induction by fasting was observed in a PPARα knock out mice (Langhi and Baldán 2014). The result shown here (Figure R 17E) could somehow conciliate contradictory data, since appears that *Fsp27β* could be a target of PPARα in extrahepatic tissues.

As so, the induction of PPARα signaling in BAT, during lack of hepatic *Fsp27β* expression, uncovered an adaptative mechanism in which the fatty acids obtained from diet or the liver de novo synthesis will regulate FAO in extra-hepatic tissues.

The report of the β form (Xu et al. 2015) generated from an alternative promoter has an obviously impact regarding our second of our objective in this Thesis, the mechanism that controls *Fsp27β* expression during early and late fasting. In the putative role of the *Fsp27β* on PPARa signaling could be important the induction during the early fasting, but also the down-regulation observed during late fasting (Figure R 2 and(Vilà-Brau et al. 2013)).

The gene transcription program during the liver-fasting adaptation can be divide into two temporally phases separated by the status of SIRT1 activation (Dominy et al. 2010). With sustained fasting (>12–18 h), SIRT1 becomes activated and deacetylates proteins like CRTC2 (Y. Liu et al. 2009) or CREBH(Hyunbae Kim et al. 2015c). This event allows the ubiquitination of the protein and subsequent degradation (Y. Liu et al. 2009). *Fsp27β* expression was induced in the liver of SIRT1 KO animal (Vilà-Brau et al. 2013), and originally a role for CRTC2 was proposed in the early expression of FSP27, suggesting that CRTC2 degradation could be involved in *Fsp27* down regulation during late fasting (Vilà-Brau et al. 2013). Nonetheless, we now know that the liver expresses only the beta form of FSP27, through a mechanism that involves CREBH (Xu et al. 2015). Thus, a more plausible pathway is that deacetylation events mediated by SIRT1 attenuate CREBH activity (Hyunbae Kim et al. 2015c) and diminish *Fsp27β* expression during late fasting.

In fact, we show herein that expression (Figure 3A) and acetylation status of CREBH (Figure 7) is important for its transcriptional activity on the *Fsp27β* promoter.

However, the exact mechanism is still elusive since PPARα appears not to be involved in *Fsp27β* liver expression (Figure 6 and(Vilà-Brau et al. 2013; Matsusue et al. 2008)).

Other possible mechanism for the down regulation of *Fsp27β* is the existence of a repressor expressed and/or activated during long fasting period. We studied the putative role of REV-ERBα and HNF6 since deletion of each of those genes generates animal models with hepatic steatosis (Y. Zhang et al. 2016b). In addition, the expression pattern of REV-ERBα was compatible with this role (Figure R 3B), and a putative binding site of Rev-Erbα has been described in the 5´ flanking region of mouse *Fsp27* gene by Chromatin Immunoprecipitation analysis. Lack of response of the cloned promoter to ROR and REV-ERBα (Figure R 9) was probably due to the length of the cloned promoter (Figure R 5). Please note that ChIp analysis were performed with wild type and DBD mutant proteins. REV-ERBα can repress gene expression in a tissue specific way by interacting with tissue specific factors like HNF6 (Y. Zhang et al. 2016b). In our hands, HNF6 was capable to reduce reporter assay activities, but promoter-deletion experiments shows that this effect map in the CREBH responsive element, suggesting a non-physiologic squelching phenomena (Figure R 12).

That PPARα ligands are products of the de novo synthesis of FA provides a link between hepatic lipogenesis and peripheral FAO. This link can explain how tissues like muscle oxidize fatty acids, depending on circadian hepatic synthesis (S. Liu et al. 2013), at specific times coinciding to the animal activity. However, the requirement of de novo synthesis to activate FAO presents a significant problem during the fasting state, where PPARα in liver becomes active to promote FAO and ketogenesis (Kersten et al. 1999), but there is not any endogenous ligand supply available by diet or de novo synthesis. In HepG2 cells, the forced expression of FSP27α, blunts the PPARα response when measured by using a PPRE-TK reporter (Figure R 14). The response of the luciferase can be rescued, in the presence of FSP27α, by using a synthetic ligand of PPARα. That the synthetic ligand did not have an effect in the absence of PPARα was attributed to the presence of endogenous ligands that, after all, make the assay works.

The peculiar expression pattern of *Fsp27β* during fasting (Vilà-Brau et al. 2013) may explain at least in part this paradox. The liver of a fasted animal becomes steatotic during fasting because of the fatty acids (NEFA) coming from white adipose tissue, where lipolysis is stimulated. In the liver, these fatty acids can serve as fuel to produce ATP and reducing power necessary for gluconeogenesis(McGarry and Foster 1995). The fatty acids liberated from the adipose tissue are not capable to activate PPARα, but could increase, via CREBH, *Fsp27β* expression (Xu et al. 2015; Jaeger et al. 2015), thus promoting the generation of LDs. The LDs created will transitorily accommodate, not only the flood of fatty acids coming from WAT, but also the endogenous phospholipids, needed for the LDs generation.

Therefore, we speculate that in liver during the early fasting, *Fsp27β* expression allows trapping of endogenous newly synthetized PPARα ligands, which in fed condition will be acting as PPARα activators in extra hepatic tissues. During late fasting, physiologic down regulation of *Fsp27β* will allow PPARa activation characteristic of the fasted liver. According with this hypothesis, when we turn down liver *Fsp27β* expression, the serum of these animals carries higher concentration of PPARα endogenous ligands (Figure R 18B). This effect correlates with a higher expression of PPARα target genes in BAT (Figure R 19 A-E) and lower in liver (Figure R 16).

In summary, our model proposes that during early fasting fatty acids delivered by WAT will induce, through CREBH-FSP27β axis, the formation of LDs in liver, which are needed to produce a transitory steatosis and, in addition, avoid the release of endogenous PPARα ligands from the liver. Conversely, during the late fasting, SIRT1 activity, also through CREBH modulation (Figure R 7), will mediate FSP27 clearance from a liver that is already prepared to oxidize fatty acids. In turn, the increased FAO capacity from liver could alleviated ER stress contributing to CREBH downregulation. During fed states, the absence of *Fsp27β* in liver will allow the new synthetized fat to leave the liver and actuate as PPARα agonist in extrahepatic tissues like BAT. Our working hypothesis is summarized in scheme I.

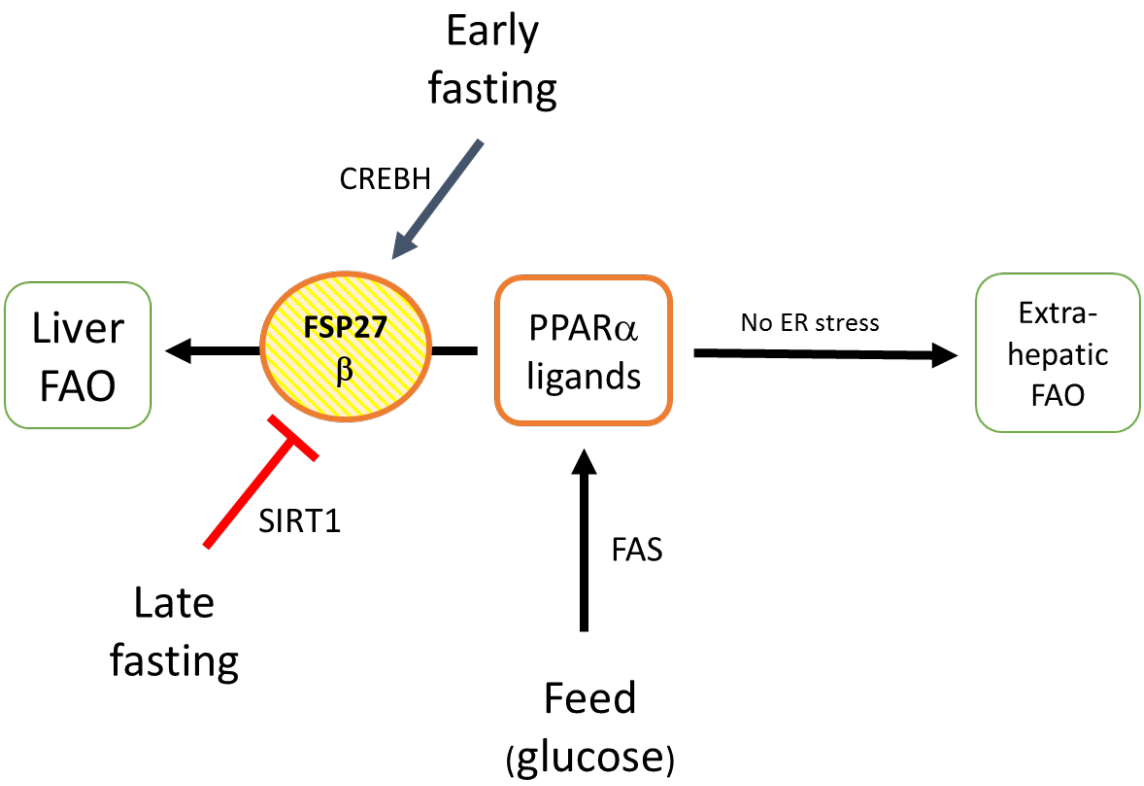

Scheme I.- putative role of FSP27β during the transition od early to late fasting in liver. Early response (CREBH) will allow accumulation of NEFA and PGC. Late downregulation (SIRT1) will be concomitant to strong FAO.

CONCLUSIONS

FSP27 isoform expression

Fsp27β is the main isoform expressed in tissues that actively oxidize fatty acids such as liver and BAT. However, its function must be broader because its expression is also predominant, with respect to Fsp27α, in the small intestine.

The expression of Fsp27β fluctuates in the liver during fasting: it increases during the early fasting (<12h) but decreases during the late fasting (> 12h), according with a more complex function than the simple accumulation of NEFAs, coming from the WAT, prior to their oxidation.

FSP27β Transcriptional regulation

Fsp27β is a target gene of CREBH, but not of PPARα. There is no cross talk between both transcription factors in the hepatic expression of Fsp27β.

Fsp27β expression depends on the level of acetylation of CREBH. This data could explain, at least in part, the expression pattern of Fsp27β during prolonged fasting where the acetylation state of CREBH diminishes.

FSP27β Function

FSP27β expression is necessary for the hepatic accumulation of TAG in liver and plays a fundamental role in the development of the physiological hepatic steatosis that occurs during fasting during.

The hepatic expression of FSP27β is necessary for the correct signaling of PPARa during fasting at least in part because FSP27β plays a key role in the storage/release of phospholipids proposed as endogenous ligands of PPARa form the liver lipid droplets.
In vitro, Fsp27β interferes with the PPARα signaling as it was determined by the use of a TK-luciferase reporter under the control of three PPRE.

Lack of Fsp27β expression Increases the concentration of PPARα endogenous ligands in serum, which triggers the PPARα signaling of in peripheral tissues such as BAT, while decreasing its signaling in the liver. Concretely, Fsp27β plays a role in the down-regulation of PPARα target genes in BAT during fasting.

References

Altarejos, J.Y., and M. Montminy. 2011. “CREB and the CRTC Co-Activators: Sensors for Hormonal and Metabolic Signals.” *Nat Rev Mol Cell Biol* 12: 141–51.

Ayté, J, G Gil-Gómez, D Haro, P F Marrero, and F G Hegardt. 1990. “Rat Mitochondrial and Cytosolic 3-Hydroxy-3-Methylglutaryl-CoA Synthases Are Encoded by Two Different Genes.” *Proceedings of the National Academy of Sciences of the United States of America* 87 (May): 3874–78. doi:10.1073/pnas.87.10.3874.

Badman, Michael K., Pavlos Pissios, Adam R. Kennedy, George Koukos, Jeffrey S. Flier, and Eleftheria Maratos-Flier. 2007. “Hepatic Fibroblast Growth Factor 21 Is Regulated by PPARα and Is a Key Mediator of Hepatic Lipid Metabolism in Ketotic States.” *Cell Metabolism* 5: 426–37. doi:10.1016/j.cmet.2007.05.002.

Barish, Grant D, Vihang a Narkar, and Ronald M Evans. 2006. “PPAR Delta: A Dagger in the Heart of the Metabolic Syndrome.” *The Journal of Clinical Investigation* 116 (3): 590–97. doi:10.1172/JCI27955.

Burris, T. P.. 2008. “Nuclear Hormone Receptors for Heme: Rev-Erb and Rev-Erb Are Ligand-Regulated Components of the Mammalian Clock.” *Molecular Endocrinology* 22 (February): 1509–20. doi:10.1210/me.2007-0519.

Burstein, R, M Ashina, K Nozaki, R P Kraig, N T Zervas, M a Moskowitz, S a Raymond, and R Burstein. 2013. “A Circadian Rhythm Orcheastrated by Histone Deacetylase 3 Controls Lipid Metabolism” 339 (March): 1095–99. doi:10.1126/science.1229223.

Chakravarthy, Manu V, Irfan J Lodhi, Li Yin, Raghu R V Malapaka, H Eric Xu, and Clay F Semenkovich. 2010. “Identification of a Physiologically Relevant Endogenous Ligand for PPARa in Liver” 138 (3): 476–88. doi:10.1016/j.cell.2009.05.036.Identification.

Chakravarthy, Manu V, Zhijun Pan, Yimin Zhu, Karen Tordjman, Jochen G Schneider, Trey Coleman, John Turk, and Clay F Semenkovich. 2005. “‘New’ Hepatic Fat

Activates PPARalpha to Maintain Glucose, Lipid, and Cholesterol Homeostasis." *Cell Metabolism* 1 (5): 309–22. doi:10.1016/j.cmet.2005.04.002.

Danesch, U., W. Hoeck, and G. M. Ringold. 1992. "Cloning and Transcriptional Regulation of a Novel Adipocyte-Specific Gene, FSP27. CAAT-Enhancer-Binding Protein (C/EBP) and C/EBP-like Proteins Interact with Sequences Required for Differentiation-Dependent Expression." *Journal of Biological Chemistry* 267 (8): 7185–93.

Danno, H., K.A. Ishii, Y. Nakagawa, M. Mikami, T. Yamamoto, S. Yabe, M. Furusawa, S. Kumadaki, K. Watanabe, and H. Shimizu. 2010. "The Liver-Enriched Transcription Factor CREBH Is Nutritionally Regulated and Activated by Fatty Acids and PPARalpha." *Biochem Biophys Res Commun* 391: 1222–27.

Desvergne, B, Liliane Michalik, and Walter Wahli. 2006. "Transcriptional Regulation of Metabolism." *Physiological Reviews* 86: 465–514. doi:10.1152/physrev.00025.2005.

Dominy, John E., Yoonjin Lee, Zachary Gerhart-Hines, and Pere Puigserver. 2010. "Nutrient-Dependent Regulation of PGC-1a's Acetylation State and Metabolic Function Through the Enzymatic Activities of Sirt1/GCN5." *Biochim Biophys Acta.* 1804 (8): 1676–83. doi:10.1016/j.bbapap.2009.11.023.

Duez, Hélène, and Bart Staels. 2008. "Rev-Erbα Gives a Time Cue to Metabolism." *FEBS Letters* 582: 19–25. doi:10.1016/j.febslet.2007.08.032.

Estall, Jennifer L, Jorge L Ruas, Cheol Soo Choi, Dina Laznik, Michael Badman, Eleftheria Maratos-Flier, Gerald I Shulman, and Bruce M Spiegelman. 2009. "PGC-1alpha Negatively Regulates Hepatic FGF21 Expression by Modulating the heme/Rev-Erb(alpha) Axis." *Proceedings of the National Academy of Sciences of the United States of America* 106: 22510–15. doi:10.1073/pnas.0912533106.

Evans, Ronald M. 2004. "PPARs and the Complex Journey to Obesity." *Keio Journal of Medicine* 53 (4): 53–58. doi:10.2302/kjm.53.53.

Feige, J.N., L. Gelman, L. Michalik, B. Desvergne, and W. Wahli. n.d. “From Molecular Action to Physiological Outputs: Peroxisome Proliferator-Activated Receptors Are Nuclear Receptors at the Crossroads of Key Cellular Functions.” *Prog Lipid Res* 45: 120–59.

Gong, Jingyi, Zhiqi Sun, and Peng Li. 2009. “CIDE Proteins and Metabolic Disorders.” *Current Opinion in Lipidology* 20: 121–26. doi:10.1097/MOL.0b013e328328d0bb.

Hanson, R.W., and L. Reshef. 2003. “Glyceroneogenesis Revisited.” *Biochimie* 85: 1199–1205.

Hegardt, F.G. 1995. “Regulation of Mithocondrial 3-Hydroxy-3-Methylglutaryl-CoA Synthase Gene Expression in Liver and Intestine from the Rat.” *Biochem Soc Trans* 23: 486–90.

Hsu, M.H., U. Savas, K.J. Griffin, and E.F. Johnson. 2001. “Identification of Peroxisome Proliferator-Responsive Human Genes by Elevated Expression of the Peroxisome Proliferator-Activated Receptor Alpha in HepG2 Cells.” *J Biol Chem* 276: 27950–58.

Inagaki, T., P. Dutchak, G. Zhao, X. Ding, V. Gautron, L., Parameswara, and et al. Li, Y., Goetz, R., Mohammadi, M., Esser, V. 2007. “Endocrine Regulation of the Fasting Response by PPARalpha-Mediated Induction of Fibroblast Growth Factor 21.” *Cell Metabolism* 5: 415–25.

Inohara, Naohiro, Takeyoshi Koseki, Shu Chen, Xiaoyu Wu, and Gabriel Núñez. 1998. “CIDE, a Novel Family of Cell Death Activators with Homology to the 45 kDa Subunit of the DNA Fragmentation Factor.” *EMBO Journal* 17 (9): 2526–33. doi:10.1093/emboj/17.9.2526.

Jaeger, D., G. Schoiswohl, Schreiber Hofer, P., Schweiger R., Eichmann M., Pollak T.O., N.M. Poecher, Grabner N., and et al. G.F., Zierler, K.A. 2015. “Fasting-Induced G0_G1 Switch Gene 2 and FGF21 Expression in the Liver Are under Regulation of Adipose Tissue Derived Fatty Acids.” *Journal of Hepatology* 63: 437–45.

Jones, Julie R, Cordelia Barrick, Kyoung-Ah Kim, Jill Lindner, Bertrand Blondeau, Yuka Fujimoto, Masakazu Shiota, Robert a Kesterson, Barbara B Kahn, and Mark a Magnuson. 2005. “Deletion of PPARgamma in Adipose Tissues of Mice Protects against High Fat Diet-Induced Obesity and Insulin Resistance.” *Proceedings of the National Academy of Sciences of the United States of America* 102 (17): 6207–12. doi:10.1073/pnas.0306743102.

Kalhan, Satish C., Supriya Mahajan, Edward Burkett, Lea Reshef, and Richard W. Hanson. 2001. “Glyceroneogenesis and the Source of Glycerol for Hepatic Triacylglycerol Synthesis in Humans.” *Journal of Biological Chemistry* 276 (16): 12928–31. doi:10.1074/jbc.M006186200.

Kersten, S, J Seydoux, J M Peters, F J Gonzalez, B Desvergne, and W Wrahli. 1999. “Peroxisome Proliferator-Activated Receptor Alpha Mediates the Adaptive Response to Fasting.” *Journal of Clinical Investigation* 103 (11): 1489–98. doi:10.1172/JCI6223.

Kharitonenkov, A. Shiyanova, T.L., A. Koester, A.M. Ford, R. Micanovic, E.J. Galbreath, L.J. Sandusky, G.E., Hammond, J.S. Moyers, and R.A. Owens. 2005. “FGF-21 as a Novel Metabolic Regulator.” *J Clin Invest*, no. 115: 1627–35.

Kim, H., R. Mendez, Z. Zheng, L. Chang, J. Cai, R. Zhang, and K. Zhang. 2014. “Liver-Enriched Transcription Factor CREBH Interacts with Peroxisome Proliferator-Activated Receptor A to Regulate Metabolic Hormone FGF21.” *Endocrinology* 155: 769–82.

Kim, Hyunbae, Roberto Mendez, Xuequn Chen, Deyu Fang, and Kezhong Zhang. 2015a. “Lysine Acetylation of CREBH Regulates Fasting-Induced Hepatic Lipid Metabolism.” *Molecular and Cellular Biology* 35 (October): 4121–34. doi:10.1128/MCB.00665-15.

Kim, J.H., J. Song, and K.W. Park. 2015. “The Multifaceted Factor Peroxisome Proliferator-Activated Receptor Γ (PPARγ) in Metabolism, Immunity, and Cancer.” *Arch Pharm Res* 38: 302.312.

Krahmer, N., Y. Guo, F. Wilfling, M. Hilger, S. Lingrell, K. Heger, H.W. Newman, D.E. Schmidt-Supprian, M. Vance, and et al Mann, M. 2011. “Phosphatidylcholine Synthesis for Lipid Droplet Expansion Is Mediated by Localized Activation of CTP:phosphocholine Cytidylyltransferase.” *Cell Metab* 14: 504–15.

Krahmer, Natalie, Robert V. Farese, and Tobias C. Walther. 2013. “Balancing the Fat: Lipid Droplets and Human Disease.” *EMBO Molecular Medicine* 5: 905–15. doi:10.1002/emmm.201100671.

Langhi, Cédric, and Ángel Baldán. 2014. “CIDEC/Fsp27 Is Regulated by PPARα and Plays a Critical Role in Fasting- and Diet-Induced Hepatosteatosis.” *Hepatology*, November, n/a – n/a. doi:10.1002/hep.27607.

Lay, John Le, Geetu Tuteja, Peter White, Ravindra Dhir, Rexford Ahima, and Klaus H Kaestner. 2010. “CRTC2 (TORC2) Contributes to the Transcriptional Response to Fasting in the Liver but Is Not Required for the Maintenance of Glucose Homeostasis.” *Molecular and Cellular Biology* 10 (1): 55–62. doi:10.1016/j.cmet.2009.06.006.CRTC2.

Lazar, M.A. 2002. “Becoming Fat.” *Genes Dev* 16: 1–5.

Lee, Chih-Hao, Peter Olson, Andrea Hevener, Isaac Mehl, Ling-Wa Chong, Jerrold M Olefsky, Frank J Gonzalez, et al. 2006. “PPARδ Regulates Glucose Metabolism and Insulin Sensitivity.” *Proceedings of the National Academy of Sciences of the United States of America* 103: 3444–49. doi:10.1073/pnas.0511253103.

Lee, J.H., P. Giannikopoulos, S.A. Duncan, J. Wang, C.T. Johansen, J.D. Brown, J. Plutzky, R.A. Hegele, L.H. Glimcher, and A.H. Lee. 2011. “The Transcription Factor Cyclic AMP-Responsive Element-Binding Protein H Regulates Triglyceride Metabolism.” *Nat Med*, no. 17: 812–15.

Lee, M.W., D. Chanda, J. Yang, H. Oh, S.S. Kim, Y.S. Yoon, S. Hong, K.G. Park, I.K. Lee, and C.S. et al. Choi. 2010. “Regulation of Hepatic Gluconeogenesis by an ER-Bound Transcription Factor, CREBH.” *Cell Metab*, no. 11: 331–39.

Lehmann, J M, L B Moore, T a Smith-Oliver, W O Wilkison, T M Willson, and S a Kliewer. 1995. “An Antidiabetic Thiazolidinedione Is a High Affinity Ligand for Peroxisome Proliferator-Activated Receptor Gamma (PPAR Gamma).” *The Journal of Biological Chemistry*. doi:10.1074/jbc.270.22.12953.

Lemberger, T, B Desvergne, and W Wahli. 1996. “Peroxisome Proliferator-Activated Receptors: A Nuclear Receptor Signaling Pathway in Lipid Physiology.” *Annu Rev Cell Dev Biol* 12: 335–63. doi:10.1146/annurev.cellbio.12.1.335.

Liu, Sihao, Jonathan D Brown, Kristopher J Stanya, Edwin Homan, Mathias Leidl, Karen Inouye, Prerna Bhargava, et al. 2013. “A Diurnal Serum Lipid Integrates Hepatic Lipogenesis and Peripheral Fatty Acid Use.” *Nature* 502: 550–54. doi:10.1038/nature12710.

Liu, Sihao, Ben Hatano, Minghui Zhao, Chen Chung Yen, Kihwa Kang, Shannon M. Reilly, Matthew R. Gangl, et al. 2011. “Role of Peroxisome Proliferator-Activated Receptor Δ/β in Hepatic Metabolic Regulation.” *Journal of Biological Chemistry* 286 (2): 1237–47. doi:10.1074/jbc.M110.138115.

Liu, Yi, Renaud Dentin, Danica Chen, Susan Hedrick, Kim Ravnskjaer, Jill Milne, David J Meyers, et al. 2009. “A Fasting Inducible Switch Modulates Gluconeogenesis Via Activator-Coactivator Exchange” 456 (7219): 269–73. doi:10.1038/nature07349.A.

Matsusue, Kimihiko, Takashi Kusakabe, Takahiro Noguchi, Shouichi Takiguchi, Toshimitsu Suzuki, Shigeru Yamano, and Frank J Gonzalez. 2008. “Hepatic Steatosis in Leptin-Deficient Mice Is Promoted by PPARγ Target Gene, Fat-Specific Protein 27.” *Cell* 7 (4): 302–11. doi:10.1016/j.cmet.2008.03.003.Hepatic.

McGarry, J.D., and D.W. Foster. 1995. “Regulation of Hepatic Fatty Acid Oxidation and Ketone Body Production.” *Annu Rev Biochem* 49: 395–420.

Monsalve, F a, R D Pyarasani, F Delgado-Lopez, and R Moore-Carrasco. 2013. "Peroxisome Proliferator-Activated Receptor Targets for the Treatment of Metabolic Diseases." *Mediators of Inflammation* 2013: 549627. doi:10.1155/2013/549627.

Nadal, Alı, Pedro F Marrero, and Diego Haro. 2002. "Down-Regulation of the Mithocondrial 3-Hydroxy-3-Methylglutaril-CoA Synthase Gene by Insulin: The Role of the Forkhead Transcription Factor FKRL1" 297: 289–97.

Napal, L., P.F. Marrero, and D. Haro. 2005. "An Intronic Peroxisome Proliferator-Activated Receptor-Binding Sequence Mediates Fatty Acid Induction of the Human Carnitine Palmitoyltransferase 1A." *Mol Biol* 354: 751–59.

Nemoto, Shino, Maria M. Fergusson, and Toren Finkel. 2004. "Nutrient Availability Regulates SIRT1 Through a Forkhead-Dependent Pathway." *Science* 306: 2105–8. doi:10.1126/science.1101731.

Nishimoto, Yuki, Shinsuke Nakajima, Sanshiro Tateya, Masayuki Saito, Wataru Ogawa, and Yoshikazu Tamori. 2017. "Cell Death-Inducing DNA Fragmentation Factor A-like Effector A and Fat-Specific Protein 27β Coordinately Control Lipid Droplet Size in Brown Adipocytes." *Journal of Biological Chemistry* 292: 10824–34. doi:10.1074/jbc.M116.768820.

Nishimoto, Yuki, and Yoshikazu Tamori. 2017. "CIDE Family-Mediated Unique Lipid Droplet Morphology in White Adipose Tissue and Brown Adipose Tissue Determines the Adipocyte Energy Metabolism." *J Atheroscler Thromb* 24: 0–0. doi:10.5551/jat.RV17011.

Nishino, Naonobu, Yoshikazu Tamori, Sanshiro Tateya, Takayuki Kawaguchi, Tetsuro Shibakusa, Wataru Mizunoya, Kazuo Inoue, et al. 2008. "FSP27 Contributes to Efficient Energy Storage in Murine White Adipocytes by Promoting the Formation of Unilocular Lipid Droplets" 118 (8). doi:10.1172/JCI34090DS1.

Ong, Kuok Teong, Mara T. Mashek, So Young Bu, Andrew S. Greenberg, and Douglas G. Mashek. 2011. “Adipose Triglyceride Lipase Is a Major Hepatic Lipase That Regulates Triacylglycerol Turnover and Fatty Acid Signaling and Partitioning.” *Hepatology* 53 (1): 116–26. doi:10.1002/hep.24006.

Ortiz, J.A., J. Mallolas, C. Nicot, J. Bofarull, J.C. Rodriguez, F.G. Hegardt, D. Haro, and P.F. Marrero. 1999. “Isolation of Pig Mitochondrial 3-Hydroxy-3-Methylglutaryl-CoA Synthase Gene Promoter: Characterization of a Peroxisome Proliferator-Responsive Element.” *Biochem* 337(Pt2): 329–35.

Puri, Vishwajeet, Silvana Konda, Srijana Ranjit, Myriam Aouadi, Anil Chawla, My Chouinard, Abhijit Chakladar, and Michael P. Czech. 2007. “Fat-Specific Protein 27, a Novel Lipid Droplet Protein That Enhances Triglyceride Storage.” *Journal of Biological Chemistry* 282 (47): 34213–18. doi:10.1074/jbc.M707404200.

Rodríguez, Joan C., Gabriel Gil-Gómez, Fausto G. Hegardt, and Diego Haro. 1994. “Peroxisome Proliferator-Activated Receptor Mediates Induction of the Mitochondrial 3-Hydroxy-3-Methylglutaryl-CoA Synthase Gene by Fatty Acids.” *Journal of Biological Chemistry* 269: 18767–72.

Sanderson, Linda M, Mark V Boekschoten, Béatrice Desvergne, Michael Müller, and Sander Kersten. 2010. “Transcriptional Profiling Reveals Divergent Roles of PPARα and PPARβ/δ in Regulation of Gene Expression in Mouse Liver.” *Physiological Genomics* 41: 42–52. doi:10.1152/physiolgenomics.00127.2009.

Sever, Richard, and Christopher K Glass. 2013. “Signaling by Nuclear Receptors.” *Cold Spring Harb Perspect Biol* 5: a016709. doi:10.1101/cshperspect.a016709.

Tamori, Yoshikazu, Sanshiro Tateya, Takeshi Ijuin, Yuki Nishimoto, Shinsuke Nakajima, and Wataru Ogawa. 2016. “Negatively-Charged Residues in the Polar Carboxy-Terminal Region in FSP27 Are Indispensable for Expanding Lipid Droplets.” *FEBS Letters* 590: 750–59. doi:10.1002/1873-3468.12114.

REFERENCES

Tanaka, Naoki, Shogo Takahashi, Tsutomu Matsubara, Changtao Jiang, Wataru Sakamoto, Tatyana Chanturiya, Ruifeng Teng, Oksana Gavrilova, and Frank J. Gonzalez. 2015. “Adipocyte-Specific Disruption of Fat-Specific Protein 27 Causes Hepatosteatosis and Insulin Resistance in High-Fat Diet-Fed Mice.” *Journal of Biological Chemistry* 290: 3092–3105. doi:10.1074/jbc.M114.605980.

Tsai, Y.S., and Maeda, N. 2005. “PPARgamma: A Critical Determinant of Body Fat Distribution in Humans and Mice.” *Trends Cardiovasc Med* 15: 81–85.

Vilà-Brau, Anna, Ana Luísa De Sousa-Coelho, Joana F Gonçalves, Diego Haro, and Pedro F Marrero. 2013. “Fsp27/CIDEC Is a CREB Target Gene Induced during Early Fasting in Liver and Regulated by FA Oxidation Rate.” *Journal of Lipid Research* 54: 592–601. doi:10.1194/jlr.M028472.

Vilà-Brau, Anna, Ana Luísa De Sousa-Coelho, Cristina Mayordomo, Diego Haro, and Pedro F Marrero. 2011a. “Human HMGCS2 Regulates Mitochondrial Fatty Acid Oxidation and FGF21 Expression in HepG2 Cell Line.” *The Journal of Biological Chemistry* 286 (23): 20423–30. doi:10.1074/jbc.M111.235044.

Wang, Wenshan, Na Lv, Shasha Zhang, Guanghou Shui, Hui Qian, Jingfeng Zhang, Yuanying Chen, et al. 2012. “Cidea Is an Essential Transcriptional Coactivator Regulating Mammary Gland Secretion of Milk Lipids.” *Nature Medicine* 18 (2): 235–43. doi:10.1038/nm.2614.

Wang, Yong Xu, Chun Li Zhang, Ruth T. Yu, Helen K. Cho, Michael C. Nelson, Corinne R. Bayuga-Ocampo, Jungyeob Ham, Heonjoong Kang, and Ronald M. Evans. 2004. “Regulation of Muscle Fiber Type and Running Endurance by PPARδ.” *PLoS Biology* 2 (10). doi:10.1371/journal.pbio.0020294.

Wu, Congyang, Yinxin Zhang, Zhirong Sun, and Peng Li. 2008. “Molecular Evolution of Cide Family Proteins: Novel Domain Formation in Early Vertebrates and the Subsequent Divergence.” *BMC Evolutionary Biology* 8 (January): 159. doi:10.1186/1471-2148-8-159.

Wu, Zhidan, Evan D. Rosen, Regina Brun, Stefanie Hauser, Guillaume Adelmant, Amy E. Troy, Catherine McKeon, Gretchen J. Darlington, and Bruce M. Spiegelman. 1999. "Cross-Regulation of C/EBPα and PPARγ Controls the Transcriptional Pathway of Adipogenesis and Insulin Sensitivity." *Molecular Cell* 3: 151–58. doi:10.1016/S1097-2765(00)80306-8.

Xu, Xu, Jong-Gil Park, Jae-Seon So, and Ann-Hwee Lee. 2015. "Transcriptional Activation of Fsp27 by the Liver-Enriched Transcription Factor CREBH Promotes Lipid Droplet Growth and Hepatic Steatosis." *Hepatology* 61: 857–69. doi:10.1002/hep.27371.

Yu, Songtao, Kimihiko Matsusue, Papreddy Kashireddy, Wen Qing Cao, Vaishalee Yeldandi, Anjana V. Yeldandi, M. Sambasiva Rao, Frank J. Gonzalez, and Janardan K. Reddy. 2003. "Adipocyte-Specific Gene Expression and Adipogenic Steatosis in the Mouse Liver due to Peroxisome Proliferator-Activated Receptor γ1 (PPARγ1) Overexpression." *Journal of Biological Chemistry* 278 (1): 498–505. doi:10.1074/jbc.M210062200.

Zhang, C., G. Wang, Z. Zheng, K.R. Maddipati, X. Zhang, G. Dyson, P. Williams, S.A. Duncan, R.J. Kaufman, and K. Zhang. 2012. "Endoplasmic Reticulum-Tethered Transcription Factor cAMP Responsive Element-Binding Protein, Hepatocyte Specific, Regulates Hepatic Lipogenesis, Fatty Acid Oxidation, and Lipolysis upon Metabolic Stress in Mice." *Hepatology* 55: 1070–82.

Zhang, Yuxiang, Bin Fang, Manashree Damle, Dongyin Guan, Zhenghui Li, Yong Hoon Kim, Maureen Gannon, and Mitchell A Lazar. 2016a. "HNF6 and Rev-Erbα Integrate Hepatic Lipid Metabolism by Overlapping and Distinct Transcriptional Mechanisms." *Genes and Development* 30: 1636–44. doi:10.1101/gad.281972.116.

Zhang, Yuxiang, Bin Fang, Manashree Damle, Dongyin Guan, Zhenghui Li, Yonghoon Kim, Maureen Gannon, and Mitchell A. Lazar. 2016b. "HNF6 and Rev-Erb??

Integrate Hepatic Lipid Metabolism by Overlapping and Distinct Transcriptional Mechanisms." *Genes and Development*. doi:10.1101/gad.281972.116.

Zhang, Yuxiang, Bin Fang, Matthew J Emmett, Manashree Damle, Zheng Sun, Dan Feng, Sean M Armour, et al. 2015. "Discrete Functions of Nuclear Receptor Rev-Erbα Couple Metabolism to the Clock." *Science (New York, N.Y.)* 348 (6242): 1488–92. doi:10.1126/science.aab3021.

ANNEXES

ANNEX 1: LIST OF ABBREVIATURES

A

AcOH
: Acetic Acid

AML12
: Alpha Mouse Liver 12

B

BAT
: Brown Adipose Tissue

C

CE
: Collision Energy

CHCl3
: Chloroform

CHO
: Carbohydrate

CHRE
: CREBH Response Elements

CMV
: Citomegalovirus

Cpt1b
: Carnitine palmitoyltransferase I

Cpt2
: Carnitine palmitoyltransferase 2

CRE
: CREB Response Elements

CREB
: Creb-Responsive Element Binding Protein

CREBH
: cyclic-AMP-responsive element binding protein H

CsCl
: Caesium Chloride

Ct
: Threshold Cycle

CXP
: Colision Cell Exit Potential

D

DEPC
: Diethylpyrocarbonate

DMEM
: Dulbecco's Modified Eagle Medium

DMEM:F12
: Dulbecco's Modified Eagle Medium and Ham's F12 medium

DNA
: Deoxyribonucleic Acid

dNTPs
: Deoxyribonucleotide Triphosphate

DP
: Declustering Potential

F

FBS
Fetal Bovine Serum
FoxA2
Forkhead box A2
FoxO3a
Forkhead box O3a
FSP27
Fat-Specific Protein 27
Fsp27α:Fat-Specific Protein alpha
Fsp27β:Fat-Specific Protein beta

G

GFP
Green Fluorescence Protein

H

H2O
Water
HEK-293
Human Embryonic Kidney
HFD
High-Fat Diet
Hmgcs2
3-hydroxy-3-methylglutaryl-CoA synthase 2
HNF6
Hepatocyte Nuclear Factor 6
HPLC
High-Performance Liquid Chromatography

L

LC-MS
Liquid Chromatography - Mass Spectroscopy · 23

M

MEM
Eagle's Minimum Essential Medium · 11, 12
MeOH
Methanol · 22, 23
MRM
Multiple Reaction Monitoring · 23
mRNA
messeger RNA · 25, 65, 66
MS/MS
Mass spectrometry · 23
MTBE
Methyl-tert-butyl-ether · 22

P

PBS

Phosphate Buffer Solution

PC
Pyruvate Carboxylase

PCAF
P300/CBP-associated factor

PCR
Polymerase Chain Reaction

PPAR
Peroxisome Proliferator-Activated Receptor

PPRE
Peroxisome Proliferaor Responsive Element
Peroxisome Proliferator Responsive Element

Prot
Protein

Q

qPCR
quantitative real time Polymerase Chain Reaction

R

RNA
Ribonucleic Acid

RORa:Retinoid-related orphan receptor alpha

S

SEM
Standard Error of the Mean

shRNA
short hairpin RNA

SIRT1
Sirtuin 1

T

TAG
Triglycerides

TGF
Transforming Growth Factor

TK
Thymidine-Kinase

U

UcpI
Uncoupling protein one

Z

ZT
Zeitgeber time

ANNEX 2:A Low Protein Diet Induces Body Weight loss and Browning of subcutaneous White Adipose Tissue Through Enhanced Expression of Hepatic Fibroblast Growth Factor 21 (FGF21) – Article

RESEARCH ARTICLE

A low-protein diet induces body weight loss and browning of subcutaneous white adipose tissue through enhanced expression of hepatic fibroblast growth factor 21 (FGF21)

*Albert Pérez-Martí[1,2], Maite Garcia-Guasch[1,2], Anna Tresserra-Rimbau[1,3,4], Alexandra Carrilho-Do-Rosário[1,2], Ramon Estruch[4,5], Jordi Salas-Salvadó[4,6], Miguel Ángel Martínez-González[4,7], Rosa Lamuela-Raventós[1,3,4], Pedro F. Marrero[1,2], Diego Haro[1,2] and Joana Relat[1,2]**

[1] Department of Nutrition, Food Sciences and Gastronomy, School of Pharmacy and Food Science, University of Barcelona, Torribera Food Campus, Santa Coloma de Gramenet, Barcelona, Spain
[2] Institute of Biomedicine of the University of Barcelona (IBUB), Barcelona, Spain
[3] Insitute of Nutrition and Food Safety of the University of Barcelona (INSA-UB), Barcelona, Spain
[4] CIBEROBN, Instituto de Salud Carlos III, Madrid, Spain
[5] Department of Internal Medicine, Hospital Clinic, IDIBAPS, University of Barcelona, Spain
[6] Human Nutrition Department, Hospital Universitari Sant Joan, Institut d'Investigació Sanitària Pere Virgili, University Rovira i Virgili, Reus (Tarragona), Spain
[7] Department of Preventive Medicine and Public Health, Universidad de Navarra-Institute of Health Research of Navarra (IDISNA), Pamplona, Spain

Scope: Fibroblast growth factor 21 (FGF21) is considered a promising therapeutic candidate for the treatment of obesity. Since FGF21 production is regulated by various nutritional factors, we analyze the impact of low protein intake on circulating levels of this growth hormone in mice and in a sub cohort of the PREDIMED (*Prevención con Dieta Mediterránea*) trial. We also describe the role of hepatic FGF21 in metabolic adaptation to a low-protein diet (LPD).

Methods and results: We fed control and liver-specific *Fgf21* knockout (L*Fgf21*KO) mice a LPD. This diet increased FGF21 production by inducing its overexpression in liver, and this correlated with a body weight decrease without changes in food intake. The LPD also caused FGF21-dependent browning in subcutaneous white adipose tissue (scWAT), as indicated by an increase in the expression of uncoupling protein 1 (UCP1). In a subgroup of 78 individuals from the PREDIMED trial, we observed an inverse correlation between protein intake and circulating FGF21 levels.

Conclusion: Our results reinforce the involvement of FGF21 in coordinating energy homeostasis under a range of nutritional conditions. Moreover, here we describe an approach to increase the endogenous production of FGF21, which if demonstrated functional in humans, could generate a treatment for obesity.

Received: August 18, 2016
Revised: November 22, 2016
Accepted: December 21, 2016

Keywords:
Adipose tissue / Browning / Fibroblast growth factor 21 / Low-protein diet / Uncoupling protein 1

Additional supporting information may be found in the online version of this article at the publisher's web-site

Correspondence: Dr. Diego Haro
E-mail: dharo@ub.edu

Abbreviations: **(FGF21)**, Fibroblast growth factor 21; **(LPD)**, Low-protein diet; **(WAT)**, white adipose tissue; **(UCP1)**, Uncoupling protein 1; **(EE)**, Energy expenditure; **(DIO2)**, Type 2 iodothyronine deiodinase protein 2; **(BAT)**, Brown adipose tissue; **(PPAR)**, Peroxisome proliferator-activated receptor; **(FAO)**, Fatty acid oxidation; **(ATF4)**, Activating transcription factor 4; **(DIO)**, Diet-induced obesity; **(HFD)**, High fat diet; **(CD)**, Control diet; **(FFQ)**, Quantitative food frequency questionnaire; **(PGC1a)**, Peroxisome proliferator-activated receptor gamma coactivator 1-alpha; **(PRDM16)**, PR domain containing 16

*Additional correspondence: Joana Relat
E-mail: jrelat@ub.edu

1 Introduction

FGF21 (Fibroblast growth factor 21) is considered a promising therapeutic candidate for the treatment of obesity and type-2 diabetes. Its administration to obese rodents and monkeys leads to decreased plasma concentrations of glucose, insulin, triglycerides and cholesterol, as well as a reduction in body weight through increased energy expenditure (EE) [1]. The injection of FGF21 in experimental animals induces increased thermogenic capacity by stimulating the expression of uncoupling protein 1 (UCP1) and type 2 iodothyronine deiodinase protein 2 (DIO2) in brown adipose tissue (BAT), and UCP1 in white adipose tissue (WAT), where it produces the so-called browning process [2, 3]. Although most of the effects of FGF21 have been related to UCP1 expression, it has also been reported that *Ucp1*-null mice respond positively to the pharmacological administration of this growth factor [4, 5].

FGF21 is a member of the FGF family, which is characterized by endocrine properties. It is produced mainly by the liver, but also by other tissues such as WAT, BAT, skeletal muscle, and pancreas [6–9]. Expression of FGF21 in the liver is induced by fasting, and its transcriptional activity is tightly controlled by peroxisome proliferator-activated receptor alpha (PPAR-α) [10–13]. The expression of this growth factor in liver activates fatty acid oxidation (FAO), ketogenesis, and gluconeogenesis in this organ, thereby triggering a metabolic state that mimics long-term fasting [14].

In addition to fasting, FGF21 expression is also induced in various tissues in response to a number of nutritional challenges and also to cold exposure. In this regard, FGF21 expression in BAT is produced in response to cold temperature [9, 15], although it is unclear whether BAT-derived FGF21 acts as an endocrine factor or whether it is simply an autocrine factor in the adipose tissue itself.

In mouse liver and HepG2 cells, FGF21 is induced by leucine-deprivation as part of the transcriptional program initiated by increased levels of activating transcription factor 4 (ATF4) [16]. The ATF4-dependent increase in FGF21 expression has been confirmed in mice with autophagy deficiency in skeletal muscle and in liver [17]. Interestingly, these mice are protected from diet-induced obesity (DIO) and insulin resistance. The similarities in the metabolic responses between the effects to leucine-deprivation [18] and to FGF21 overexpression allowed us to consider FGF21 as a key mediator between amino acid deprivation and lipid metabolism in liver, WAT, and BAT. In this regard, results from the evaluation of the metabolic response of *Fgf21*-deficient mice to a leucine-deficient diet previously led us to conclude that, as expected, most of the effects caused by leucine deprivation in liver, WAT, and BAT are impaired in the absence of this growth factor [19].

Likewise, methionine-deprived mice show a phenotype comparable to that of leucine-deprivation, including resistance to a high-fat diet (HFD), improved glucose homeostasis, increased fatty acid activation and FAO in liver, enhanced lipolysis in WAT, and increased UCP1 expression in BAT [20, 21]. Of note, the induction of hepatic FGF21 expression under leucine- or methionine-restricted diets was found to be accompanied by an increase in FGF21 protein levels in serum.

In order to facilitate the translation of these findings to humans, here we focussed on low-protein diets (LPD) instead of amino acid-deficient diets. Protein restriction brings about weight loss and an increase in both food intake and EE [22]. Moreover, a LPD induces thermogenic markers in BAT of obese rats [23]. Moreover, serum concentrations of FGF21 in both rodents and humans increase upon exposure to an LPD, regardless of total calorie intake. This observation thus reveals that FGF21 is likely to be involved in the metabolic response to protein-restricted diets [24].

Here we addressed whether a LPD exerts similar effects on lipid metabolism to those of a leucine-deficient diet and whether these effects are dependent on hepatic FGF21 production. To this end, we examined the metabolic response of wild-type and *Fgf21* liver-specific knockout mice (L*Fgf21*KO) to a LPD (up to 5% of energy as protein). A decreased in dietary protein content induced a huge increase in FGF21 serum levels, significant weight loss, and an increase in the expression of UCP1 in the subcutaneous WAT (scWAT) of wild-type mice. Remarkably, no effects were observed in *Fgf21*-deficient mice, thereby indicating that the absence of FGF21 blunts or completely blocks the response to a LPD in this mouse model.

To corroborate these results in humans, we evaluated whether protein intake is associated with circulating levels of FGF21. We calculated protein intake through nutritional questionnaires and determined the serum levels of FGF21 in 78 individuals randomly selected from two nodes of the PREDIMED (*Prevención con Dieta Mediterránea*) trial. As with the animal model, an inverse correlation between circulating FGF21 levels and protein intake was observed.

To summarize, here we define the molecular mechanisms by which a LPD exerts its metabolic effects through the induction of hepatic FGF21 expression and browning of scWAT. Furthermore, the data collected from humans raises the possibility of investigate the dietary modulation of circulating levels of FGF21 as an alternative approach to its pharmacological administration. In this regard, we propose the modification of protein intake to enhance FGF21 production.

2 Material and methods

2.1 Animals

To generate the L*Fgf21*KO mice, $Fgf21^{loxP}$ mice ($Fgf21^{tm1.2Djm}$/J) that have *Fgf21* flanked by two *loxP* sites (Jackson Laboratory, USA) were crossed with Albumin-cre (Tg(Alb1-cre)1Dlr/J) mice (kindly provided by Dr. A. Zorzano). The latter express the CRE recombinase enzyme under control of albumin promoter/enhancer elements, thus allowing liver-specific gene deletions [25]. $Fgf21^{LoxP}$

mice were used as controls. Animals were housed in a temperature-controlled room (22 ± 1°C) on a 12/12 h light/dark cycle and were provided free access to commercial rodent chow and tap water prior to the experiments.

2.1.1 Dietary intervention

The control diet (CD) (Ref. D10001) and LPD (Ref. D12010401) were obtained from Research Diets, Inc. (USA). Both diets were isocaloric. They had the following composition (in percentage of mass): 20% protein, 66% carbohydrates and 5% fat for the CD, and 5% protein, 81% carbohydrates and 5% fat for the LPD (detailed composition shown in Supporting Information Table 1). For the feeding experiment, 8-week-old male mice were first fed the CD for 7 days and then randomly assigned to either the CD or LPD group with free access to food and water for 7 days. Food intake and body weight were recorded daily. Animals were then anesthetized by isoflurane inhalation, and blood was collected by cardiac puncture. After euthanizing the animals, tissues were isolated and immediately snap-frozen and stored at −80°C for future analysis. The Animal Ethics Committee of the University of Barcelona approved these experiments (CEEA register: 48/15)

2.1.2 Human samples for plasma measurements

We used plasma samples from 78 men and women randomly selected from the participants of the centers in Hospital Clinic (Barcelona) and Reus (Tarragona) of the PREDIMED trial (www.predimed.es). This study was a 5-year randomized clinical trial to compare the effects of either a Mediterranean diet supplemented with extra virgin olive oil or nuts versus a low-fat control diet. A total of 7447 asymptomatic men but at high cardiovascular risk (aged 55–80 years) and women (aged 60–80 years) were recruited. All participants had type 2 diabetes or three or more cardiovascular risk factors. Details of the recruitment method and study design have been described elsewhere [26] and are also available at www.predimed.es. In addition to the plasma samples, we also gathered information from these 78 individuals, including a 137-item semi-quantitative food frequency questionnaire (FFQ), and a general questionnaire that provided data on lifestyle habits, concurrent diseases, anthropometry, and medication use. Total energy intake and nutrient intake were calculated on the basis of Spanish food composition tables [27]. The study protocol was approved by the institutional review boards of the participating centers (ISRCTN35739639).

2.1.3 Plasma measurements

Mouse plasma samples were obtained by centrifuging whole blood collected in EDTA-treated tube. The plasma was stored at −80°C. FGF21 in mouse and human plasma was measured by means of a Human (ref. EZHFGF21-19K) and Mouse/Rat (ref. EZRMFGF21-26K) FGF21 ELISA obtained from EMD Millipore (Germany). The assay was conducted following the manufacturer's protocol. Briefly, a calibration curve was constructed by plotting the difference in absorbance values at 450 and 590 nm versus the FGF21 concentrations of the calibrators, and concentrations of unknown samples (performed in duplicate) were determined using this calibration curve. Free fatty acids (non-esterified fatty acids, NEFA) were determined in mice plasma by an enzymatic colorimetric assay. The Free fatty acids, Half-micro test (ref. 11383175001) was obtained from Sigma-Aldrich (USA). The measure was performed according to the manufacturers' instructions.

2.1.4 RNA isolation and relative quantitative RT-PCR

Total RNA was extracted from the frozen tissues [liver, epididymal WAT (eWAT), BAT and inguinal scWAT] using TRI reagent solution (ref. AM9738 Ambion, Thermo Fisher Scientific, USA) followed by DNase I treatment (ref. AM1906, Ambion, Thermo Fisher Scientific, USA) to eliminate genomic DNA contamination. To measure the relative mRNA levels, quantitative (q)RT-PCR was performed using SYBR Green or TaqMan reagents. cDNA was synthesized from 1 μg of total RNA by MLV reverse transcriptase (ref. 28025021, Invitrogen, Thermo Fisher Scientific, USA) with random hexamers (ref. 11034731001, Roche Diagnostics, Germany), following the manufacturer's instructions. The TaqMan Gene Expression Master Mix (ref. 4369514) and SYBR® Green PCR Master Mix (ref. 4364344), supplied by Applied Biosystems (ThermoFisher Scientific, USA), were used for the PCR step. Amplification and detection were performed using the StepOne Plus Real-Time PCR System (Applied Biosystems, ThermoFisher Scientific, USA). Each mRNA from a single sample was measured in duplicate, using 18S, Beta-Actin, and 36b4 as housekeeping genes. The primer sequences are shown in Supporting Information Table 2. Results were obtained by the Relative Standard Curve Method and expressed as fold increase versus the experimental control.

2.1.5 Protein extracts preparation

To obtain liver nuclear extracts, frozen liver was triturated with a mortar in liquid nitrogen and immediately homogenized with a Dounce in 1 mL of HB buffer [15 mM Tris-HCl (pH 8), 15 mM NaCl, 60 mM KCl, 0.5 mM EDTA], and centrifuged at 800 × *g* for 5 min. The resulting pellet was resuspended in 100 μL of HB buffer supplemented with 0.05% Triton X-100 (Sigma, USA) and centrifuged for 10 min at 1000 × *g*. Nuclear pellets were washed with 1 mL of HB buffer supplemented with 0.05% Triton X-100 and 1 mL of HB buffer. Nuclei were incubated at 4°C for 30 min in 50 μL of HB buffer containing 360 mM of KCl and then centrifuged for 5 min at 10 000 × *g*. The supernatants corresponding to the

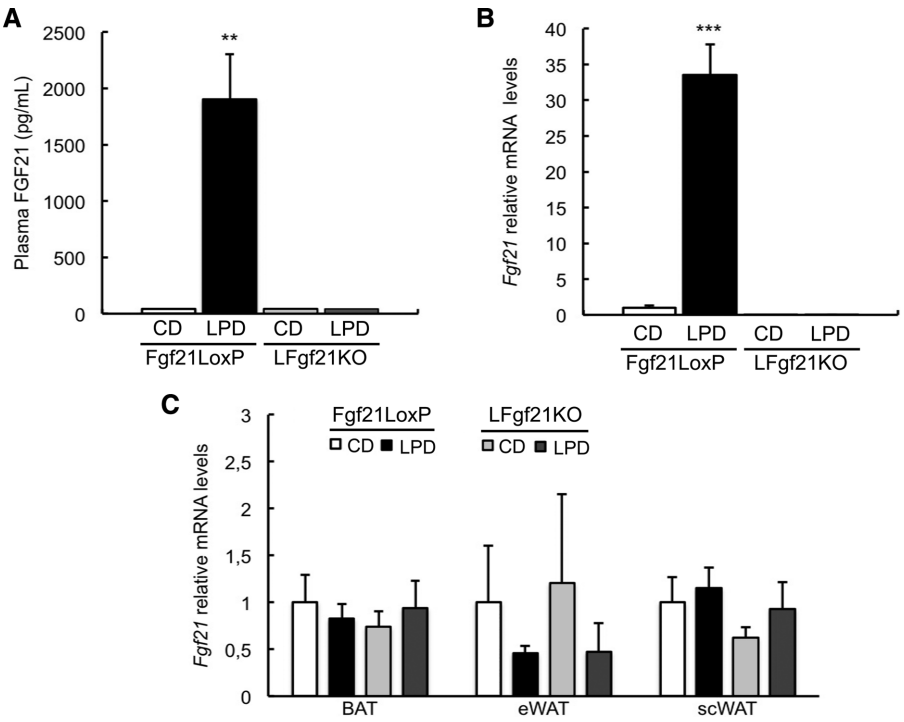

Figure 1. FGF21 is induced by an LPD in liver but not in BAT or WAT, and this induction correlates positively with plasma concentration in mice. Plasma protein concentration of FGF21 was measured by ELISA (A). Fgf21 mRNA levels in liver (B) and WAT and BAT (C) were measured by qRT-PCR. Error bars represent the mean ± SEM. $^{**}p<0.01$ $^{***}p<0.001$ versus $Fgf21^{LoxP}$ mice fed a CD ($n = 7$–9/group).

nuclear extracts were collected, frozen, and stored at −80°C. Protein concentration was determined using the Bio-Rad Protein Assay Dye Reagent Concentrate (Ref. 5000006, Bio Rad, USA). All buffers were supplemented with a mixture of protease inhibitors (Ref. P8340, Sigma-Aldrich, USA), 0.1 mM of PMSF, and a phosphatase inhibitor cocktail 3 (Ref. P0044, Sigma-Aldrich, USA).

2.1.6 Immunoblotting

Nuclear proteins were resolved by SDS-polyacrylamide gel electrophoresis and transferred onto a Hybond-P PVDF membrane (Millipore). Membranes were blocked (Tris-HCl 50 mM pH 8, 150 mM, 5% skimmed milk, 0.1% Tween) for 1 h at room temperature. The blots were then incubated with ATF4 primary antibody (sc-200, Santa Cruz Biotechnology, Inc., USA) in blocking solution (1:200). After an overnight incubation at 4°C, the blots were washed and incubated with an anti-rabbit horseradish peroxidase-conjugated secondary antibody (ref. NA934, Amersham, GE Healthcare, UK) in blocking buffer for 2 h at room temperature. The blots were developed using the EZ-ECL Chemiluminescence Detection Kit for HRP (ref. 20-500-500, Biological Industries, Israel). Quantification was performed using Image J software.

2.1.7 Data analysis/statistics

For human samples, baseline characteristics are presented as means ± standard error of the mean (SEM) for continuous variables, frequencies and percentages for categorical variables across quartiles of protein intake at baseline. Differences between quartiles were tested by a 1-factor ANOVA test for continuous variables and by the chi-square test for the categorical ones. We performed multiple linear regressions to evaluate the relationship between protein intake (exposure variable) and FGF21 hormone levels (dependent variable). Protein intake was previously adjusted for calories using the residual method. Regression analyses were unadjusted (model 1) or adjusted by body mass index (BMI) and total energy intake (model 2).

All statistical analyses were conducted using SAS software, version 9.3 (SAS Institute, Inc., USA). All t tests were two-sided and p values below 0.05 were considered statistically significant.

3 Results and discussion

3.1 A LPD induces FGF21 gene expression in the liver of control mice, but not in BAT or WAT

According to previously reported results, mice on an LPD show a dramatic increase in serum levels of FGF21 [22–24] (Fig. 1A). To check the origin of this FGF21, we analyzed the *Fgf21* mRNA levels in several tissues. The liver is the main site of FGF21 production and release into the blood. Accordingly, we observed a great induction of *Fgf21* mRNA synthesis in the liver of mice on the LPD (Fig. 1B). This increase correlated positively with serum levels. In contrast,

Fgf21 expression was unchanged in BAT, eWAT and scWAT of control mice (*Fgf21*^{loxP}) on the same diet (Fig. 1C).

To determine the specific role of hepatic FGF21 in the metabolic response to a LPD, we fed L*Fgf21*KO mice a LPD diet. As expected, *Fgf21* mRNA levels were undetectable in the livers of these animals (Fig. 1B), while no statistically significant changes were detected in BAT, eWAT, or scWAT when compared to the same tissues in control mice (Fig. 1C).

This mouse model shows that protein restriction almost exclusively affects the hepatic expression of FGF21 and that there is no compensatory response in other tissues, such as BAT or WAT.

We measured the circulating FFA levels as a possible signaling factor for the induction of FGF21 in mice under a low protein diet. The absence of statistically significant changes in FFA (data not shown) allow us to rule out the PPAR-FA axis in the signaling mechanism responsible for the induction of the hepatic expression of FGF21 in these conditions.

3.2 A LPD increases ATF4 protein levels in mouse liver

GCN2 is a kinase that acts as a sensor of amino acid supply [28]. When activated, GCN2 phosphorylates EIF2a, which results in the slowing or stalling of the initiation step of mRNA translation. Hence, phospho-EIF2a reduces general protein synthesis rates. Paradoxically, in these circumstances there is an increase in the translation of discrete mRNAs, including ATF4 [29, 30]. A LPD increases GCN2-dependent phosphorylation of eIF2a, resulting in greater levels of ATF4 protein [31, 32]. ATF4 is a transcriptional factor that directly or indirectly induces a subset of specific genes to regulate metabolic adaptation to amino acid restriction. The 5' region of Fgf21 contains two evolutionarily conserved functional ATF4-binding sequences responsible for its ATF4-dependent transcriptional activation [16, 33]. To determine the effect of an LPD on ATF4 expression, we analyzed liver protein extracts of mice fed an LPD or a CD for 7 days. ATF4 expression was induced in liver in response to the LPD, as revealed by Western blot assays (Fig. 2A and B). These results are consistent with previous published data reporting that ATF4 triggers the expression of FGF21 and that Gcn2 -/- mice show a partially blunted induction of FGF21 under protein restriction [24]. On the basis of the aforementioned published data, our results support the notion that the GCN2-ATF4 pathway is likely to be the main mechanism underlying hepatic FGF21 overexpression upon protein restriction.

GCN2-independent mechanisms that induce hepatic FGF21 in response to methionine-restricted diets have recently been described [34]. This observation points to a different response program in liver via a non-canonical PERK/nuclear respiratory factor 2 (NRF2) pathway. This alternative pathway could effectively sense and translate the metabolic responses to methionine restriction in the absence of GCN2. In parallel, the absence of GCN2 during long-term

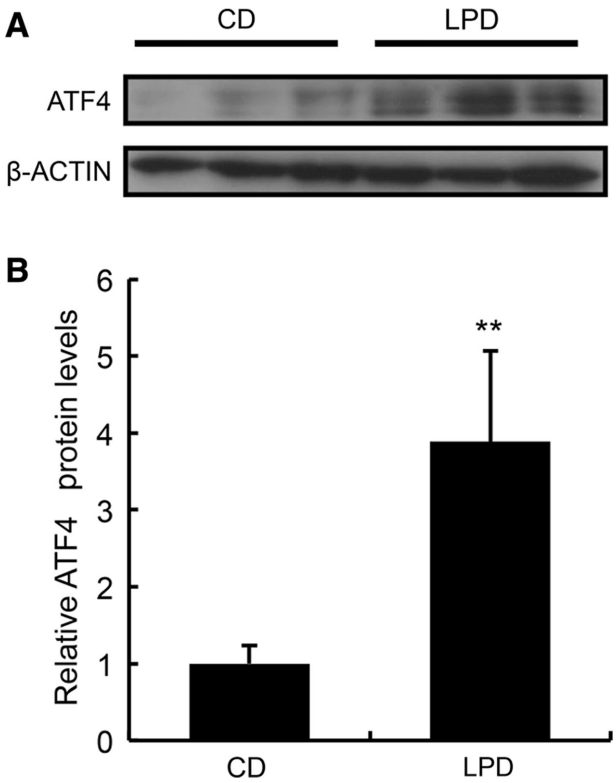

Figure 2. An LPD increases ATF4 protein levels in liver. ATF4 protein levels were determined by Western blot analysis using hepatic nuclear extracts obtained from *Fgf21*^{LoxP} mice administered a CD or LPD (A). The experiment was normalized by actin protein levels as loading control and the intensity of the bands were quantified by densitometry with the Image J software (B). Error bars represent the mean ± SEM. $^{**}p<0.01$ versus CD (n = 3/group).

dietary protein restriction has been reported to be compensated upstream of ATF4 to induce FGF21 [35]. Globally, the impact of alternative pathways to stimulate FGF21 expression under a LPD, whether they involve ATF4 or not, should be addressed in greater depth.

3.3 *Fgf21* deficiency significantly attenuates weight loss under an LPD

Mice fed an LPD presented rapid weight loss. Here we addressed whether this phenomenon is dependent on hepatic FGF21. For this purpose, *Fgf21*^{LoxP} mice and L*Fgf21*KO mice were fed a CD or LPD for 7 days.

Our data showed that weight loss was partially blunted in L*Fgf21*KO mice (Fig. 3A and B). However, the reduction in food intake observed under an LPD, that can account for some of the loss in body weight, was unchanged between genotypes (Fig. 3C). It is remarkable that these results contradicted previous publications describing either no change or an increase in food intake in response to protein restriction

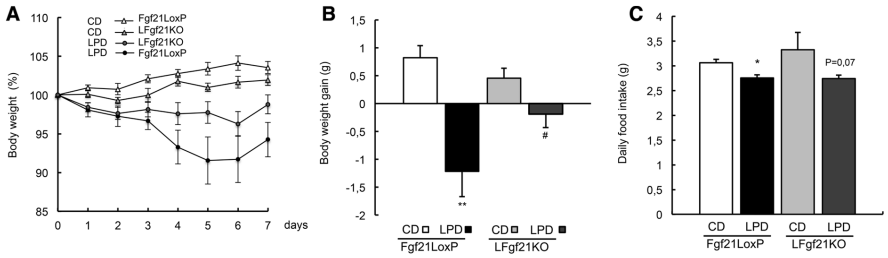

Figure 3. Hepatic FGF21 expression is required for the weight loss caused by LPD but does not affect food consumption. Body weight progression of mice fed a CD or LPD expressed as percentage of the initial weight, which was considered 100% (A). Total body weight change (g) after 7 days on a CD or LPD (B). Daily food intake (C). Error bars represent the mean ± SEM. $^{**}p<0.01$ versus *Fgf21*^{LoxP} mice fed a CD, $^{\#}p<0.05$ versus L*Fgf21*KO fed a CD; 0.07 represents *p* value versus L*Fgf21*KO mice fed a CD ($n = 7$–9/group).

[24]. Nonetheless, the present results are consistent with the decreased food intake described in mice fed leucine-deficient diets [19]. Minor changes in diet composition affecting amino acid bioavailability may explain these discrepancies. Moreover, although FGF21 has the potential to modulate food preferences [36, 37]. In our mouse model this FGF21 did not contribute to the food aversion caused by the LPD.

To determine the importance of each tissue in overall weight loss, we calculated the change in weight of individual tissues. All tissues analyzed tended to weigh less in mice on the LPD, reaching statistical significance in heart, liver, scWAT and $p = 0.06$ in eWAT (Fig. 4). Regarding the role of FGF21, our results show that the weight loss observed in scWAT and heart was dependent on hepatic FGF21 expression, as weight loss was blunted in L*Fgf21*KO mice under the same diet. The effect of the LPD on liver tissue weight was partially abolished by hepatic *Fgf21* deficiency (Fig. 4).

Taken together, FGF21 produced by the liver is, at least in part, responsible for the body weight loss experienced by the mice on the LPD. Our results point to scWAT as one of the target tissues of hepatic FGF21 regarding the weight loss effect. Since hepatic FGF21 exerts its effects mainly in WAT and BAT through regulating lipid metabolism, the following experiments are focused on describing the role of LPD-induced FGF21 on the metabolic response of adipose depots.

3.4 LPD induces metabolic changes in response to FGF21 in scWAT, but not in eWAT or BAT

Thermogenesis in BAT is mediated by the upregulation of UCP1 [38]. It has been proposed that the induction of FGF21 production by the liver mediates direct activation of brown fat thermogenesis during the fetal-to-neonatal transition [39]. FGF21 also regulates peroxisome proliferator-activated receptor gamma coactivator 1-alpha (PGC1a) and browning of WAT in adaptive thermogenesis [40].

Contrary to what happens under leucine deprivation [19], no statistically significant induction of *Ucp1* or *Dio2* mRNA levels were observed in BAT or eWAT of control mice under the LPD (Fig. 5A and B). In contrast, the analysis of gene expression in scWAT revealed that the LPD induced the expression of *Ucp1*, *Pgc1a*, *Cidea* and PR domain containing 16 (*Prdm16*), reaching a statistically significant value for *Ucp1* and *Pgc1a* (Fig. 6). This expression pattern was not detected in the L*Fgf21*KO mice (Fig. 6), thereby indicating the role

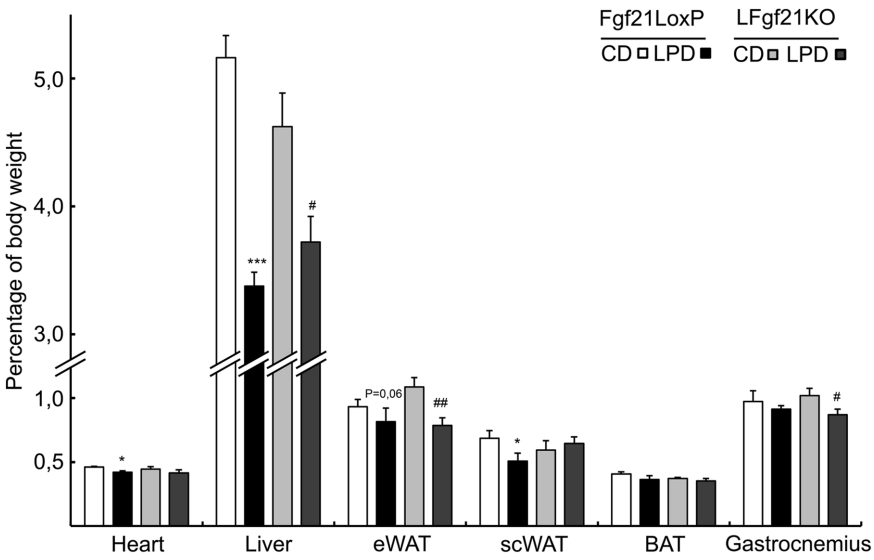

Figure 4. Hepatic FGF21 is required for the weight loss caused by an LPD. The weight of heart, liver, eWAT, scWAT, BAT, and gastrocnemius in mice fed a CD or LPD is presented as the mg of tissue per 100 mg of total body weight. Error bars represent the mean ± SEM. $^{*}p<0.05$, $^{***}p<0.001$ versus *Fgf21*^{LoxP} mice fed a CD; $^{\#}p<0.05$, $^{\#\#}p<0.01$ versus L*Fgf21*KO mice fed a CD; 0.06 represents the *p* value with respect to *Fgf21*^{LoxP} mice fed a CD ($n = 7$–9/group).

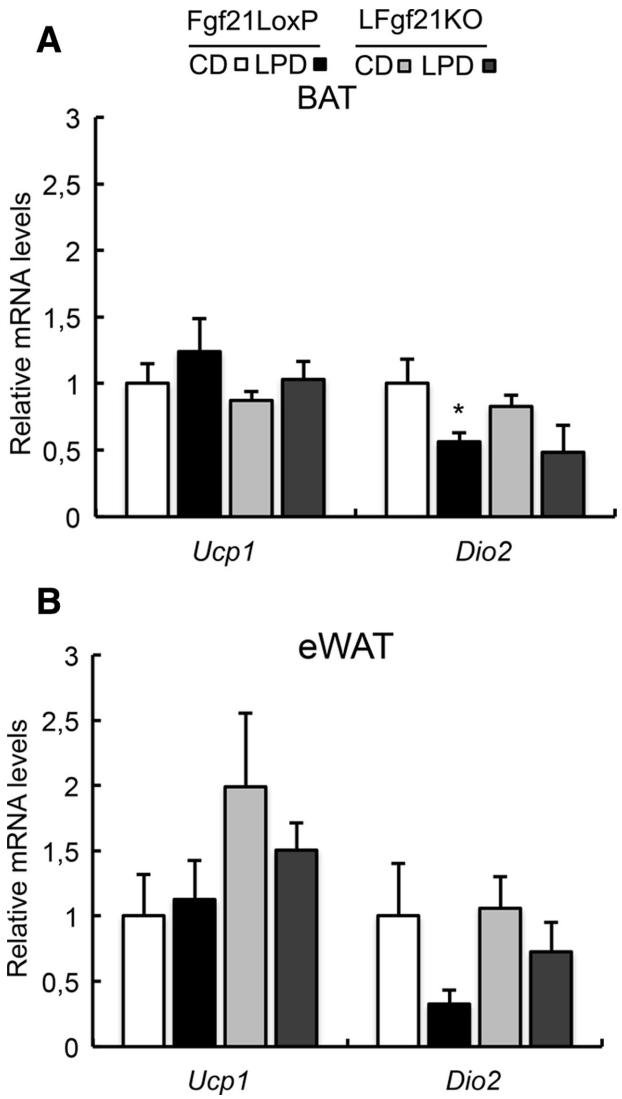

Figure 5. A LPD does not alter thermogenic genes in BAT or eWAT. *Ucp1* and *Dio2* expression was measured by qRT-PCR in mouse BAT and eWAT. Error bars represent the mean ± SEM. $^{*}p<0.05$ versus $Fgf21^{LoxP}$ mice fed a CD ($n = 7$–9/group).

of FGF21 in the metabolic adaptation of scWAT to protein restriction.

As UCP1 activity is related to EE, the blunted induction of UCP1 in the L*Fgf21*KO mice under LPD may contribute to the lower weight loss observed in this mouse model under these circumstances. In conclusion, hepatic FGF21 induces the browning of scWAT and increases the thermogenic capacity of mice on an LPD.

3.5 FGF21 plasma levels correlate negatively with protein intake in humans

To translate our results to humans, we evaluated the relationship between protein intake and circulating levels of FGF21 in 78 individuals randomly selected from the PREDIMED trial. Baseline data for these subjects are shown in Table 1. Protein intake was obtained from FFQs and was expressed as grams of protein per day (g/day). We used baseline samples (T = 0). Results from the multiple linear regression analyses showed a significant inverse relationship between plasma FGF21 concentrations and dietary intake of protein. At baseline, FGF21 levels decreased by 3.39 pg/mL for each gram of protein ingested (Table 2). The participants with a high intake of protein showed statistically significant lower values of circulating FGF21.

We also performed regression analyses using quartiles of protein intake and obtained similar results. After adjustment for BMI and total energy intake, FGF21 decreased (−30.7 pg/mL) when moving from the lower to higher quartiles ($p = 0.015$)(Fig. 7).

Similarly to the data from mice, these results indicate that the serum concentrations of FGF21 are inversely proportional to dietary protein intake.

4 Concluding remarks

Here we addressed the role of hepatic FGF21 in the metabolic changes triggered by an LPD. Our results demonstrate that the effects of an LPD depend, at least in part, on the circulating levels of FGF21 and consequently on the liver production of

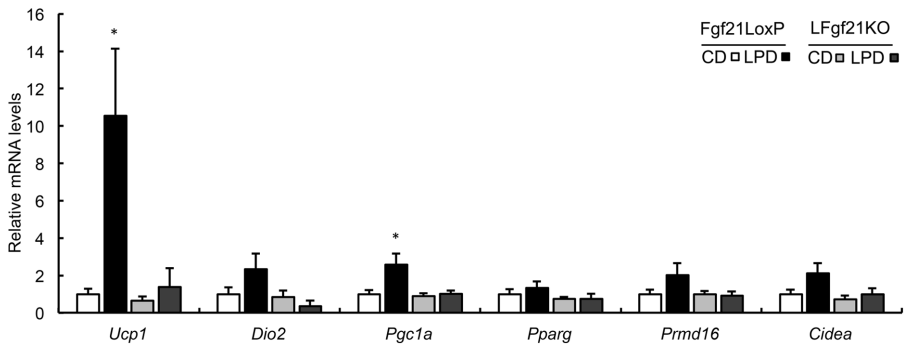

Figure 6. Hepatic FGF21 is required for inducing thermogenic gene expression during an LPD. *Ucp1, Dio2, Pgc1a, Pparg, Prmd16,* and *Cidea* expression was measured by qRT-PCR in mouse scWAT. Error bars represent the mean ± SEM. $^{*}p<0.05$ versus $Fgf21^{LoxP}$ mice fed a CD ($n = 7$–9/group).

Table 1. Baseline characteristics of participants from the PREDIMED cohort included in this study, divided into quartiles of energy-adjusted protein intake at baseline[a)]

	Quartiles of energy-adjusted protein intake				*p* value[b)]
	Q1	Q2	Q3	Q4	
No subjects (78)	19	20	20	19	
Age (years)	67.1 ± 5.9	65.7 ± 4.8	67.0 ± 6.4	65.3 ± 4.0	0.30
Sex (women)	6 (31)	10 (50)	9 (45)	15 (79)	0.03
Body mass index (kg/m^2)	28.1 ± 3.2	30.0 ± 3.4	27.7 ± 2.7	30.8 ± 2.9	0.006
Energy intake (kcal/day)	2370 ± 350	2192 ± 603	2227 ± 433	2390 ± 571	0.51
Protein intake (g/day)	80 ± 6	90 ± 2	97 ± 3	110 ± 5	<0.0001
FGF21 (pg/mL)	289 ± 116	276 ± 143	256 ± 117	190 ± 115	0.07

[a)]Categorical variables: subjects (percentage), continuous variables: mean ± SD
[b)]One-way ANOVA tests (continuous variables) or chi-squared tests (categorical variables).

Table 2. Multivariable regression analyses with FGF21 (pg/mL) as dependent variable and energy-adjusted protein intake at baseline (g/day) as independent variable

		β[a)]	*p* value	95% CI
Protein intake (continuous variable)	Model 1[b)]	−3.42	0.006	−5.83, −1.02
	Model 2[c)]	−3.39	0.007	−5.86, −0.92
Quartiles of protein intake	Model 1[b)]	−31.5	0.01	−56.5, −6.5
	Model 2[c)]	−30.8	0.02	−56.5, −5.0

CI: Confidence interval.
[a)]Parameter estimates.
[b)]Unadjusted.
[c)]Adjusted for body mass index (BMI) and total energy intake.

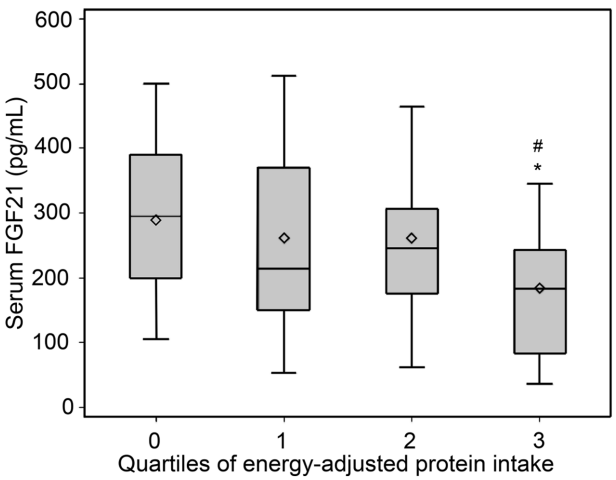

Figure 7. Circulating FGF21 levels correlate negatively with protein intake. Plasma FGF21 concentration divided into quartiles of protein intake adjusted for the calorie intake of 78 participants in the PREDIMED trial. Error bars represent the mean ± SEM. $^{*}p<0,05$ from first quartile; $^{\#}p<0,05$ from the second quartile.

this growth factor. The L*Fgf21*KO mice revealed the relevance of FGF21 in the response to an LPD, but also in the metabolic and transcriptional pathways activated or repressed by protein restriction.

Given the parallelism between the results of our study in humans and those in mice, we postulate that dietary protein content is crucial for the modulation of circulating FGF21 levels and thus for the activity of this hormone in target tissues in mice and that it could also be in humans. We propose to investigate a dietary intervention consisting of a reduction in protein intake as a non-invasive approach to induce the hepatic expression of FGF21. We also describe the molecular mechanisms through which a LPD—via FGF21—could be beneficial to restore lipid/glucose homeostasis.

Studies performed in humans provide contradictory results regarding the correlation between plasma levels of FGF21, BMI, and insulin resistance [41–43]. Also, the FGF21-resistant state described in mice [44] is not well established in humans and the beneficial effects of FGF21 induction have yet to be demonstrated in the latter.

Our findings provide new insight into the modulation of dietary protein as a strategy to induce elevated serum concentrations of FGF21. Further studies will be needed to evaluate the effects of an LPD / FGF21 induction on the metabolic profile of obese and insulin-resistant subjects.

This project was supported by grant SAF2013-41093 (to P.F.M. and D.H.) from the Ministerio de Economia y Competitividad, by funding from the Catalan government, Generalitat de Catalunya (Ajut de Suport als Grups de Recerca de Catalunya 2014SGR916 to D.H and 2014SGR773 to R.L.M.), by CICYT (AGL2013-49083-C3-1-R and AGL2016-79113-R to R.L.R.) and the Instituto de Salud Carlos III, ISCIII (CIBEROBN) from the Ministerio de Economía y Competitividad (MEC) (AEI/FEDER, UE) (to R.L.M.). A.P.M. was supported by Scholarship from Spain's Ministerio de Educación Cultura y Deporte. A.C.D.R. was supported by Scholarship from University of Barcelona.

A.P.M. performed the experiments with mice. M.G.G. performed the ELISA and the statistical analysis of human samples.

A.T.R. performed the statistical analysis of human samples with M.G.G. A.C.D.R. has made the FFA analysis during the revision of the manuscript. R.E., J.S.S., M.A.M.G. provided the human samples P.F.M., D.H., J.R. conceived the project and wrote the paper. All authors read, approved and contributed with important intellectual content to the final version of the manuscript.

The authors have declared no conflict of interest.

5 References

[1] Kharitonenkov, A., Shanafelt, A.-B., FGF21: a novel prospect for the treatment of metabolic diseases. *Curr. Opin. Investig. Drugs.* 2009, *10*, 359–364.

[2] Fisher, F.-M., Kleiner, S., Douris, N., Fox, E.-C. et al., FGF21 regulates PGC-1α and browning of white adipose tissues in adaptive thermogenesis. *Genes Dev.* 2012, *26*, 271–281.

[3] Lee, P., Swarbrick, M.-M., Greenfield, J.-R., The sum of all browning in FGF21 therapeutics. *Cell Metab.* 2015, *21*, 795–796.

[4] Véniant, M.-M., Sivits, G., Helmering, J., Komorowski, R. et al., Pharmacologic effects of FGF21 are independent of the 'browning' of white adipose tissue. *Cell Metab.* 2015, *21*, 731–738.

[5] Samms, R.-J., Smith, D.-P., Cheng, C.-C., Antonellis, P.-P. et al., Discrete aspects of FGF21 in vivo pharmacology do not require UCP1. *Cell Rep.* 2015, *11*, 991–999.

[6] Nishimura, T., Nakatake, Y., Konishi, M., and Itoh, N., Identification of a novel FGF, FGF-21, preferentially expressed in the liver. *Biochim. Biophys. Acta - Gene Struct. Expr.* 2000, *1492*, 203–206.

[7] Johnson, C.-L., Weston, J.-Y., Chadi, S.-A., Fazio, E.-N. et al., Fibroblast growth factor 21 reduces the severity of cerulein-induced pancreatitis in mice. *Gastroenterology.* 2009, *137*, 1795–1804.

[8] Izumiya, Y., Bina, H.-A., Ouchi, N., Akasaki, Y. et al., FGF21 is an Akt-regulated myokine. *FEBS Lett.* 2008, *582*, 3805–3810.

[9] Hondares, E., Iglesias, R., Giralt, A., Gonzalez, F.-J. et al., Thermogenic activation induces FGF21 expression and release in brown adipose tissue. *J. Biol. Chem.* 2011, *286*, 12983–12990.

[10] Badman, M.-K., Pissios, P., Kennedy, A.-R., Koukos, G., Hepatic fibroblast growth factor 21 is regulated by PPARa and is a key mediator of hepatic lipid metabolism in ketotic states. *Cell Metab.* 2007, *5*, 426–437.

[11] Inagaki, T., Dutchak, P., Zhao, G., Ding, X. et al., Endocrine regulation of the fasting response by PPARa-mediated induction of fibroblast growth factor 21. *Cell Metab.* 2007, *5*, 415–425.

[12] Gälman, C., Lundåsen, T., Kharitonenkov, A., Bina, H.-A., et al,. The circulating metabolic regulator FGF21 is induced by prolonged fasting and PPARα activation in man. *Cell Metab.* 2008, *8*, 169–174.

[13] Lundåsen, T., Hunt, M.-C., Nilsson, L.-M., Sanyal, S. et al., PPARα is a key regulator of hepatic FGF21. *Biochem. Biophys. Res. Commun.* 2007, *360*, 437–440.

[14] Reitman, M.-L., FGF21: a missing link in the biology of fasting. *Cell Metabolism* 2007, *5*, 405–407.

[15] Chartoumpekis, D.-V., Habeos, I.-G., Ziros, P.-G., Psyrogiannis, A.-I. et al., Brown adipose tissue responds to cold and adrenergic stimulation by induction of FGF21. *Mol. Med.*, 2011, *17*, 736–740.

[16] De Sousa-Coelho, A.-L., Marrero, P.-F., Haro, D., Activating transcription factor 4-dependent induction of FGF21 during amino acid deprivation. *Biochem. J.*, 2012, *443*, 165–171.

[17] Kim, K.-H., Jeong, Y.-T., Oh, H., Kim, S.-H. et al., Autophagy deficiency leads to protection from obesity and insulin resistance by inducing Fgf21 as a mitokine. *Nat Med.* 2013, *19*, 83–92.

[18] Cheng, Y., Meng, Q., Wang, C., Li, H. et al., Leucine deprivation decreases fat mass by stimulation of lipolysis in white adipose tissue and upregulation of uncoupling protein 1 (UCP1) in brown adipose tissue. *Diabetes*, 2010, *59*, 17–25.

[19] De Sousa-Coelho, A.-L., Relat, J., Hondares, E., Pérez-Martí, A. et al., FGF21 mediates the lipid metabolism response to amino acid starvation. *J. Lipid Res.* 2013, *54*, 1786–1797.

[20] Ables, G.-P., Perrone, C.-E., Orentreich, D., Orentreich, N., Methionine-restricted C57BL/6J mice are resistant to diet-induced obesity and insulin resistance but have low bone density. *PLoS One.* 2012, *7*, e51357.

[21] Stone, K.-P., Wanders, D., Orgeron, M., Cortez, C.-C. et al., Mechanisms of increased in vivo insulin sensitivity by dietary methionine restriction in mice. *Diabetes.* 2014, *63*, 1–28.

[22] Ozaki, Y., Saito, K., Nakazawa, K., Konishi, M. et al., Rapid increase in fibroblast growth factor 21 in protein malnutrition and its impact on growth and lipid metabolism. *Br. J. Nutr.* 2015, *114*, 1410–1418.

[23] Pezeshki, A., Zapata, R.-C., Singh, A., Yee, N.-J. et al., Low protein diets produce divergent effects on energy balance. *Sci. Rep.* 2016, *6*, 25145.

[24] Laeger, T., Henagan, T.-M., Albarado, D.-C., Redman, L.-M. et al., FGF21 is an endocrine signal of protein restriction. *J. Clin. Invest.* 2014, *124*, 3913–3922.

[25] Yakar, S., Liu, J.-L., Stannard, B., Butler, A. et al., Normal growth and development in the absence of hepatic insulin-like growth factor I. *Proc. Natl. Acad. Sci.* 1999, *96*, 7324–7329.

[26] Estruch, R., Ros, E., Salas-Salvadó, J., Covas, M.-I. et al., Primary prevention of cardiovascular disease with a Mediterranean diet. *N. Engl. J. Med.* 2013, *368*, 1279–1290.

[27] Mataix, J., *Tabla de composición de alimentos.* 2003, 5a ed. Granada: Universidad de Granada.

[28] Qiu, H., Dong, J., Hu, C., Francklyn, C.-S. et al., The tRNA-binding moiety in GCN2 contains a dimerization domain that interacts with the kinase domain and is required for tRNA binding and kinase activation. *EMBO J.*, 2001, *20*, 1425–1438.

[29] Hao, S., Sharp, J.-W., Ross-Inta, C.-M., McDaniel, B.-J. et al., Uncharged tRNA and sensing of amino acid deficiency in mammalian piriform cortex. *Science* 2005, *307*, 1776–1778.

[30] Shan, J., Ord, D., Ord, T., Kilberg, M.-S., Elevated ATF4 expression, in the absence of other signals, is sufficient for transcriptional induction via CCAAT enhancer-binding

protein-activating transcription factor response elements. *J. Biol. Chem.* 2009, *284*, 21241–21248.

[31] Anthony, T.-G., McDaniel, B.-J., Byerley, R.-L., McGrath, B.-C. et al., Preservation of liver protein synthesis during dietary leucine deprivation occurs at the expense of skeletal muscle mass in mice deleted for eIF2 kinase GCN2. *J. Biol. Chem.* 2004, *279*, 36553–36561.

[32] Guo, F., Cavener, D.-R., The GCN2 eIF2a kinase regulates fatty-acid homeostasis in the liver during deprivation of an essential amino acid. *Cell Metab.*, 2007, *5*, 103–114.

[33] Wan, X.-S., Lu, X.-H., Xiao, Y.-C., Lin, Y. et al., ATF4- and CHOP-dependent induction of FGF21 through endoplasmic reticulum stress. *Biomed Res. Int.*, vol. 2014, *>2014*, 807874.

[34] Wanders, D., Stone, K.-P., Forney, L.-A., Cortez et al., Role of GCN2-independent signaling through a non-canonical PERK/NRF2 pathway in the physiological responses to dietary methionine restriction. *Diabetes*, 2016, *65*, db151324.

[35] Laeger, T., Albarado, D.-C., Burke, S.-J., Trosclair, L. et al., Metabolic responses to dietary protein restriction require an increase in FGF21 that is delayed by the absence of GCN2. *Cell Rep.*, 2016, *16*, 707–716.

[36] von Holstein-Rathlou, S., BonDurant, L.-D., Peltekian, L., Naber, M.-C. et al., FGF21 mediates endocrine control of simple sugar intake and sweet taste preference by the liver. *Cell Metab.* 2016, *23*, 335–343.

[37] Chu, A.-Y., Workalemahu, T., Paynter, N.-P., Rose, L.-M. et al., Novel locus including FGF21 is associated with dietary macronutrient intake. *Hum. Mol. Genet.* 2013, *22*, 1895–1902.

[38] Matthias, A., Ohlson, K.-B., Fredriksson, J.-M., Jacobsson, A. et al., Thermogenic responses in brown fat cells are fully UCP1-dependent. UCP2 or UCP3 do not substitute for UCP1 in adrenergically or fatty SCID-induced thermogenesis. *J. Biol. Chem.* 2000, *275*, 25073–25081.

[39] Hondares, E., Rosell, M., Gonzalez, F.-J., Giralt, M. et al., Hepatic FGF21 expression is induced at birth via PPARalpha in response to milk intake and contributes to thermogenic activation of neonatal brown fat. *Cell Metab.* 2010, *11*, 206–212.

[40] Fisher, F.-F., Kleiner, S., Douris, N., Fox, E.-C. et al., FGF21 regulates PGC-1a and browning of white adipose tissues in adaptive thermogenesis. *Genes Dev.* 2012, *26*, 271–281.

[41] Zhang, X., Yeung, D.-C.-Y., Karpisek, M., Stejskal, D. et al., Serum FGF21 levels are increased in obesity and are independently associated with the metabolic syndrome in humans. *Diabetes.* 2008, *57*, 1246–1253.

[42] Chen, W.-W., Li, L., Yang, G.-Y., Li, K. et al., Circulating FGF-21 levels in normal subjects and in newly diagnose patients with Type 2 diabetes mellitus. *Exp. Clin. Endocrinol. Diabetes.* 2008, *116*, 65–68.

[43] Chavez, A.-O., Molina-Carrion, M., Abdul-Ghani, M.-A., Folli, F. et al., Circulating fibroblast growth factor-21 is elevated in impaired glucose tolerance and type 2 diabetes and correlates with muscle and hepatic insulin resistance. *Diabetes Care* 2009, *32*, 1542–1546.

[44] Fisher, F.-M., Chui, P.-C., Antonellis, P.-J., Bina, H.-A. et al., Obesity is a fibroblast growth factor 21 (FGF21)-resistant state. *Diabetes* 2010, *59*, 2781–2789.

ANNEX 3:A Low Protein Diet Induces Body Weight loss and Browning of subcutaneous White Adipose Tissue Through Enhanced Expression of Hepatic Fibroblast Growth Factor 21 (FGF21) – *Communication at the Wine and Health Meeting 2017 (La Rioja)*

A low-protein diet induces body weight loss and browning of subcutaneous white adipose tissue through enhanced expression of hepatic Fibroblast Growth Factor 21 (FGF21).

Albert Pérez-Martí[1,2], Maite Garcia-Guasch[1,2], Anna Tresserra-Rimbau[1,3,4], Alexandra Carrilho-Do-Rosário[1,2], Ramon Estruch[4,5], Jordi Salas-Salvadó[4,6], Miguel Ángel Martínez-González[4,7], Rosa Lamuela-Raventós[1,3,4], Pedro F. Marrero[1,2], Joana Relat[1,2], Diego Haro[1,2].

[1]Department of Nutrition, Food Sciences and Gastronomy, School of Pharmacy and Food Science, University of Barcelona, Torribera Food Campus, Santa Coloma de Gramenet, (Barcelona) Spain.
[2]Institute of Biomedicine of the University of Barcelona (IBUB).
[3]Insitute of Nutrition and Food Safety of the University of Barcelona (INSA-UB).
[4]CIBEROBN, Instituto de Salud Carlos III, Madrid, Spain.
[5]Department of Internal Medicine, Hospital Clinic, IDIBAPS, University of Barcelona, Spain.
[6]Human Nutrition Department, Hospital Universitari Sant Joan, Institut d'Investigació Sanitària Pere Virgili, University Rovira i Virgili, Reus (Tarragona), Spain.
[7]Department of Preventive Medicine and Public Health, Universidad de Navarra-Institute of Health Research of Navarra (IDISNA), Pamplona, Spain.

SUMMARY

Fibroblast growth factor 21 (FGF21) is considered a promising therapeutic candidate for the treatment of obesity and metabolic disorders. Since FGF21 production is regulated by various nutritional factors, we analyze the impact of low protein intake on circulating levels of this growth hormone in mice and in a sub cohort of the PREDIMED (*Prevención con Dieta Mediterránea*) trial. We also describe the role of hepatic FGF21 in metabolic adaptation to a low-protein diet (LPD).

RESULTS

We fed control and liver-specific *Fgf21* knockout (L*Fgf21*KO) mice a LPD. This diet increased FGF21 production by inducing its overexpression in liver (**Figure 1**), and this correlated with the induction of the transcription factor ATF4 (**Figure 2**) and a body weight decrease without changes in food intake (**Figure 3**).

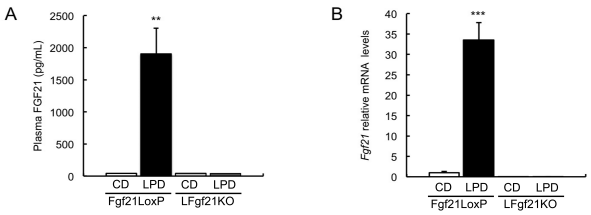

Figure 1. FGF21 is induced by a LPD in liver, and this induction correlates positively with plasma concentration in mice. Plasma protein concentration of FGF21 was measured by ELISA (A). Fgf21 mRNA levels in liver (B) were measured by qRT-PCR. Error bars represent the mean ± SEM. ** p<0.01 ***p<0.001 versus *Fgf21LoxP* mice fed a CD (n=7–9/group).

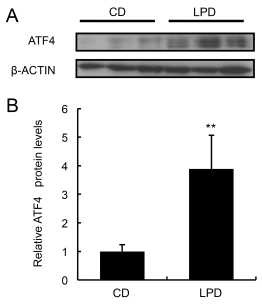

Figure 2. A LPD increases ATF4 protein levels in liver. ATF4 protein levels were determined by Western blot analysis using hepatic nuclear extracts obtained from *Fgf21LoxP* mice administered a CD or LPD (A). The experiment was normalized by actin protein levels as loading control and the intensity of the bands were quantified by densitometry with the Image J software (B). Error bars represent the mean ± SEM. **p<0.01 versus CD. (n=3/group).

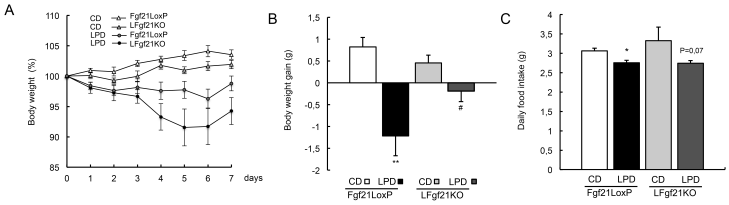

Figure 3. Hepatic FGF21 expression is required for the weight loss caused by LPD but does not affect food consumption. Body weight progression of mice fed a CD or LPD expressed as percentage of the initial weight, which was considered 100% (A). Total body weight change (g) after 7 days on a CD or LPD (B). Daily food intake (C). Error bars represent the mean ± SEM. ** p<0.01 versus *Fgf21LoxP* mice fed a CD, # p<0.05 versus L*Fgf21*KO fed a CD; 0.07 represents p value versus L*Fgf21*KO mice fed a CD (n=7–9/group).

The LPD also caused FGF21-dependent browning in subcutaneous white adipose tissue (scWAT), as indicated by an increase in the expression of uncoupling protein 1 (UCP1) (**Figure 4**).

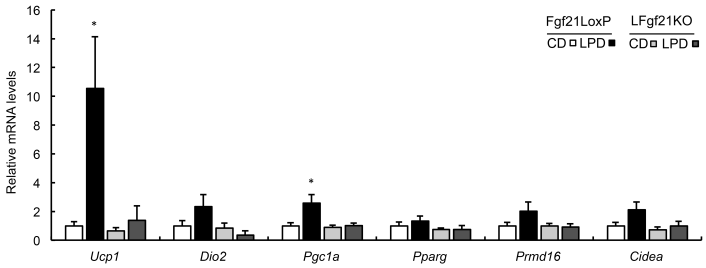

Figure 4. Hepatic FGF21 is required for inducing thermogenic gene expression during a LPD. *Ucp1, Dio2, Pgc1a, Pparg, Prmd16* and *Cidea* expression was measured by qRT-PCR in mouse scWAT. Error bars represent the mean ± SEM. * p<0.05 versus *Fgf21LoxP* mice fed a CD (n=7–9/group).

In a subgroup of 78 individuals from the PREDIMED trial, we observed an inverse correlation between protein intake and circulating FGF21 levels (**Figure 5**).

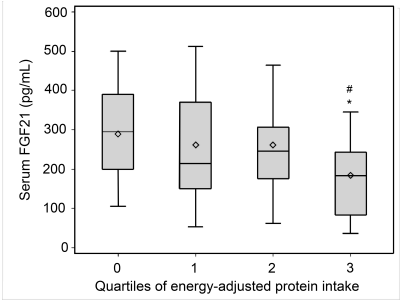

Figure 5. Circulating FGF21 levels correlate negatively with protein intake. Plasma FGF21 concentration divided into quartiles of protein intake adjusted for the calorie intake of 78 participants in the PREDIMED trial. Error bars represent the mean ± SEM. * p<0,05 from 1st quartile; # p<0,05 from the 2nd quartile.

GRAPHIC ABSTRACT

Our results reinforce the involvement of FGF21 in coordinating energy homeostasis under a range of nutritional conditions. Moreover, here we describe an approach to increase the endogenous production of FGF21, which if demonstrated functional in humans, could generate a treatment for obesity.

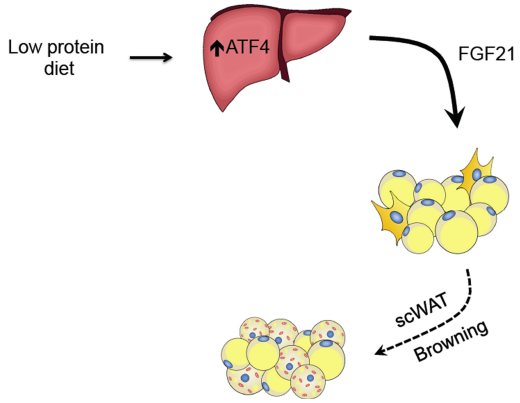

UNIVERSITAT DE BARCELONA

Campus de l'Alimentació Universitat de Barcelona